uOttawa

L'Université canadienne
Canada's university

FACULTÉ DES ÉTUDES SUPÉRIEURES ET POSTOCTORALES

uOttawa

L'Université canadienne
Canada's university

FACULTY OF GRADUATE AND POSDOCTORAL STUDIES

Miressa Ebisa Fola

AUTEUR DE LA THÈSE / AUTHOR OF THESIS

M.A.Sc. (Civil Engineering)

GRADE / DEGREE

Department of Civil Engineering

FACULTÉ, ÉCOLE, DÉPARTEMENT / FACULTY, SCHOOL, DEPARTMENT

Downstream Hydraulic Geometry of Clay-Dominated Cohesive Bed Stream Channels

TITRE DE LA THÈSE / TITLE OF THESIS

Dr. C. Rennie

DIRECTEUR (DIRECTRICE) DE LA THÈSE / THESIS SUPERVISOR

CO-DIRECTEUR (CO-DIRECTRICE) DE LA THÈSE / THESIS CO-SUPERVISOR

EXAMINATEURS (EXAMINATRICES) DE LA THÈSE / THESIS EXAMINERS

Dr. S. Sivathayalan

Dr. O. Seidou

Dr. I Nistor

Gary W. Slater

Le Doyen de la Faculté des études supérieures et postdoctorales / Dean of the Faculty of Graduate and Postdoctoral Studies

Downstream Hydraulic Geometry of Clay-Dominated Cohesive Bed Stream Channels

Miressa Ebisa Fola

Thesis submitted to the
Faculty of Graduate and Postdoctoral Studies
in partial fulfillment of the requirements
for the Master of Applied Science degree in Civil Engineering

The Ottawa-Carleton Institute for Civil Engineering
Department of Civil Engineering
Faculty of Engineering
University of Ottawa

Your file Votre référence
ISBN: 978-0-494-49195-9
Our file Notre référence
ISBN: 978-0-494-49195-9

Acknowledgements

The author wants to give a special thanks to his supervisor Professor Colin D. Rennie for his invaluable input during the entire thesis. In addition to his guidance and valuable comments, Professor Rennie spent significant time in providing training for deploying modern river surveying methods using the Acoustic Doppler Current Profiler (ADCP) and Real Time Kinematic Differential Global Position System (RTK-DGPS). He also spent countless hours in assisting the author with field surveying and provided matlab code for processing ADCP data.

The author also wants to express great appreciation to hydraulics lab technical officer Gavin Post and fellow students Elizabeth Jamieson and Soheil Movafagh for spending their time, energy and expertise in assisting him during the field survey days. He wants to say thank you to Shalini Kashyap for her assistance in troubleshooting the matlab code for ADCP data processing. The author would also like to thank Civil Engineering Department Support staff Yolande Hogan and Manon Racine for their collaboration for requests related to administration issues. Finally, the author would like to say thank you to members of Oromo Community of Ottawa: Abdisa, Yimam, Lelise, Kamal, Feleke, Hadha-biyya, Teshome, Mohamad, Labu, Sultan, Yeshitila and many others for their friendship and help in settling in Ottawa.

Abstract

Empirical downstream hydraulic geometry equations for clay-dominated cohesive bed (semi-alluvial) streams were derived using the data from five streams in eastern Ontario and four streams from other regions. The width exponent (0.57) is comparable to the exponents reported for previous studies; however, depth exponent (0.52) was greater for clay-dominated cohesive bed than for typical gravel-bed and sand-bed rivers. Furthermore, the recurrence intervals of bankfull discharges of those streams range from 1 to 2 years. To the author's knowledge, this is the first study which related bankfull hydraulic variables and discharges to derive downstream hydraulic geometry equations specifically for clay-dominated cohesive bed streams. Assessment of width:depth ratio depicted that large channels were deeper and narrower than comparable gravel-bed channels, but small channels were actually wider and shallower than typical gravel-bed rivers. This can likely be attributed to the resistance of stiff and consolidated cohesive-bed to erosive effects of more frequent flows.

Table of Contents

Page

Page

List of Tables

List of Figures

Page

Page

List of Symbols and Abbreviations

✓ Abbrevations

ADCP	Acoustic Doppler Current Profiler
AMS	Annual maximum series
BC	British Columbia
bf	Bankfull
BFD	Bankfull discharge
BFD-RI	Bankfull discharge recurrence interval
bfr	Bankfull based on rating data
BT	Bottom track
cm	Centimeter
CA	Canada
cfs	Cubic feet per second
DA	Drainage Area
DGPS	Differential Global Positioning System
DMS	Degree Minute Second
EON	Eastern Ontario
Eq	Equation
ETS	Electronic Total Station
HDOP	GPS Horizontal Dilution of Position
Fig	Figure
GGA	GPS Fix data
GPS	Global Positioning System
IACWD	Interagency Advisory Committee on Water Data
ID	Identification
IFIM	Instream Flow Incremental Methodology
KHz	Kilo-Hertz
KM / km	Kilometer

Lat	Latitude
Lon	Longitude
L_R	Left to right
R_L	Right to left
m	Meter
mdr	Measured based on rating
Mi / mi	Mile
MT	Montana
NAVSTAR	Navigation Satellite Timing and Ranging
No	Number
NY	New York
ON	Ontario
PDS	Partial duration series
RDI	RD Instruments
REC	Number of record years
RI	Recurrence interval
RTK-DFGPS	Real Time Kinematic-Differential Global Positioning System
s or sec	Second
Sq	Square
UK	United Kingdom
US	United States
USGS	United States Geological Survey
WM	Water Mode
BM	Bottom Mode
Ave	Average

✓ Symbols

A	Area, [L^2]
a	Constant; width coefficient
A_{bf}	Bankfull Area, [L^2]
b	Constant; width exponent
c	Constant; hydraulic depth coefficient
C	Speed of sound, [L/T]
D	Mean depth, [L]
D_{50}	Grain size defined as the size for which 50% by weight of the material is finer, [L]
D_{84}	Grain size defined as the size for which 84% by weight of the material is finer, [L]
D_{bf}	Bankfull mean depth, [L]
f	Constant; hydraulic depth exponent
F_d	Doppler shift, [1/T]
ff	Friction factor
Fr_{min}	Minimum Froude number
F_s	Frequency of the transmitted sound, [1/T]
G	Skew coefficient
H	Stage or level, [L]
k	Constant; velocity coefficient
K	Frequency factor
m	Constant; velocity exponent
M	Ordered sequence of flood events from largest to lowest flood
n	Manning's roughness, [$T/L^{1/3}$]
N	total number of flood events (samples) in the data set.
nr	Number of current meter propeller revolutions per unit time
p	Index number
Q	Discharge, [L^3/T]
Q_B	BT discharge, [L^3/T]

Q_{bf}	Bank full discharge, [L^3/T]
Q_G	GGA discharge, [L^3/T]
Q_M	Measured discharge, [L^3/T]
Q_T	T year return period discharge, [L^3/T]
r	Average number of floods per year selected for PDS
r^2	Coefficient of determination
S	Slope, [L/L]
SD	Standard deviation
T	Recurrence period, [T]
T_{PDS}	PDS recurrence interval, [T]
v	Velocity, [L/T]
v_{bf}	Bankfull mean velocity, [L/T]
w	Width [L]
w_{bf}	Bankfull width, [L]
y	Depth, [L]
z	Constant, slope exponent
$\%$	Percent
Δ	Characteristic meter constant, [L/T]
λ	Hydraulic pitch of current meter propeller
τ	Shear stress, [M/T^2L]
γ	Specific weight [M/L^2T^2]
Ω	Stream power per unit length [ML^5/L^4T^3]
δ	Change

Chapter One

1 Introduction

1.1 General Background

Natural river channels are thought to tend toward an equilibrium condition by changing their geometric and hydraulic variables in response to changes of water and sediment discharge. The adjustments of river channels take place by erosion and deposition as well as by variation in bed forms, which affects the hydraulic resistance and thus the local competence to carry sediment (Langbein and Leopold, 1966; Knighton, 1998). It is commonly assumed that an alluvial channel adjusts particularly its width, depth, velocity, slope and resistance to achieve a stable condition in which it can transport a certain amount of water and sediment discharge (Langbein and Leopold, 1966; Phillips, 1990). However, Hey (1978) argued that a natural channel possesses up to nine degrees of freedom to adjust in response to the imbalance between sediment input and output. Channel adjustments in response to water sediment discharge depend on several factors along the river channel such as channel material, bank vegetation, and sediment supply from the basin as well as basin characteristics (Church, 1992). A number of factors such as basin topography, geographic location, geology, land use, climate and other hydrologic factors could influence basin characteristics.

The observation of correlation among the hydraulic and geometric variables of regime (stable) channels dates back more than one century. The regime theory of the behavior of alluvial channels was fathered by Lindley (1919) and the complete theory was formulated by Lacey in 1930 based on observations of irrigation channels in India (Henderson, 1966; Hey, 1978; Stevens and Nordin, 1987). Several attempts have been made during the past half century to predict the hydraulic and geometric parameters of stable alluvial river channels. Hydraulic geometry is a relation between hydraulic and/or geometric variables and discharge of stable or quasi-stable river channels. The concept of hydraulic geometry was first introduced by Leopold and Maddock (1953) as empirical power equations 1.1 - 1.3. which relate the main hydraulic variables such as channel width, mean depth and

mean velocity to water and sediment discharge. The relations are similar to the empirical equations derived for regime irrigation canals (US-FISRWG, 1998) and intended to extend the regime concept to natural rivers (Knighton, 1998).

Hydraulic geometry approaches can be divided in to two broad categories: the empirical (regime) and theoretical (analytical) or semi-theoretical methods (White et al., 1982; Knighton, 1998). The most widely used and reliable approach is the empirical one, which stems directly from the observations of Leopold and Maddock (1953). The empirical (regime) approach relies on collection and analysis of field data in order to establish appropriate relations from the data (White et al., 1982; Knighton, 1998). The analytical method, on the other hand, solves for river geometry from the basic equations for flow continuity, sediment transport, and flow resistance, but requires postulation of an additional hypothesis about river behaviour in order to generate sufficient equations (White et al., 1982; Knighton, 1998). The empirical approach pioneered by Leopold and Maddock (1953) provides a basis for analysing stream response to changing discharge, both at particular cross-sections and in the downstream directions (Knigton, 1998). A primary test of any theoretical formulation would be to replicate the values of the exponents of the empirical approaches (Millar, 2004). More detailed reviews of both approaches are presented in Chapter Two of this thesis.

The empirical hydraulic geometry equations of Leopold and Maddock take the following form:

$$w = aQ^{b} \tag{1.1}$$

$$d = cQ^{f} \tag{1.2}$$

$$v = kQ^{m} \tag{1.3}$$

Where:

w, d, v and *Q* are water surface width, mean depth, mean velocity and discharge respectively. *a, b, c, f, k* and *m* are constants.

These equations must satisfy continuity:

$$Q = w \cdot d \cdot v \tag{1.4}$$

Hence, the product of coefficients and sum of exponents of equations 1.1 - .1.3 must also be unity:

$$a \cdot c \cdot k = 1 \tag{1.5}$$

$$b + f + m = 1 \tag{1.6}$$

Generally, hydraulic geometry study of natural rivers is considered from two different contexts: at-a-station and downstream hydraulic geometry (Maddock and Leopold, 1953; Leopold et al., 1964; Knighton, 1998). At-a-station hydraulic geometry relates channel geometry and flow hydraulics to the variation of discharge at a particular cross-section of a river reach. Downstream hydraulic geometry relates channel geometry and flow hydraulics to the spatial variation of discharge. It can be considered as an integration of the individual adjustment of channel dimensions and shapes of cross-sections from several reaches to accommodate some channel forming discharge (Rhodes, 1987). Downstream hydraulic geometry can be thought of as a scaling relation of channel variables with water and sediment discharge (Ellis and Church, 2005). Recently, reach based hydraulic geometry has been also introduced as a third option (Stewardson, 2005). Reach hydraulic geometry relates the reach-averaged parameters (width, mean depth and mean velocity), instead of parameters at single point (at-a-station), to changes in discharge with time. Reach hydraulic geometry is not a popular approach among hydraulic geometry researchers; the term has been rarely used, perhaps because it is very similar to at-a-station hydraulic geometry. Reviews of all kinds of hydraulic geometries are presented in more detail in Chapter Two of this thesis.

Equations 1.1 -1.3 are the most commonly used hydraulic geometry relations. However, the scope of hydraulic geometry study in the form of power equations has been expanded to include several other kinds of river channel geometry and hydraulic variables such as bed slope, meander length, suspended sediment load, dissolved load, resistances

(Manning's roughness or Darcy-Weisbach friction factor) and shear stress. Chiefly, hydraulic geometry relations are described in the form of power equations with discharge. In all kinds of hydraulic geometry approaches, discharge is assumed as a primary force and hence the single independent variable by which much of the changes in channel morphology are dictated. At-a-station and reach hydraulic geometry (a special case of at-a-station) relations are derived from the ranges of discharge from minimum to bankfull flow and the corresponding channel geometry and hydraulic variables. However, downstream or regional hydraulic geometry relations are usually derived from geometric and hydraulic variables corresponding to a morphologically significant water level in the channel, such as bankfull or active channel depth, and the channel forming discharge.
Bankfull width shows one of the strongest basin scale relationships when it is related to bankfull discharge (Annable, 1996; Ellis and Church, 2005). Channel forming discharge is most commonly represented by bankfull discharge. Bankfull discharge is the flow that completely fills the channel up to the elevation of the flood plain without overtopping the channel banks. In fact, some workers such as Leopold and Maddock (1953), Jowett (1998) and others used mean annual discharge and hydraulic variables computed from it in order to derive the downstream hydraulic geometry equations. The mean annual discharge usually fills a river channel to about one-third of its bankfull level (Leopold et al., 1964). More detailed review of different approaches used to estimate channel-forming discharge is presented in Chapter Two.

Types of bank and bed materials as well as types of sediment being transported highly influence the level and mode of adjustments that a river channel undergoes in response to variation of water and sediment discharge. River channels can be classified as alluvial, semi-alluvial and non-alluvial based on the type of their channel material and sediment load transported by the rivers. An alluvial channel has bed and banks composed of the same material as sediment transported by the flow. Alluvial streams are free to adjust their shape and dimensions, such as width, depth and slope, in response to changes in discharge and watershed sediment (US-FISRWG, 1998; Trenhaile, 2005). However, semi-alluvial channels have at least either one of their banks or a bed composed of a material resistant to erosion and slightly or fully different from sediment that the river transports for most

flow conditions of a year. The adjustment of the geometry of these channels to the changes of discharge and sediment load may not be uniform over a cross-section or reach. Semi-alluvial channels are expected to adjust slowly in comparison to that of fully alluvial ones. Non-alluvial channels have banks and bed composed of materials that are completely different from the materials that a river transports. They are highly resistant to erosion or they are not active fluvial units. Non-aluvial channels are less sensitive to disturbances than semi-alluvial or alluvial channels unless there are weak sections that allow channel migration (Horel, 2006; FPBM, 2004; US-FISRWG, 1998). Non-alluvial channel reaches are typically transport zones (Horel, 2006).

The majority of extant hydraulic geometry relations are derived for alluvial channels. Moreover, hydraulic geometry research is lacking for rivers incising into different sediment deposits of variable erodibility. This situation, in addition to the complex nature of river systems, limits the validity of the hydraulic geometry application in areas where rivers flow through a variety of complex geologic formations. Hydraulic geometry of erosion resistant cohesive (clay-silt) river channels is the focus of this research. They are treated as semi-alluvial channels.

1.2 Purpose and Scope of the Study

Hydraulic geometry (regime) theory is one of the simple but very useful approaches that civil and environmental engineers, geomorphologists, and geologists employ to describe and predict the complex nature of a river system. Hydraulic geometry represents one methodology for studying the behavior of a complex river system with more unknowns than independent equations (Knighton, 1998). The concept of hydraulic geometry is applicable from small to big rivers; specifically, there is no particular drainage area or unit discharge limit beyond which the concepts of downstream hydraulic geometry do not apply (Wohl, 2004). In fact, the entire concept of downstream hydraulic geometry relations depends upon the premise that the relations between channel geometry and discharge are scale independent.

Where the cost of obtaining actual channel data is prohibitive, Allen et al. (1994) suggested that hydraulic geometry relationships are adequate to be used in planning-level models such as for flow routing techniques, sediment routing models, or aquatic production models. Combined with other analytical techniques such as site specific hydraulic and sediment transport analysis, hydraulic geometry relations can result in a cost-effective design method, which is adapted to site-specific conditions (Burns, 1998).

The material into which the channel incises is one of the most important factors in determining fluvial morphology. Bed material composition dictates the degree and nature of adjustment of stable channel geometry in response to change of water and/or sediment discharge. The bed and bank material of the river is critical for sediment transport and hydraulic influences, and thereby modifies the channel form, plan and profile of the river (Rosgen, 1994). The cohesiveness (high percentage of silt-clay) of channel material results in narrow channel geometry, but if the alluvium lacks cohesion (has a small percentage of silt-clay) the channel will widen to a greater extent (Shumm, 1960; Osterkamp and Hedman, 1982). Hydraulic geometry relations of stable channels derived by regression analysis (empirical), available in the literature, are mostly from data collected from alluvial streams. Moreover, theoretical or semi-analytical approaches used to estimate stable channel parameters generally base their assumptions on granular alluvial channel materials.

However, there are many rivers across the Canadian fluvial system which can be classified as semi-alluvial because they are flowing over, and/or cutting into, erosion resistant glacial deposits (e.g. glaciomarine and glaciolacustrine clays, glacial tills), and/or are controlled by bedrock outcrops. Consequently, it is difficult to predict their channel morphology using hydraulic geometry relations derived for alluvial river channels. Particularly, in eastern Ontario, surface geology maps indicate that glacial origin cohesive sediment deposits such as glaciomarine and glaciolacustrine clays and silts are widespread, and hence many rivers have made their channels through them. Field observations conducted by the author and his supervisor during summer 2006 confirmed the presence of many rivers incising into glacially deposited material formations such as

fine (cohesive) glaciolacustrine and glaciomarine sediments. Understanding the dynamics of their channel morphology can be very essential for many purposes such as conducting environmental impact assessments, planning stream corridor restoration projects and assessing the suitability of riverine habitat for healthy life of aquatic animals. Unfortunately, few of these channels are equipped with flow monitoring (gauging) facilities within or close to the reaches that have channel materials of glacial fine (cohesive) glaciolacustrine and glaciomarine sediments.

Cohesive material generally consists of particles in the silt-clay range. While resistance to erosion for non-cohesive material (fully granular alluvial) depends on the physical properties of particles, to a larger extent resistance to erosion of cohesive sediment depends on the strength of electrochemical bonds between particles, adding considerably to the complexity of the erosion problem (Knighton, 1998). This fundamental difference between fully granular alluvial channel (non-cohesive) and cohesive channel demands the study of hydraulic geometry of cohesive (erosion resistant) river channels. However, as discussed above, the majority of extant hydraulic geometry research studied alluvial channels comprised of non-cohesive bed and bank material. The author is unaware of previous hydraulic geometry research for rivers incising into relatively stiff glaciomarine cohesive clay-silt deposits.

1.3 Objectives of the Study

The primary purpose of this study is to understand how the main geometric and hydraulic parameters (width, mean depth and mean velocity) of erosion resistant clay dominated cohesive bed (semi-alluvial) natural river channels are related to water and sediment discharge variation. Moreover, recurrence intervals of measured or calculated bankfull discharges of those river channels are to be determined using flood frequency analysis based on annual maximum series. This research is expected to be a valuable input to the field of river hydraulics and geomorphology that can be used in predicting channel morphology of complex fluvial systems, in particular the morphology of cohesive river channels.

The objectives of this study are the following:

1) Derive downstream hydraulic geometry (regional scaling relation) of clay dominated cohesive bed (semi-alluvial) river channels using data collected from eastern Ontario rivers as well as data gleaned from the literature for other rivers from neighboring regions with similar geographic and climatic conditions.
2) Analyze the recurrence interval of bankfull discharge for the Study Rivers based on annual maximum flow series.

1.4 Organization of the Thesis

The thesis is organized into six chapters. The first chapter (i.e., this chapter) gives the general background information about hydraulic geometry and bankfull discharge, describes the scope and purposes of the study and specifies the objectives of the research.

Chapter Two incorporates detailed review of all types of hydraulic geometries and channel forming discharges. Broad coverage of extant at-a-station, downstream and reach hydraulic geometry studies are included. Furthermore, in this Chapter theories about different methods of estimating channel forming (bankfull) discharge are covered in detail.

The methodologies used to obtain the data required for hydraulic geometry analysis are described in Chapter Three. Methods used to identify Study Rivers, data collection methods, general background review of deployed instruments, data processing methods (interpolation, projection, and digitization using ArcGIS) and in the end extraction of discharge and geometric data required for hydraulic geometry analysis are the focus of Chapter Three.

Chapter Four includes the analyses and results of the thesis which are flood frequency analysis and estimating the recurrence intervals of bankfull discharges of the study rivers, derivation of downstream hydraulic geometry equations and summarizing of results obtained in tables and diagrams.

Chapters Five and Six are discussion and conclusion respectively. The first part of Chapter Five incorporates in depth discussion about possible approaches of determining bankfull discharge, difficulties in defining bankfull levels in the field, and comparison of recurrence intervals of bankfull discharges of study rivers with recurrence intervals of bankfull discharges reported in the literature. The second part of Chapter Five includes interpretation of the derived hydraulic geometry equations, comparison of the equations with the previous suitable findings and discussion about the departure and consistency of the results of this study with previous researches. In Chapter Six the summary of the findings of this study are presented. Conclusions made based on the results of this study related to previous research are also incorporated.

Chapter Two

2 Review of Hydraulic Geometry and Dominant Discharge

2.1 Empirical Hydraulic Geometry Study

2.1.1 At-A-Station Hydraulic Geometry

At-a-station hydraulic geometry describes how channel geometry and flow hydraulics change as discharge varies at an individual cross-section over time (Leopold and Maddock, 1953; Knighton 1998; Beyer, 2006). At-a-station hydraulic geometry can be reduced to a simple consideration of "hydraulics plus geometry" at a given cross section, and offers a concise, quantitative description of channel form (Ellis and Church, 2005). The three basic at-a-station hydraulic geometry relations are described by simple empirical equations relating width, depth and velocity to a range of discharges from low up to bankfull flow at a single cross-section (Eqs. 1.1 – 1.3). The six numerical parameters (*a, b, c, f, k, and m*) are estimated by regression using measured data of geometric and hydraulic parameters at a cross-section for a range flows.

The at-a-station discharge and sediment load variation from low to high (flood) is generally the result of fluctuations in sources of water such as groundwater, storm runoff, snowmelt as well as many other factors that happen in a watershed and influence flows toward rivers or creeks. Sediment load and discharge are characteristics of hydrology, geology, and physiognomy of the drainage basin (Leopold and Maddock, 1953). Natural streams respond to variations of flow and sediment load by changing their cross-sectional shape and dimension over time mostly through either scouring and/or deposition. Moreover, for rivers in cold climate regions such as Canadian rivers the effects of ice jams and ice scouring are also expected to play a role in channel size and shape adjustment (Trenhaile, 2004). At-a-station hydraulic geometry relations imply that alluvial channels adjust their width, depth and shape in order to attain quasi-equilibrium conditions in which it is capable of transporting a certain amount of water and sediment (Singh, 2003).

At-a-station width exponents are highly variable (Table 2.1) in comparison to the downstream or regional hydraulic geometry. This might be because cross-sectional adjustments are highly controlled by variations in bed and bank materials (clay, silt, sand, gravel, pebble and cobble), vegetation (thick wood, grass or no vegetation), woody debris, bed topography, channel pattern and others (Singh, 2003; Trenhaile, 2004; Anderson et al., 2004). For instance, streams with cohesive banks (higher silt/clay) have narrow and steep channels, hence water surface width variations with discharge become negligible (Knighton, 1998) while channels with non-cohesive materials are usually wide. At-a-station hydraulic geometry exponents such as width exponent (b), largely reflect the composition of bank material in a cross-section, particularly silt/clay, which influences the cohesiveness of the material and thus the erodibility of banks (Knighton, 1974; Beyer, 2006).

Furthermore, erosional adjustments are very difficult in rivers flowing through coarse glacial deposits, which often have beds that are heavily armored or paved with stony material (Trenhalie, 2004). Anderson et al. (2004), after analyzing data from 39 different sources, also concluded that bank vegetative conditions strongly influence the width of a channel. In relatively humid climates, vegetative influences are very high and even tend to override the influences of channel materials although interactions between bank vegetation and bank material exist (Anderson et al., 2004). Apparently, grass, shrub and tree roots reinforce stream banks against erosion and can also promote deposition of sediment, and thereby make the channel narrower. However, woody debris in forest area streams can also block and divert the flow and locally destabilize stream channels, causing bank slumping, lateral channel migration, and formation of erosional or depositional features (Beebe, 2001 cited in Trenhaile, 2004). A list of at-a-station hydraulic geometry relations collected from the literature is summarized in Table 2.1.

2.1.2 Downstream Hydraulic Geometry

A river's drainage area and the number of tributaries that join the main channel increase in the downstream direction. Therefore, flows from tributaries and seepages from banks are typical causes of increase of flow in the downstream direction. This increase in discharge

is accommodated by change in channel variables such as width, depth, velocity, roughness, slope and planform. From the context of hydraulic geometry, given local bed and bank conditions, each cross-section adjusts its dimension and shape to accommodate some channel forming discharge. Downstream hydraulic geometry is a sampling of these individual adjustments, an integration of the individual at-a-station hydraulic geometries (Rhodes, 1987). The three most commonly used downstream hydraulic geometry relations are described by the power equations (1.1 – 1.3) relating the width, mean depth and mean velocity to changes of water and sediment discharge in the downstream direction. In fact, the reaches to be considered for downstream hydraulic geometry relations can be either on a single river system moving downstream or on many rivers, i.e. regional scaling, provided that the characteristic discharge has the same frequency at all reaches and all rivers are situated in similar geographic and physiographic regions (Jowett, 1998).

Dudley (2004) derived regional hydraulic geometry relations for rivers in coastal and central Maine, USA using data from 10 USGS stations and 5 IFIM sites, referenced to bankfull flow. He concluded that about 50% of increase of flow in the downstream direction is accommodated by an increase in channel width and 32% by an increase in depth. The remaining 18% is accommodated by an increase in stream flow velocity. Width usually increases in a more consistent manner than any other morphologic variable, as a square root of the discharge, and mean velocity tends to increase slightly downstream in most rivers (Leopold et al., 1964).

Frequency distribution of downstream hydraulic geometry exponents of 110 data sets (Rhodes, 1987) clearly showed that largely the exponents of width, mean depth and mean velocity were falling in the range of 0.40 to 0.60, 0.20 to 0.50, and 0 to 0.30, respectively. Park (1977) also analyzed 72 worldwide downstream hydraulic geometry data and showed the modal classes of width, depth and velocity exponents fall within the range of 0.4 to 0.5, 0.3 to 0.4, and 0.1 to 0.2, respectively. Table 2.2 summarizes downstream hydraulic geometry relation exponents for width, depth and velocity, collected from a wide range of literature.

Downstream hydraulic geometry parameters are affected by many factors such as sediment supply, downstream fining of bank sediments, plan form geometry, and bank vegetation (Singh, 2003; Trenhaile, 2004; Anderson et al., 2004; Stewardson et al., 2005). Moreover, Wohl (2004) used data sets from 10 mountain rivers in United States, Panama, Nepal and New Zealand to study the limits of downstream hydraulic geometry and concluded that for hydraulic geometry to be well developed the hydraulic deriving forces should sufficiently exceed the substrate's resisting forces. Mountain rivers commonly have more resistant channel boundaries than lower-gradient alluvial channels. Wohl (2004) showed that where the ratio of stream power to sediment size (Ω/D_{84}) exceeds 10,000 kg/s^3, downstream hydraulic geometry is well developed. In general, downstream hydraulic geometry relations are principally a function of discharge (Knighton, 1974), and the variability in the minimum drainage area at which well-developed downstream hydraulic geometry relationships exist suggests that there is no specific area or unit discharge threshold beyond which the concept of hydraulic geometry applies (Wohl, 2004).

Either mean annual or bankfull discharges were used to derive empirical downstream hydraulic geometry equations. Leopold and Maddock (1953) and Jowett (1998) used mean annual discharge and geometric and/or hydraulic variables computed from it to derive their downstream hydraulic geometry equations. In fact, the majority of workers use bankfull discharge as a characteristic discharge for downstream hydraulic geometry study. Several reasons can be listed to support the concept of bankfull discharge for being a preferable reference flow for down stream hydraulic geometry study. The following points are summarized from Leopold et al. (1964), Andrew (1980), Copeland et al. (2000), Dudley (2004) and Beyer (2006):

- ✓ It can be estimated at ungauged sites based on observable physical channel features and does not require knowledge of frequency of flow in the river.
- ✓ Most workers agree on its being a single discharge that generally best approximates the discharge which determines the dominant morphological characteristics of river channel.
- ✓ It is anticipated that bankfull discharge has similar frequency of occurrence through out a river system; it provides a unifying concept for studying a river system.

- ✓ It represents the break point between the processes of channel formation and flood plain.
- ✓ It is also a single discharge that better approximates the effective discharge – the discharge that transports maximum sediment load over time.

Moreover, it may be argued that in alluvial channels the maximum competence of the stream is normally that associated with bankfull conditions (Harvey, 1969) and, hence bankfull discharge is an index of stream flow considered to be closely related to channel morphology (Lawlor, 2004).

2.1.3 Reach Hydraulic Geometry

Reach hydraulic geometry relates the reach averaged channel parameters (width, mean depth and mean velocity) to changes in discharge. The reach based variations of width, depth and velocity would be represented by power equations (1.1 – 1.3) the same way as the classical at-a-station and downstream hydraulic geometries. The cross-sectional data (width, depth and velocity) would be collected from a reach in which the spatial variation of discharge is none or negligible. Hence, the change in discharge is due to seasonal variation of flow just like for at-a- station hydraulic geometry.

Stewardson (2005) questioned the use of at-a-station hydraulic geometry relations in catchment management. Stewardson's (2005) main argument is that at-a-station hydraulic geometry relations are constrained by its application to single cross-sections and in many cases, hydraulic conditions, including variability along the reach is more important than at a single cross-section. Hence, reach hydraulic geometry can be taken as a new approach to reduce the bias in at-a-station hydraulic geometry due to using data from a single cross-section to represent the characteristics of the whole reach. Jowett (1998) used reach-averaged parameters rather than parameters from a single cross-section in his study of hydraulic geometry of 73 reaches of New Zealand Rivers. He reported the average at-a-station hydraulic geometry of the 73 reaches and suggested the results to be used for a preliminary habitat assessment. Stewardson (2005), using data surveyed in 17 reaches, 16 of theses are on rivers in Victoria, Australia and one on Hoder River in England, obtained the reach hydraulic geometry exponents of surface width (b), mean depth (f) and mean

velocity (m) equal to 0.11, 0.28 and 0.52. These values are consistent with the results of at-a-station hydraulic geometry relations reported by other workers, such as Jowett (1998) for New Zealand Rivers and Wilcox (1971) for upper Hodder Basin (see Table 2.1).

2.2 Theoretical or Semi-theoretical Hydraulic Geometry

Most river channels display stable or relatively stable hydraulic geometry that only the basic flow relationships of continuity, resistance and sediment transport cannot by themselves explain (Knighton, 1998; Huang et al., 2002). Because of the large number of variables involved and the basic indeterminate nature, river researchers are incapable of solving directly for river hydraulic geometry (Chang, 1979). A review of studies in the field of hydraulic geometry indicates that in addition to the classical empirical (regime) method introduced by Leopold and Maddock (1953) which relies on available data and regression analysis, a multitude of theoretical and semi-theoretical approaches have been employed for deriving relations between hydraulic variables of river channels and water and sediment discharges. In general, theoretical and semi-theoretical approaches propose one or more additional theories or relations (hypotheses) that the rivers must satisfy in addition to the three classical basic hydraulic equations of mass conservation (continuity), flow resistance and sediment transport to describe the relations among dependent channel variables and independent flow variables (Knighton, 1998; White et al., 1982). The behavior of river channels involves several dependent variables including mean flow channel width (w), water depth (y), velocity (v), channel gradient (S), and the resistance factor, Manning's n, which adjust to independent channel forming agent such as water and sediment discharge (Jia, 1990). A brief review of the most common theoretical and semi-theoretical hydraulic geometry approaches, for both at-a-station and downstream contexts, is provided in the following paragraphs.

Langbein (1964) introduced the minimum variance theory. In accommodating a change such as in discharge, rivers can change components such as width, depth, velocity, and slope. These changes are assumed to be uniformly distributed among these components insofar as possible. In other words the dependent variables adjust by an equal percentage of their former values, subject to the restrictions of the situation (Williams, 1978a). As

explained by Williams (1978a), the Langbein (1964) minimization theory applies the concept on which many laws of science are established: a system tends to react to an imposed stress so as to minimize the disturbance to the system. Therefore, in order to accommodate the variation due to independent variables such as discharge, the theory suggests that the most probable state is minimum and equal variations of all components. From the perspective of hydraulic geometry relations introduced by Leopold and Maddock (1953), Langbein (1964), Knighton (1977), Williams (1978a) demonstated that the minimization theory means minimization of the sum of the squares of hydraulic exponents. For example Williams (1978a) and Knighton (1998) applied the minimization theory using independent variable discharge (Q) and adjustable dependent variables such as width (w), depth (y), velocity (v), shear stress (τ), slope (S) and friction factor (ff). From the context of hydraulic geometry relations (power relationship):

$$Q = w \cdot d \cdot v \propto Q^{1} \tag{2.1}$$

$$v \propto Q^{m};\ d \propto Q^{f};\ w \propto Q^{b} \propto Q^{1-m-f} \tag{2.2}$$

$$S \propto Q^{z} \tag{2.3}$$

$$\tau \propto d \cdot S \propto Q^{f} \cdot Q^{z} \propto Q^{f+z} \tag{2.4}$$

$$ff \propto \frac{y \cdot S}{v^{2}} \propto \frac{Q^{f} \cdot Q^{z}}{Q^{2m}} \propto Q^{f+z-2m} \tag{2.5}$$

Where: m, f, b, and z are constants.

The variance sum to be minimized, according to the minimum variance theory:

$$m^{2} + f^{2} + (1-m-f)^{2} + z^{2} + (f+z)^{2} + (f+z-2m)^{2} \rightarrow \text{minimum} \tag{2.6}$$

Assuming the constraints, b = 0.19f (suggested by Williams (1978a) for channels having movable beds and relatively firm banks) and z = 0 (slope constant for at-a–station hydraulic geometry) and setting the partial derivatives with respect to m and f equal to

zero to find the minimum, the values of b, f, and m are 0.1, 0.53 and 0.37 respectively. Langbein's (1964) theory has been admired by Williams (1978a) for it applicability to a wide range of channel types and to both at-a-station and downstream hydraulic geometry. "Langbein (1964) has presented a rationale for river channel adjustment that allows quantitative computation of important hydraulic and form parameters that, insofar as they have been adequately observed in the field data, are in good agreement with field data (Emmet and Leopold, 1964)." On the other hand the hypothesis has been also criticized for paying insufficient attention for possible effects of sediment transport (Knighton, 1974, 1998 and Williams, 1978a), for depending on the log-linear form of hydraulic geometry, which may not be always the most appropriate (Richrad, 1973 cited in Knighton, 1977) and the difficulty with the selection of adjustable variables to be included in minimum variance (Knighton, 1998). However, Williams (1978a) indicated that for at-a-station hydraulic geometry, water surface width, mean depth, mean velocity, shear stress and friction factor are the most reliable variables, which are the same as Langbein's (1964) original choice.

Smith (1974) used the conservation principle and sediment transport laws to derive the theoretical downstream hydraulic geometry of steady state channels. He represented a stream channel of finite width as a surface $z = z(x,y,t)$ in which x and y are coordinates along longitudinal and cross-sectional directions respectively, and t is time. Smith (1974) used three necessary conditions for the existence of a river channel of finite width: sediment mass is conserved during transport, the channel has form just sufficient to transport its total water discharge and the fact that channel has a form just sufficient to transport its total sediment load. Applying Manning's equation and an empirical law of sediment load (a function of only specific discharge (q) and channel slope (S)), and by taking partial derivative of z with respect to time (t) and setting to zero, Smith (1974) was able to derive the theoretical downstream hydraulic geometry relations. The theoretical values of downstream hydraulic geometry exponents of width (b), depth (f) and velocity (m) obtained were 0.6, 0.3, and 0.1 respectively.

Chang (1979a, 1979b), used a theory of minimum stream power — subject to given constraints, the channel geometry corresponding to that of minimum stream power represents the condition of stability and equilibrium. Bagnold (1960) introduced the concept of stream power to the study of sediment transport: "*when any real substance (water) impels any other real substances (sediment) to move, all experience shows that energy must be expended by first substance in maintaining the motion of the second against some kind of dynamic opposition. And power — that is, the time rate of energy expenditure — is necessary to maintain the motion at a given time rate. Thus a stream can be regarded as a transporting machine; and we have the dynamic relation: rate of work done = efficiency x available power.*" The stream power per unit channel length is given by γQS for uniform flows (Bagnold, 1960; Chang, 1979a, Knighton, 1998) in which γ is specific unit weight of fluid, S is slope and Q is discharge. Chang (1979a) developed an analytical model based on a sediment transport formula, a flow resistance relationship, and the minimum stream power assumption to compute the equilibrium geometry of sand-bed river channels. Assuming γ is constant, minimization of stream power implies minimization of QS. The procedure proposed by Chang (1979a) begins with the assumption of a width, and depth and slope are computed for a given water and sediment discharge and sediment size, using an iterative process. He showed that channel geometry corresponding to the minimum stream power represents that of the best hydraulic section for the given water and sediment rates. Then, he concluded that if one accepts the concept of minimum stream power, this geometry also represents the stable equilibrium condition. An alluvial channel attains a stable width when the rate of unit stream power (γQS) with respect to its width (w), $\gamma QS/w$ is a minimum (Cheema et al., 1997).

Yang et al. (1981) also used the theory of minimum energy dissipation to derive at-a-station hydraulic geometry relations of stable channels. Yang (1972) introduced the concept of unit stream power (velocity-slope product) to estimate total sediment concentration or discharge, which is similar to Bagnold's (1960) stream power concept and showed that the total sediment transported in a channel is dominated by effective unit stream power and vice versa. Unit stream power is defined as the time rate of potential energy expenditure per unit weight of water in alluvial channel. More accurate total

sediment load equations were derived directly or indirectly from the concept that the rate of sediment transport in an open channel flow should be related to the rate of energy dissipation of the flow (Yang and Molinas, 1982). The theory of minimum energy dissipation states that a system is in an equilibrium condition when its rate of energy dissipation is at its minimum value (Yang and Molinas, 1982 and Yang et al. 1981). Minimization of unit stream power implies minimization of velocity-slope product (vS). Applying theory of minimum rate of energy dissipation in conjunction with the Manning-Strickler equation and the dimensionless unit stream power equation for sediment transport, Yang et al. (1981) derived the theoretical hydraulic geometry exponents of width (b), depth (f) and velocity (m) equal to 9/22, 9/22 and 2/11, respectively. These values are in general agreement with observed at-a-station values from natural river gaging stations as well as laboratory studies.

Davies and Sutherland (1980) put forward the hypothesis of maximum friction factor to describe the general principle covering the deformation of alluvial boundaries. The hypothesis has been stated (Davies and Sutherland, 1980, 1983):

> *if the flow of a fluid past an originally plane boundary is able to deform the boundary to non-planar shape, it will do so in such a way that the friction factor increases. The deformation will cease when the shape of the boundary is that which gives rise to local maximum of friction factor. Thus, the equilibrium shape of the non-planar self-formed flow boundary or channel corresponds to a local maximum of friction factor. The empirical hypothesis of maximum friction factor seems preferable to the minimization hypotheses such as minimum energy dissipation rate, minimum stream power and minimum unit stream power, because it is compatible with the known behavior of turbulent flows and non-linear processes, it is applicable with a wider range of independent variables, and it is more in keeping with trends shown by experimental data under all constraints.*

They further argued that empirical success of the minimization theory hypothesis is confined to situations in which they predict similar behavior to the maximum friction factor hypothesis; they may be considered as special cases of this more general hypothesis. Davies and Sutherland (1983) criticized the maximum stream power

hypothesis, because its success is limited to the assumption of water discharge (Q) and sediment discharge (Q_s) as independent variables, under which conditions it predicts similar behavior to that predicted by maximum friction factor (MEF).

White et al. (1982) developed a method based on maximizing sediment transport to predict the hydraulic and geometrical characteristics of stable alluvial channels. Their hypothesis is based on the assumption that an alluvial channel adjusts its geometric characteristics and gradient in such a way that the sediment transporting capacity is maximized. More precisely, for a particular water discharge and slope, the width of the channel adjusts itself to maximize the sediment transport rate. They acknowledged a lack of physical justification to support the principle of maximizing the sediment transporting capacity, but were able to show that the hypothesis leads to acceptable predictions over a large range of flow conditions. The method uses the sediment transport equations of Ackers and White, the frictional relationships of White, Paris and Bettess (1980) and of course the maximum sediment transporting capacity principle. Just like other analytical methods, White et al. (1982) also used some simplifying assumptions such as flow is steady and uniform and the bed and bank materials are non-cohesive. Moreover, they also showed the principle of maximizing the sediment transport rate is equivalent to the concept of minimum stream power. Furthermore, the hypothesis of maximum friction factor (Davies and Sutherland, 1980, 1983) supports the hypothesis of maximum sediment transport. "For given water input and unlimited sediment supply the channel will adjust its boundaries to carry the largest possible amount of sediment. This would occur if the channel adopted a shape offering the maximum hydraulic resistance to flow so that the forces exerted on the boundary by the flow will be a maximum, which is a condition for maximization of sediment movement (Davies and Sutherland, 1980)".

Jia (1990) introduced a minimum Froude number theory for stable alluvial sand rivers. He stated that as alluvial channels approach stable conditions, the Froude number of the flow will tend to attain a minimum value which reflects bed material motion and maximum channel stability, under the constraints imposed by water discharge, sediment load and particle size. He used computer simulation and found a minimum Froude number (Fr_{min})

can be used to identify a unique stable equilibrium state. The simulation was based on the following main assumptions: the channel of the sand-bed river is alluvial; the adjustment of slope and cross-sectional form should satisfy the water and sediment transport equilibrium conditions; the adjustment should be associated with flow resistance of bed forms and sediment particles. He used natural sand-bed river and stable canal data to test his hypothesis; the result was in good agreement with the data. His Eqs. (2.7) and (2.8) may apply to designing stable sand alluvial channels or judging their stability. Jia (1990) suggested that Eqs. (2.7) and (2.8) are suitable only for sand bed rivers; if the size of the bed material exceeds 2 mm or the channel banks are particularly resistant to erosion, the equation may not be applicable.

$$F_{r_{min}} = 4.49 \cdot D_{50}^{-0.186} \cdot (v \cdot S)^{0.377} \tag{2.7}$$

$$y = 0.00507 \cdot D_{50}^{0.371} \cdot S^{-0.755} \cdot v^{1.25} \tag{2.8}$$

Where:

Fr_{min} is minimum Froude number and D_{50} is median sediment size (mm)

S is slope (m/m), v is velocity (m/sec) and y is depth (m).

Huang and Nanson (2000) showed that by introducing channel form factor (width/depth ratio) as a dependent variable, the self adjusting mechanism of alluvial channels can be illustrated directly with the basic flow relations of continuity, resistance and sediment transport without incorporating an extremal hypothesis in to the analysis. In their analysis, in addition to continuity, they used Lacey's flow resistance relation, and DuBoys' sediment transport formula. Their analysis was based on simplifying assumptions such as the alluvial channel flow is both steady and uniform, follows a straight path, and takes the simple form of rectangular cross-sections. Huang and Nanson (2000) and Huang et al. (2002) argued that channel flow is found to be capable of reaching a state of MFE (Maximum Flow Efficiency, defined as the maximum sediment transporting capacity per unit available stream power), at which a stable channel section is constructed with the same geometry as those widely observed in nature. Therefore, the concept of MFE embraces both maximum sediment transporting capacity (MSTC) and minimum stream power (MSP). Results from an analysis based on any of MFE, MSTC and MSP would be

highly consistent both with each other and with observations from natural fluvial systems (Huang et al., 2002). However, Dosselman (2004) challenged their conclusion of alluvial channel adjustment to MFE by introducing the alternative principle TPI (Twenty Percent Inefficiency: rivers adjust their hydraulic geometry in such a way that the resulting width-to-depth ratio (width/depth) is always 20% larger than the width-to-depth ratio of maximum sediment transport).

2.3 Channel Forming (Dominant) Discharge

2.3.1 General

Studies indicate that discharge is a primary controlling variable for changing the morphological variables (width, depth, velocity, slope, roughness, plan, competence etc) of natural stream channels. However, still there is luck of generalized consensus in determining a single discharge or clearly defined ranges of discharge by which the dynamics of channel morphology would be explained. There are several definitions and quantitative analytical approaches for estimating a representative range of discharges or a single channel-forming discharge.

The use of single dominant discharge (channel-forming discharge) is the foundation of "regime" and "hydraulic geometry" theories for determining morphological characteristics of alluvial channels (Copeland et al., 2000). Channel-forming or dominant discharge is a theoretical discharge that if constantly maintained in an alluvial stream over a long period of time, would produce the same channel geometry that is produced by the long term natural hydrograph (Pickup and Warner, 1976; US-FISRWG, 1998; Copeland et al., 2000). The concept of dominant (channel-forming) discharge simplifies modeling strategies since it replaces the frequency distribution of flow by a single discharge (Knighton, 1998).

As it is logical to assume that on average alluvial channels are adjusted to the flow which fills the available cross-section, bankfull discharge has been used to represent dominant (channel-forming) discharge, thus giving it additional morphological significance

(Knighton, 1998). Hypothetically, bankfull discharge represents the discharge that performs the geomorphic work and shapes the stream channel (Copeland et al., 2000; Beyer, 2006). Hence, it is considered to be the channel-forming agent that maintains channel dimension and transports the bulk of sediment over time (Harman, 1999). The largest clasts, as well as the largest volume of the annual bedload, are carried at discharges near the bankfull stage (Leopold, 1992). Bankfull flow is the flow that completely fills the channel up to the elevation of the flood plain, without overtopping the channel banks (Williams, 1978b; Copeland et al., 2000; Dudley, 2004). The most widely accepted definition of bankfull level is the elevation of the active flood plain (Harvey, 1969; Pickup and Warner, 1976; US-FISRWG, 1998; Copeland et al., 2005). Another popular definition of bankfull level is the level at which the width/depth ratio is a minimum (Wolman, 1955; Harvey, 1969). Williams (1978b) presented summary of 11 different ways of defining bankfull level.

Bankfull discharge is considered to have morphological significance because it represents the break point between the process of channel formation and floodplain formation (Copeland et al., 2005). Bankfull discharge (magnitude and frequency) has been largely adopted as one of the most important concepts in the analysis of river morphology, flood events, and ecological systems (Navratil et al., 2006). The three commonly prescribed methods used by several workers to estimate a single channel-forming (dominant) discharge include: field survey data, a specified recurrence interval discharge, and the effective discharge. The selection of the appropriate method for determining channel forming discharge is dependent on data availability, physical characteristics of the site, time and funding constraints, the importance of the study or project for which the discharge is required, and the expertise and availability of skilled workers. If possible, it is recommended that all three methods be used and crosschecked against one another to reduce the uncertainty in the final result (Copeland et al., 2000). Hereafter, the term channel-forming (dominant) discharge is replaced by bankfull discharge.

2.3.2 Estimation of Bankfull Discharge from Field Survey Data

Field determination of bankfull stage and the subsequent computation of bankfull discharge is a challenging task for Geomorphologists and Engineers. Defining bankfull stage of a river cross-section is subjective and in general its reliability is dependent on personal judgments of the individual and/or group who conduct the field assessment. Bankfull level indicators are not always obvious and can be significantly different from one river to the other or from one reach to the other reach on the same river. They can even vary from section to section with in the same reach or left bank to right bank. Therefore, specifying the definition of bankfull stage which best suites for specific river cross-section is dependent on the obviousness of the bankfull indicators at each site, the researchers' experience and the level of careful onsite investigation.

Williams (1978B) listed eleven possible ways of defining bankfull level proposed and used by various researchers:

1) the height of the valley flat, 2) the elevation of the active flood plain, 3) the elevation of the low bench, 4) the elevation of the 'middle bench' for rivers having three or four overflow surfaces, 5) the elevation of the most prominent bench, 6) the average elevation of the highest surfaces of the channel bars, 7) the height of the lower limit of perennial vegetation, usually trees, 8) the elevation of the upper limit of sand-sized, particles in the boundary sediment, 9) the elevation at which width to depth ratio (W/D) of the cross-section becomes a minimum, 10) the stage corresponding to the first maximum of the bench index as defined by Riley (1972) and 11) the stage corresponding to a change in the relation of cross-sectional area (A) to top width.

Williams (1978B) further commented that the above listed eleven methods of defining bankfull level can lead to eleven different bankfull discharges at the same river cross-section.

The elevation of active flood plain (top of flood plain) is the most commonly used and reliable definition of bankfull level for perennial or intermittent streams of humid regions. Top of active flood plain can be considered as the most morphologically significant stage

because it is the transition point from the main river channel to its floodplain. Therefore, geomorphologists reasonably assume active flood plain level as the most meaningful bankfull stage (Williams, 1978B; Pyrce, 2003). Other indicators could also be useful for comparison purposes, though they usually results in confusion by suggesting at significantly different level from an elevation of the top of either bank (Copeland et al., 2000). The following are some of the many factors that complicate defining bankfull stage:

- ✓ Absence of obvious bankfull indicators at a section or within a reach
- ✓ Confusions due to the presence of more than one bankfull indicators with in a reach or at a section but not referring to the same level or none of them referring to top of active flood plain
- ✓ Confusions resulted from significant variation of bankfull level with in the same reach or even at left and right bank of a single section based on similar bankfull indicators
- ✓ Presence of benches or terraces, which are usually the result of incision, also causes confusion with the reliable bankfull level indicator (top of active flood plain). Where three benches appear below the apparent flood plain, the top of uppermost "high" bench is equivalent to be the bankfull level (Woodyer, 1968).
- ✓ Any other indicator which suggests that the bankfull level is not close to the top of either bank. This condition suggests that the channel may not be in equilibrium, hence existing channel geometry may not be stable, and the channel-forming discharge would be poorly approximated by the bankfull discharge

After selecting suitable reach and defining bankful level estimation of bankfull discharge using field survey data involves collection of morphologic data such as bankfull width, left and right bank bankfull levels, thalweg elevations and associated distances along the river course, and water surface elevations at the time of survey. The best-fit line through the bankfull stage profile that would closely be parallel to the water surface profiles, can be constructed from field survey data, thereby bankfull channel parameters can be derived (Copeland et al., 2000; Lawlor, 2004). In many natural rivers, the water surface becomes nearly uniform at two-third of bankfull to nearly bankfull stage, i.e. the slope of water surface becomes equal throughout the reach (Leopold et al., 1964). Ideally, bankfull

discharge is determined using the longitudinal profiles of the bankfull levels derived from the survey data together with the stage-discharge relation at a gauge station within or close to the reach. However, nowadays, using modern river discharge measuring instruments such as an Acoustic Doppler Current Profiler (ADCP) it is possible to make more accurate measurements of discharge and depth during high flow conditions, that is, when flow is at or close to bankfull level. When an ADCP is deployed with a Real Time Kinematic Differential Global Positioning System (RTK-DGPS), it can be used to generate river cross-sectional profiles with reasonable accuracy. Please refer to Chapter Three for more details on utilization of an ADCP / RTK-DGPS system.

In the absence of the gauging data at the study site, a stage-discharge rating curve is usually estimated from backwater analysis (Copeland et al., 2000). Computer programs for calculation of water surface profile such as HEC-RAS are based on the standard step method (Lawlor, 2004). These programs can be used to calculate water surface profiles for a range of discharges including bankfull discharge so that the stage discharge curve can be generated. The HEC-RAS model uses the cross-sectional profiles, longitudinally profiles, Manning's roughness coefficients, and boundary conditions to calculate the water surface elevation at each cross-section for a selected discharge within the reach. A boundary condition (the starting downstream water surface elevation) is recommended to be set at the bankfull stage elevation, ideally based on data from a gauging station (Copeland et al., 2000, Lawlor, 2004). The discharge is varied until the simulated water surface elevations at the remaining cross-sections in the reach closely match the surveyed bankfull elevation. Therefore, the discharge corresponding to the water surface elevation equal to the bankfull stage elevation at each cross-section is taken to be the bankfull discharge. However, unless it is calibrated, it is unlikely that roughness parameters are accurately estimated only from the field data. Hence, the accuracy of estimating bankfull discharge by only depending on the model output is questionable. If discharge is measured using an Acoustic Doppler Current Profiler (ADCP) during a high flow condition at a reach close to the gage station, bankfull discharge can be estimated from the measured discharge and rating data more accurately than using the numerical modeling software (please refer to Chapter Four).

2.3.3 Bankfull Discharge as a Specified Recurrence Interval Flow

Whenever possible, direct measurement of bankfull discharge or estimating from field survey data is preferable. However, sometimes because of financial and time constraints and other unexpected reasons, measurement and/or field survey data based estimation of bankfull discharge may not be feasible. Moreover, there would be circumstances where field identification of bankfull level indicators becomes very difficult. Therefore, relating bankfull discharge to a certain recurrence interval flow is a common practice. Observations of the recurrence interval for bankfull flow are reviewed in this section. Most studies indicate that the recurrence interval of bankfull discharge based on annual maximum flow series falls with in the range of 1 to 2 years, with an average of 1.5 years. Note that the mean annual flood corresponds approximately to the 2 year return interval (2 years if the annual maximum series is normally distributed, or 2.33 years if it is Gumbel distributed) (Bedient and Huber 1992).

The peak discharge magnitude and the associated frequency (or exceedance probability) are most commonly inferred from annual flood series using a statistical approach — annual flood-frequency analysis. The annual flood series is based on the maximum flood for every year, usually called annual maximum series (AMS). Flood events can also be analyzed using partial duration series (PDS), in which more than one flood event per year is considered in the analysis. The flood frequency analysis approach based on annual maximum series (AMS) is not applicable to flood events with a recurrence interval of less than one year. Therefore, frequency analysis based on partial duration series is of interest when flow rates that are more frequent than once per year are required. Knowledge about the more frequent floods is needed in many types of problems, such as environmental studies for the protection and restoration of stream channels, aquatic habitats, and floodplains; non-point source pollution analyses, channel erosion analyses, fishery management etc (Soong et al., 2004, McCuen, 1998). Please refer Chapter Four for frequency analysis based annual maximum series (AMS) and Appendix A for short review of frequency analysis approach based on partial duration series (PDS).

From observations made on 19 rivers in US, the recurrence interval of a particular discharge considered in the field to represent a bankfull discharge varied from 1.07 to 4 years; but 15 of the 19 fell in the range 1.07 to 1.9 years (Leopold et al., 1964). The recurrence interval of bankfull discharge for Yampa River basin falls between 1.18 and 1.40 years (Andrew, 1980). For the gauged North Carolina Piedmont streams it ranged from 1.1 to 1.8, with a mean of 1.4 years (Harman, 1999). The bankfull discharge recurrence intervals for 16 streams in central New York, 14 streams in southern Tier New York, and 10 streams in western New York (region 7 adjacent to Eastern Ontario) ranged from 1.11 to 3.40, 1.01 to 2.35 and 1.05 to 3.60 years, respectively (Westergard et al, 2004; Muluihill et al., 2005, 2006). The corresponding average recurrence intervals of bankfull discharges of those regions were 1.51, 1.54 and 2.13 years respectively. Miller and Davis (2003) reported the average bankfull discharge recurrence intervals ranged from 1.2 to 2.7 years for three other hydrologic regions of New York State. For five snowmelt-dominated rivers in the northern Rocky Mountains, USA bankfull discharge recurrence interval ranged from 1.5 to 1.7, and the average was 1.6 years (Emmet and Wolman, 2001). Swift and Ledford (1993) reported that there was good agreement between flow estimated from bank survey for channel-maintaining flow level (bankfull) and a 1.5 years recurrence interval discharge estimated from frequency analyses for Southern Appalachian streams. They further suggested, where the flow rates were different, misreading of the bankfull survey criteria seemed to be at fault. Petit and Paquet (1997) conducted a study on 30 gravel bed rivers in Belgium. They reported that the recurrence interval of bankfull discharge (based on annual maximum series) for rivers with a hydrologic basin area of less than 250 km^2 was of the order of 1 year and of larger rivers was the order of 1.5 – 2 years.

Significant deviation of bankfull discharge recurrence interval from the classical 1 to 2 years has been also reported by many workers. Williams (1978b) reported a wide range of recurrence intervals (1.01 to 32 years) based on annual maximum series for the bankfull discharge of 36 active floodplain stations. Although the statistical average (mode) of recurrence interval is about 1.5 years, only about one third of the bankfull discharges of the stations that Williams (1978b) investigated had recurrence intervals near 1.5 years.

Pickup and Warner (1976) reported that the recurrence intervals of bankfull discharges of four Cuberland Basin streams, Australia lie within the range of 4 to 10 years based on the maximum annual series.

For non-equilibrium streams in urban and rural environments whose bankfull discharge recurs more than once in a year, it is not possible to estimate bankfull discharge based on annual maximum flood series. Therefore, in such causes, it is more appropriate to use a partial duration series approach rather than annual maximum series (Woodyer, 1968; Navratil et al., 2006). The recurrence interval of a flood calculated by annual series is the return period (in years) of the annual flood in excess of the stated value, whereas that calculated from the partial series is the return period of any discharge equal to or in excess of the given value (Harvey, 1969). Although for rare discharges the results produced by both annual maximum series and partial durations series methods may be comparable, for more frequent events they are distinctly different (Hervey, 1969). Navratil et al. (2006) estimated the magnitude and frequency of bankfull discharge of 16 gravel-bed reaches of three river basins in France by applying different methods. They confirmed that annual maximum series analysis is mathematically incapable of providing appropriate solutions, as top of bank discharge occurs several times per year in most of their surveyed reaches. Hence, for such rivers only partial duration series can be used to determine bankfull discharge recurrence interval.

2.3.4 Estimation of Bankfull Discharge as Effective Discharge

Wolman and Miller (1960) described effective discharge as the discharge that transports more sediment than any other discharge. They concluded that effective discharge is a relatively frequent event of moderate intensity and approximately corresponds to the bankfull discharge. The effective discharge represents the single flow increment that is responsible for transporting the most sediment over some time period (Andrews, 1980). Leopold (1992) and Goodwin (2004) also described effective discharge as the discharge that transports maximum sediment load over time. Although most studies indicated that the effective discharge is better represented by a range of discharges than a single discharge, it is usually represented by a single effective discharge approximately equal to

bankfull discharge. For stable alluvial streams, effective discharge has been shown to be highly correlated to bankfull discharge (US-FISRWG, 1998).

Figure 2.1 depicts the concept applied by Wolman and Miller (1960) and Andrews (1980): effective discharge is a function of both magnitude and frequency of occurrence of the flow events. Andrew's (1980) explained Fig. 2.1 as follows:

> *The frequency with which a given discharge occurs is represented by curve B, the distribution of stream flows. The most frequent discharges are moderate and transport relatively small amounts of sediment. Conversely, the largest discharges are rare, but transport very large amounts of sediment. The relative effectiveness (curve III) of a given discharge is the product of the sediment transport rate and the frequency of occurrence. As shown, it is a range of intermediate discharges that transports the largest part of the average annual sediment load. This range of discharge may be represented by the modal sediment-transporting discharge, which will be called the effective discharge.*
>
> Furthermore, according to Pickup and Warner (1976), the most effective discharge can be determined by: dividing the flow into small classes, finding the duration of flow within each class, calculating the mean bed-load discharge within the class and multiplying it by duration a histogram showing the bed-load transport regime, i.e. the amount of load transported by each class, may then be constructed. The most effective discharge is taken as the mid-point of the class which transports the most bed load.

Andrews (1980) estimated the effective discharge using data from 15 gauging stations in Yampa River Basin, Colorado. For all gauging stations, the bankfull discharge and effective discharge were nearly equal. Leopold (1994) also analyzed bedload transport and flow data of 12 gravel bed rivers in the mountains of Colorado and Wyoming, and reported the maximum bed load was carried in the discharge category of 0.76 – 1.2 times bankfull discharge. Emmet and Wolman (2001) conducted similar analysis on five snow-melt dominated gravel bed rivers in the northern Rocky Mountains, USA and reported the ratio of effective discharge to bankfull discharge ranged from 0.98 to 1.31.

On the other hand, several researchers have reported that effective discharge is far less than bankfull discharge determined from the bankfull indicators of channel features. The natural bankfull discharge is at least ten times the size of the most effective discharge in every case of four streams from Cumber Basin, Australia (Pickup and Warner, 1976). (Pickup and Warner, 1976) argued that the idea of single channel-forming or dominant discharge should be replaced by two groups of dominant discharges; those which shape the bed (effective discharge) and those which shape the banks (larger flows). (Crowder and Knapp, 2005) found for streams throughout Illinois that the effective discharge was less than the 1.1 year recurrence interval flow. In 23 headwater gravel-bed streams in snowmelt-dominated parts of central and northern Idaho the bed-load effective discharge had an average recurrence interval of 1.4 years and the magnitude of effective discharge averaged 80% of bankfull discharge (2.0 years average recurrence interval) (Whiting et al., 1999). The most effective discharge is found to have a return period of 1.15-1.40 years on the annual series but is much smaller than the 1.58-year flood (Pickup and Warner, 1976). Copeland et al. (2005) also showed that in most cases effective discharge is significantly lower than bankfull discharge; it provides an adequate lower bound for the range of bankfull discharges.

Of the various discharges related to the channel morphology (i.e., dominant, bankfull and effective discharges), effective discharge is the only one that can be computed directly and its value is not subject to the problems associated with determining field indicators (Copeland et al., 2005; US-FISRWG, 1998). Flow duration data and sediment load data are two basic components required for the calculation of effective discharge over a period of record at different discharges (Fig. 2.1). It is recommended that total bed material load (the near-bed material load (i.e., bedload) and suspended bed material load) data be used for the calculation of the effective discharge, as channel maintenance is mostly concerned with bed material (Knighton, 1998; Andrews, 1980; US-FISRWG, 1998; Emmet and Wolman, 2001). Using only suspended sediment generates lower effective discharge values (Crowder and Knapp, 2005). Usually, because bed load data are not sufficiently available, they are estimated using a bed load rate transport empirical formula (Andrews,

1980; Leopold 1994, Pickup and Warner, 1976). Wash load needs to be subtracted from the suspended load data portion (US-FISRWG, 1998; Goodwin, 2004).

The estimate of effective discharge can be influenced by the width to depth ratio of the channel (Petit and Paquet, 1997; Goodwin, 2004) and the composition of the bed surface material (Emmet and Wolman, 2001; Goodwin, 2004). The larger the particles of the bed surface material, the greater the critical shear stress required for particle motion, and larger flows are required to transport sediment. Thus, sediment begins to move later in the flood hydrograph. In other words, large particles on the streambed amour the channel bottom and results in larger values of incipient-motion discharge (Emmet and Wolman, 2001; Goodwin, 2004).

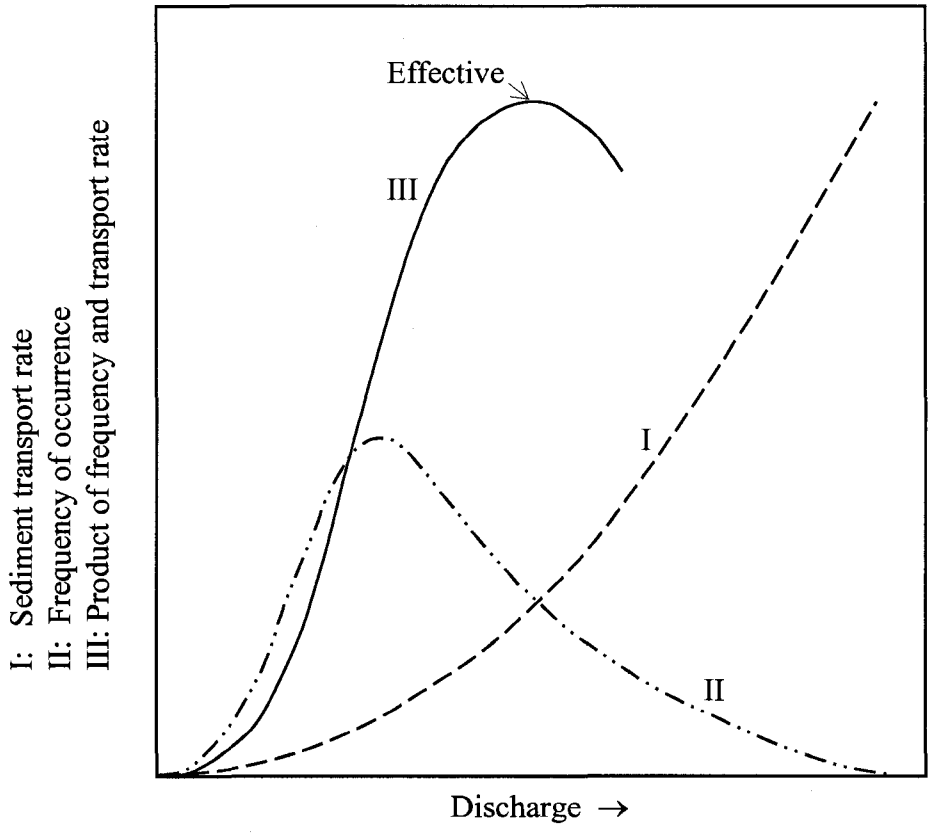

Figure 2.1 Relations between discharge and sediment-transport rate, frequency of occurrence and the product of frequency and transport rate (after Wolman and Miller, 1960).

2.3.5 Estimation of Bankfull Discharge from Regional Curves

When time and resources do not permit field determination of bankfull discharge or there are no reliable and sufficient data to use one of the other methods, empirical regional curves of bankfull discharge versus drainage area can be used to estimate bankfull discharge (US-FISRWG, 1998; Copeland et al., 2000). The regional curves are most accurate if they are derived on the basis of uniform hydrologic, climatic, and physiographic conditions and applied within that region (Mulvihill et al., 2006). However, drainage area is only one of the many parameters affecting runoff; hence extreme care must be taken while applying an empirical regional curve for evaluating bankfull discharge (Copeland et al., 2000).

Annable (1996) conducted a composite analyses of the data from 47 rural streams in southern Ontario and obtained a regional curve of bankfull discharge versus drainage area; $Q_{bf} = 0.52 \cdot A^{0.75}$. Mulvihill et al. (2006) reported, $Q_{bf} = 0.507 \cdot A^{0.765}$ for western New York of hydrologic region 7 (a region adjacent to eastern Ontario). The coefficient of determination (r^2) of the equation was 0.94, indicating that much of the range in the variables was explained by drainage area. The state wide regional curve for Vermont was $Q_{bf} = 0.175 \cdot A^{1.07}$. Using 14 natural streams from eastern Ontario Ebisa-Fola (2006) also derived a relationship between a 1.5 years recurrence interval discharge based on annual maximum series and drainage area: $Q_{1.5} = 0.26 \cdot A^{0.9}$; coefficient of determination (r^2) equal to 0.97. Q_{bf} is bankfull discharge in m^3/s, $Q_{1.5}$ is 1.5 years recurrence interval discharge in m^3/s and A is drainage area in km^2.

2.3.6 Some Limitations of Channel-Forming Discharge Concept

Although the channel-forming (bankfull) discharge concept plays an important role in the study of river morphology, flood events and ecological systems (Navratil et al., 2006), it has several limitations, as summarized below:

- ✓ It is assumed to be applicable only to stable alluvial streams (Copeland et al., 2000).

- ✓ It is not generally applicable for arid streams, because runoff is generated by localized high-intensity storms and absence of vegetation ensures that the channel will adjust to each major flood event (US-FISRWG, 1998).
- ✓ Using channel-forming discharge is not a universally accepted technique to design channel geometry (US-FISRWG, 1998).
- ✓ Bankfull discharge is not necessarily of constant frequency or the most effective flow; it is only a surrogate for the range of flows (Emmett, 2004; Knighton 1998). Natural alluvial rivers experience a wide range of discharges and may adjust their geometry to flow events of different magnitudes (including bankfull flow) by mobilizing either bank or bed sediments (US-FISRWG, 1998; Knighton, 1998).
- ✓ Field determination of bankfull channel variables is usually difficult, especially where several morphological levels exist. There is also no consistent method for specifying the bankfull stage (Knighton, 1998), and estimation of bankfull flow condition in the field is a difficult and subjective measurement (Heil and Johnson, 1995). Williams (1978b) summarized 11 different ways of defining bankfull elevation and showed that they could give as many as 11 different bankfull-levels at the same stream cross-section. In practice, not all stream reaches show consistent or reliable field indicators of bankfull stages and conflicting indicators often encountered (Williams, 1978B; Miller and Davis, 2003).
- ✓ Bankfull discharge may not be the most effective flow as regards to sediment transport (Knighton, 1998). For instance, for rivers with very resistant channel boundary, high-magnitude and low-frequency floods may control channel form or vice versa.

Table 2.1 Summary of at-a-station hydraulic geometry relations collected from the literature

Source[ς]	Exponents*			# of data	River / Location	Note
	b	f	m			
Leopold & Maddock (1953)	0.26	0.40	0.34	20	Mid-Western, US	
Wolman (1955)	0.04	0.41	0.55	7	Brandywine Creek, Pennsylvania	
Leopold & Miller (1956)	0.21	0.41	0.33	10	Ephemeral stream in the semi arid US	
Leopold & Langbein (1962)	0.23	0.42	0.36			
Leopold et al. (1964)	0.12	0.45	0.43	158	Stream gauges sites, US	
Langebein (1964)	0.23	0.42	0.35			Stable river section
Scott (1966)	0.35	0.42	0.55			Ephemeral streams
	0.24	0.56	0.20			Perennial
Leopold and Skipitzke (1967)	0.16	0.30	0.52		Middlefork Salmon River, Idaho, US	DA: 138 mi^2.
	0.06	0.43	0.53		Bear Valley Creek	DA: 180 mi^2.
	0.04	0.36	0.61		Middlefork Salmon River	DA: 2020 mi^2.
	0.08	0.41	0.52		Big Creek, Idaho US	DA: 470 mi^2.
	0.27	0.20	0.53		Salmon River	DA: 2020 mi^2.
	0.10	0.40	0.49		Salmon River	DA: 3670 mi^2.
Lewis (1969)	0.17	0.33	0.49	10	Rio Manati, Puetro Rico	
Cotes (1969)	0.36	0.20	0.44	18	Streams in the Appalachian Plateau	DA: 13 – 61 mi^2.
Cotes (1969)	0.36	0.20	0.44	18	Streams in the Appalachian Plateau	DA: 13 – 61 mi^2

Table 2.1 Continued.

Wilcock (1971)	0.09	0.36	0.53	9	Upper river Hodder basin, UK	Coarse bed, cohesive banks
Heede (1972)	0.05	0.43	0.52		Fool Creek, Central Rocky Mountains, US	
	--	0.36	0.34		Ephemeral streams in semi-arid, US	
Ponton (1972)	0.21	0.32	0.50		Coast mountain streams, BC, CA	
Knighton (1972)	0.29	0.40	0.31		River Dean at Addington Hall	Braided reach
	0.11	0.56	0.33			Right distributory, braided reach
	0.23	0.27	0.50			Left distributory, braided reach
Richards (1973)	--	0.64	0.30		Rocestor	
	--	0.44	0.47		Serlby park	
	--	0.37	0.57		Yaxall	
	--	0.576	0.32		Draycott	
	--	0.34	0.60		Beedly	
Knighton (1975a)	0.12	0.40	0.48	12	River Bollin-Dean, England	Coarse bed, Cohesive Banks
Harvey (1975)	0.12	0.42	0.43	8	River Ter	Cohesive banks
Hickin and Nanson (1975)	0.34	0.33	0.33		Beaton River, BC, CA	
Li et al. (1976)	0.24	0.46	0.30		Threshold theory of sediment transport	Theoretical
Dury (1976)	0.54	0.34	--			

Table 2.1 Continued.

Riley (1978)	0.42	0.41	0.16		Gwydir River	
	0.35	0.48	0.17		Namoi River	
	0.35	0.52	0.13		Barwon river	
	0.38	0.46	0.16		Three rivers	
Williams (1978)	0.1	0.53	0.37		Minimum variance	b =0.19f; theoretical
Beston (1979)	0.245	--	--		Watersheds in Kentucky	
Church (1980)	0.22	0.31	0.48		Baffin Island Sandurs	
Lane and Foster (1980)	0.37	0.37	0.25			
	0.32	0.32	0.36			
Yang et al. (1981).	0.41	0.41	0.18		Min. rate of energy dissipation	theoretical
Abrhams (1984)	0.42	-0.06	0.632		West channels	8 observations
	-0.67	0.86	0.75		East channels	8 observations
Philips and Harlan (1984)	0.367	0.049	0.58		Blanca Meadow	20 observations
Rhoads (1991)	0.50	0.34	--	252	Missouri River basin	
Mackey and others (1998)	0.18	0.30	0.55	24	Massachusetts, USA	Mean of 24 Rivers
Jowett (1998)	0.18	0.30	0.43	73	New Zealand rivers	Reach Averaged values

Table 2.1 Continued.

W. Dudley (2004)	0.19	0.33	0.48	10	Rivers in costal and central Maine, USA	Mean value of 10 stations
J. Beyer (2005)	0.29	0.41	0.29	14	Verde River System	South Western USA
R. Ellis and Church (2005)	0.123	0.425		10	Lower Fraser River, BC, Canada	ADCP Data

$^{\varsigma}$: Sources are the original papers but data are not necessarily taken form the original paper.

*: see Eqs. 1.1 - 1.3

Table 2.2 Summary of downstream hydraulic geometry relations collected from the literature

Source[ς]	Exponents[⊕]				River / Location	Note
	b	f	m	# of sites		
Lacey (1929)	0.50				Canals-Punjab	
Leopold and Maddock (1953)	0.50	0.40	0.10		USA	
Wolman (1955)	0.34	0.45	0.32		Ephemeral streams, USA	Q (50% chance of occurrence)
	0.38	0.42	0.32		-do-	Q (15% chance of occurrence)
	0.45	0.43	0.17		-do-	Q (2% chance of occurrence)
	0.42	0.45	0.05		-do-	Bankfull discharge
	0.57	0.40	0.03		Principal station at Brandywine creek and headwaters, USA	Q (50% chance of occurrence)
	0.58	0.40	0.02		-do-	Q (2% chance of occurrence)
Leopold and Miller (1956)	0.29	0.15	0.58		Sedalia gully near Sedalia, Colorado, USA	
	0.31	0.20	0.49		Sowbelly Creek near Hat Creek, NB, USA	
Nixon (1959)	0.49				Britain	
Miller (1958)	0.38	0.25	0.39		High mountain streams	

Table 2.2 continued.

Brush (1961)	0.55	0.36	0.09	119	Appalachian streams, central Pennsylvania USA	16 streams
Simons and Albertson (1963)	0.50	0.36	0.14		Indian and US canals	Sandy banks;
	0.50	0.36	0.14		Indian and US canals	Cohesive banks, small load
	0.50	0.36	0.14		Indian and US canals	Cohesive banks, large load
Ackers (1964)	0.42	0.43	0.15			
	0.43	0.43	0.14			
	0.53	0.35	0.12			
Langbein (1964)	0.53	0.37	0.10		Minimum variance	Theoretical
	0.50	0.40	0.1		River	Derived from data
Emmett and Leopold (1964)	0.50	0.37	0.125		Minimum variance	Graphical
Scott (1966)	0.69	0.12	0.19		Perennial rivers	
	0.03	0.48	0.43		Ephemeral streams	
Kellerhals (1966)	0.50	0.20	--			Regime theory
Kellerhals (1967)	0.50	0.40	0.10		Western Canada	Q of three years return period
Ackers (1964)	0.42	0.43	0.15			
	0.43	0.43	0.14			
Leopold and Skiptze (1967)	0.50	0.36	0.14	7	Middle Fork Salmon, Idaho USA	

Table 2.2 continued.

Leopold and Skiptze (1967)	0.50	0.36	0.14	7	Middle Fork Salmon, Idaho USA	
Blench (1969)	0.50	0.33	--			Regime theory
Carlston (1969)	0.46	0.38	0.16	10		
	0.50	0.32	0.18		Yellow river	
Thornes (1970)	0.40	0.34	0.25		Suia-Missuand Araguaia basins, Mato Gross, Brazil	Minimization of error sum of squares
	0.47	0.41	0.04		-do-	Q > 1.94 cfs
	0.11	0.32	0.59		-do-	Q < 1.94 cfs
	0.19	0.32	0.56		-do-	Maximization of explained variance Q > 5.02 cfs
	0.51	0.50	0.01		-do-	Q > 1.94 cfs
	0.14	0.36	0.54			Smaller streams
Ponton (1972)	0.60	0.40	-0.01		Green river	
	0.80	0.44	-0.23		Birkenhead river	
Knighton (1974)	0.61	0.31	0.08		Bollin-Dean River, England	Cohesive banks or Till
Smith (1974)	0.60	0.30	0.10		Conservation-sediment transport	Theoretical
	0.54	0.23	0.23			
	0.46	0.16	0.38			

Table 2.2 continued.

Rundquist (1975)	0.52	0.32	0.16			Gravel and sand bed Rivers and canals
Emett (1975)	0.56	0.34	0.12	39	Salmon River, Indaho, USA	
Li et al. (1976)	0.46	0.46	0.08			Threshold theory
Park (1977)	0.40-0.50	0.30-0.40	0.10-0.20	72	Worldwide	72 different sites
Charlton et al. (1978)	0.45	0.40	0.15			
Parker (1979)	0.50	0.415	0.085		Momentum diffusion	Theoretical
Mahmood, et al. (1979)	0.51	0.31	0.18		Canals, Pakistan	
Lane and Foster (1980)	0.46	0.46	0.081			
Chang (1980)	0.47	0.42	0.11		Minimum stream power	Theoretical-
Bray (1982)	0.53	0.33	0.14		Alberta, Canada	
Andrews (1984)	0.48	0.37	0.14		Colorado, USA	Thick bank vegetation
	0.48	0.38	0.14			Thin bank vegetation
Hey & Thorne (1986)	0.45	0.35	0.20		Britain	

Table 2.2 continued.

Rhoads (1991)	0.46	0.46	--		Missouri river basin	106,155-1,358,000 km^2.
	0.49	0.30	--		James river basin	655-55810 km^2.
	0.51	0.37	--		Smoky Hill River	9207-49,880 km^2.
Allen et al. (1994)	0.557	0.341	0.104	674	15 states in U.S. and Canada (from Bray,1979)	674 cross-sections
Henderson and Ibbitt (1996)	0.45-0.55	0.20-0.35	0.20-0.35		New Zealand	
Annable (1996)	0.28			7	Southern Ontario	Stream Type B: Rosgen Classification (1994)
	0.46			26	Southern Ontario	Stream Type C: Rosgen Classification (1994)
	0.47			8	Southern Ontario	Stream Type E: Rosgen Classification (1994)
Annable (1996)	0.23			4	Southern Ontario	Stream Type F: Rosgen Classification (1994)
	0.49			47	Southern Ontario	All types of river
Ibbitt (1997)	0.52	0.14	0.34		Hutt River, New Zealand	
Ibbitt (1997)	0.45	0.39	0.15		Buller River, New Zealand	

Table 2.2 continued.

Jowett (1998)	0.50	0.25	0.25	73	Rivers, New Zealand	
Cao and Knight (1998)	0.51	0.34	0.15		10 studies in Canada, China, UK, and USA	Field derived average
	0.50	0.33	0.17		Stream power and fluvial process probability	Theoretical
Giffiths (1998)	0.48	0.43	0.11	25	6 Large rivers in New Zealand	25 flow gauging sites
Jowett and Giffitts (1998)	0.48	0.30	0.22	98	New Zealand Rivers	
Ibbitti et al., (1998)	0.52	0.25	0.24		Ashley River, New Zealand	
McKerchar et al., (1998)	0.44	0.24	0.32		Ashley River, New Zealand	
Henderson et al., (1999)	0.47	0.31	0.22		Cropp river, New Zealand	
McCandless and Everett (2002)	0.52	0.42	--	23	Maryland Piedmont, USA	
Haung and Nanson (2000) Haung et al. (2002)	0.48	0.29	0.23		Maximum flow efficiency	Theoretical $^{\Theta}2.3 \leq \xi \leq 23$
Molnar and A. Ramirez (2002)	0.44	0.23	0.33	225	Ashley river, New Zealand	
	0.53	0.26	0.21	286	Taieri river, New Zealand	
Moody and Troutman (2002)	0.45	0.39	--		Clear creek (small), Powder river (medium), and Mississippi river USA	
	0.50			226	Various rivers	

Table 2.2 continued.

Dudley (2004)	0.50	0.32	0.18	15	Rivers in Costal and Central Maine, USA	Bankfull discharge
Mosselman (2004)	0.482	0.287	0.231		Twenty percent inefficiency	
Wohl.(2004)	0.34	0.36	0.24	40	Chagres, Panama	Mountain river
Wohl and Wilcox (2004)	0.27	0.47	0.26	18	Dudh Kosi, Nepal	Mountain river
	0.49	0.32	0.18	20	Waimakarir, New Zealand	Mountain river
Wohl, et al. (2004)	0.34	0.33	022	14	Chena, Alaska, USA	Mountain river
	0.59	0.39	0.16	15	Agua Fria, Arizona, USA	Mountain riover
Beyer (2005)	0.56-0.68	0.27-0.37	0.03-0.13	6	Verde River System, SW-USA	2 , 5 and 10 years return period discharges
Ellis and Church (2005)	0.596	0.247	0.157	18	Lower Fraser River, BC, Canada	Data were collected using ADP
Wohl and Wilcox (2005)	0.5	0.33	0.17		Kowai and Porter rivers, New Zealand	Mountain streams
	0.52	0.43	0.07		Camp creek ,New Zealand	

$^{\varsigma}$: Sources are the original papers but data are not necessarily taken form the original paper.

$^{\oplus}$: see Eqs. 1.1 - 1.3

$^{\Theta}$: ζ is width to depth ratio

Chapter Three

3 Data Collection and Processing

3.1 Selection of Study Rivers

The focus of this research is clay dominated cohesive bed rivers from eastern Ontario region (UTM zone 18 and 17) and surrounding regions. Eastern Ontario has been subject to deposition of glaciomarine or glaciolacustrine clay deposits (Ontario Geological Survey, 2003), thus several rivers in the region have cohesive beds. Rivers from eastern Ontario region have been selected based on the following conditions:

- ✓ The river must have at least one reach equipped with a gauging facility that has 10 or more years of flow records.
- ✓ The gauging station must be located in a natural flow reach of a river — the river must not have any in-stream development, restoration, or regulatory works undertaken at any location of its upstream reaches or on any of its upstream tributary / tributaries.

From all rivers in eastern Ontario region only 23 rivers (Table 3.1) fulfilled the above selection criteria. All of them are within the hydrometric networks of Water Survey Canada. The hydrometric data base (Surface Water and Sediment Data) is available on Compacted Disc (HYDAT CD-ROM) and as on-line data base from the Water Survey Canada webpage: http://www.wsc.ec.gc.ca/products/main_e.cfm?cname=products_e.cfm.

The primary objective of this research is the study of hydraulic geometry of clay dominated cohesive bed (semi-alluvial) natural stream reaches. Before conducting preliminary field survey, the primary bed material for each river reach was estimated by analysis of the local surficial geology map. Surface geology of the area and gage station coordinates were mapped together using ArcGIS software, and the resulting maps were used to predict the expected bed material of each of the selected rivers. Thus, stream reaches were further screened based meeting on at least one of the following three conditions:

- ✓ The primary material surface geology of the area at the gauge site reach should indicate the presence of glacial sedimentary deposits such as glaciomarine and glaciolacustrine silts and clays.
- ✓ The primary surficial material of the area at the gauge site reach indicates the presence of other deposits composed predominantly of clay and silt, or
- ✓ As verified by Environment Canada personnel, the gauging station is located where the bed material of the river is cohesive.

Only 12 river or creek reaches (Table 3.1) across eastern Ontario fulfilled the first and second screening assessments and were selected for preliminary survey or field visit for verification. The author with the assistance of Dr. Colin D. Rennie conducted quick field survey on all 12 rivers or creeks in August, 2006. Unfortunately, only the first six river reaches (Table 3.1 and Fig. 3.1) were confirmed by on-site survey to have cohesive bed and were selected for further detailed study. The surface geology maps of all six rivers are indicated in Figs. 3.2 - 3.7.

Table 3.1 List of natural river reaches equipped with gage station in eastern Ontario

No	ID: STATION NAME	DA	LAT	LON	REC
		KM^2	DMS	DMS	YEAR
1	02LA007: JOCK RIVER NEAR RICHMOND	559	451507	754556	33
2	02HM004: WILTON CREEK NEAR NAPANEE	112	441421	765058	37
3	02MC001: RAISIN RIVER NEAR WILLIAMSTOWN	404	450920	743817	42
4	02LB007: SOUTH NATION RIVER AT SPENCERVILLE	246	444851	753420	54
5	02HM009: WEST BRANCH LITTLE CATARAQUI CREEK AT KINGSTON	5	441424	763444	13
6	02LB008: BEAR BROOK NEAR BOURGET	440	452533	750913	46
7	02LB018: WEST BRANCH SCOTCH RIVER NEAR ST. ISIDORE DE PRESCOT	100	452231	745652	23
8	02MC027: RAISIN RIVER AT BLACK RIVER	129	450450	745204	8
9	02MC030: SOUTH RAISIN RIVER NEAR CORNWALL	26	450555	744613	16
10	02LB022: PAYNE RIVER NEAR BERWICK	152	451130	750620	22
11	02LB006: CASTOR RIVER AT RUSSELL	433	451545	752038	54
12	02HM005: COLLINS CREEK NEAR KINGSTON	155	441523	763645	33
13	02HK007: COLD CREEK AT ORLAND	159	440805	774712	21
14	02HL004: SKOOTAMATTA RIVER NEAR ACTINOLITE	712	443258	771941	47
15	02KF011: CARP RIVER NEAR KINBURN	269	452503	761155	31
16	02KF016: MISSISSIPPI RIVER BELOW MARBLE LAKE	357	445035	770712	14
17	02MB010: BUELLS CREEK AT BROCKVILLE	13	443508	754130	14
18	02MC026: RIVIERE BEAUDETTE NEAR GLEN NEVIS	124	451624	742937	19
19	02MC028: RIVIERE DELISLE NEAR ALEXANDRIA	85	451937	743839	14
20	02LB017: NORTH BRANCH SOUTH NATION RIVERNEAR HECKSTON	69	445941	753058	26
21	02LB020: SOUTH CASTOR RIVER AT KENMORE	189	451342	752445	20
22	02HL005: MOIRA RIVER NEAR DELORO	308	442958	773706	37
23	02HK008: RAWDON CREEK NEAR WEST HUNTINGDON	87	442017	772837	20

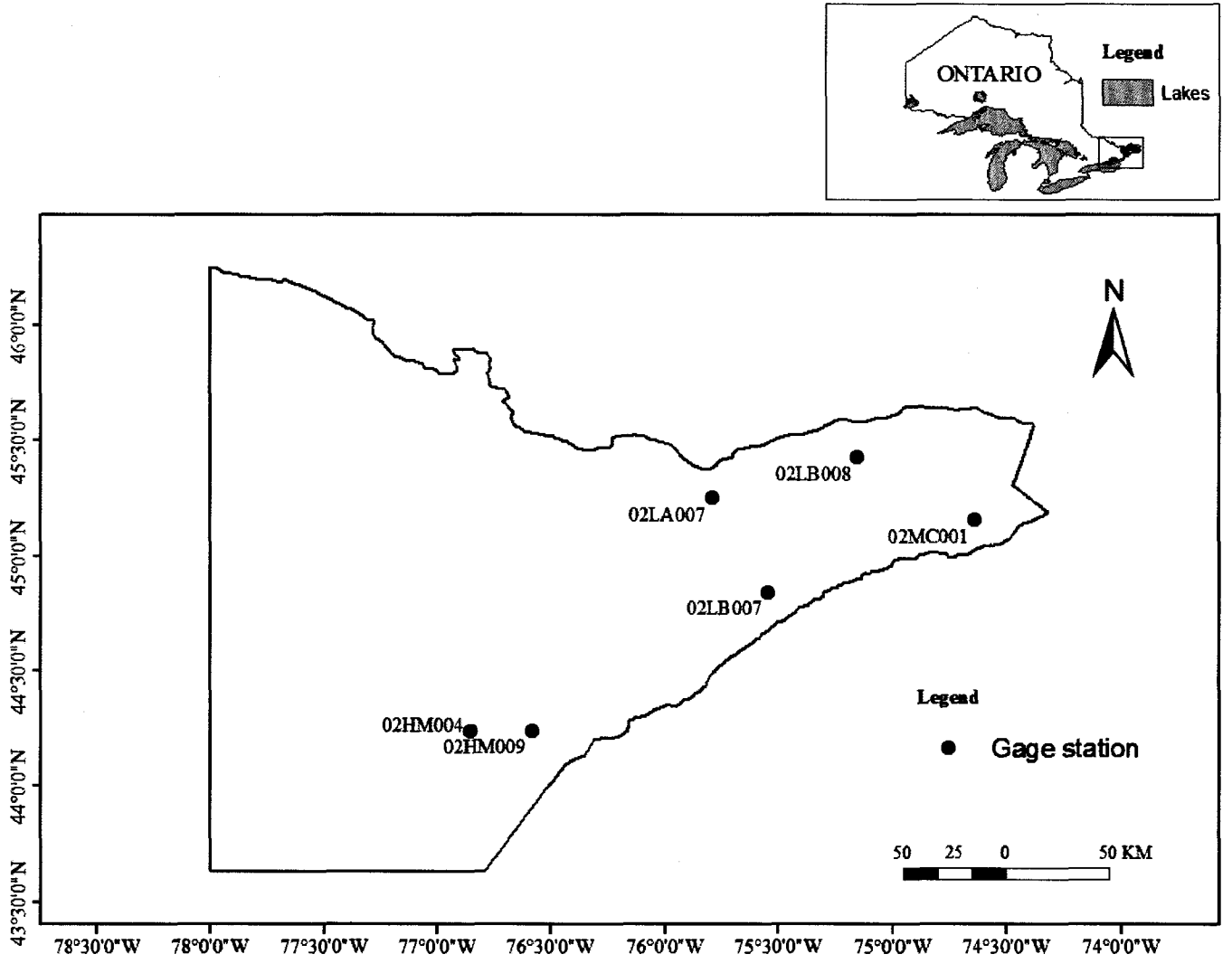

Figure 3.1 Map indicating locations of river reaches selected for detail study in Eastern Ontario

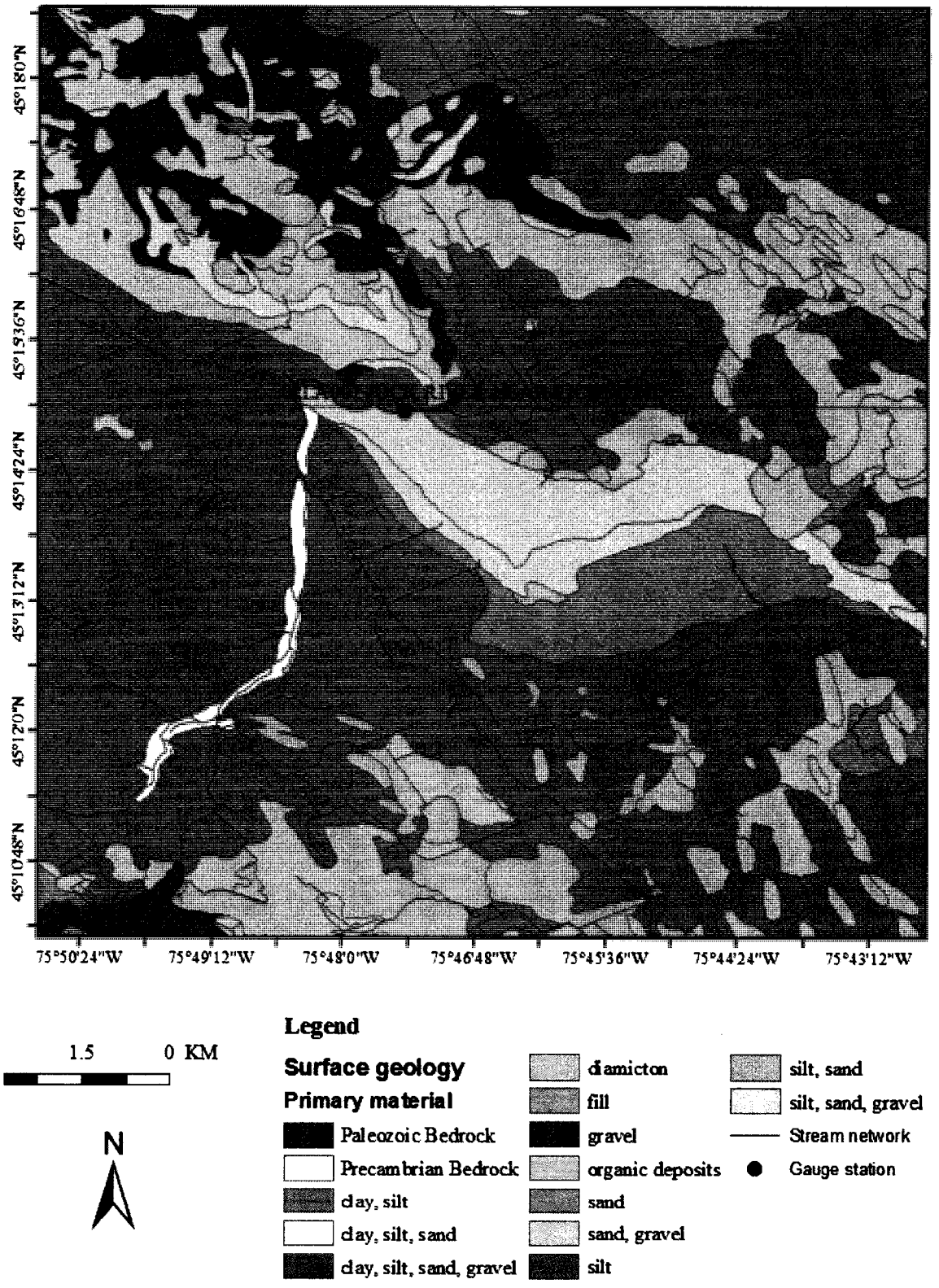

Figure 3.2 Primary material surface geology map at Jock River study reach

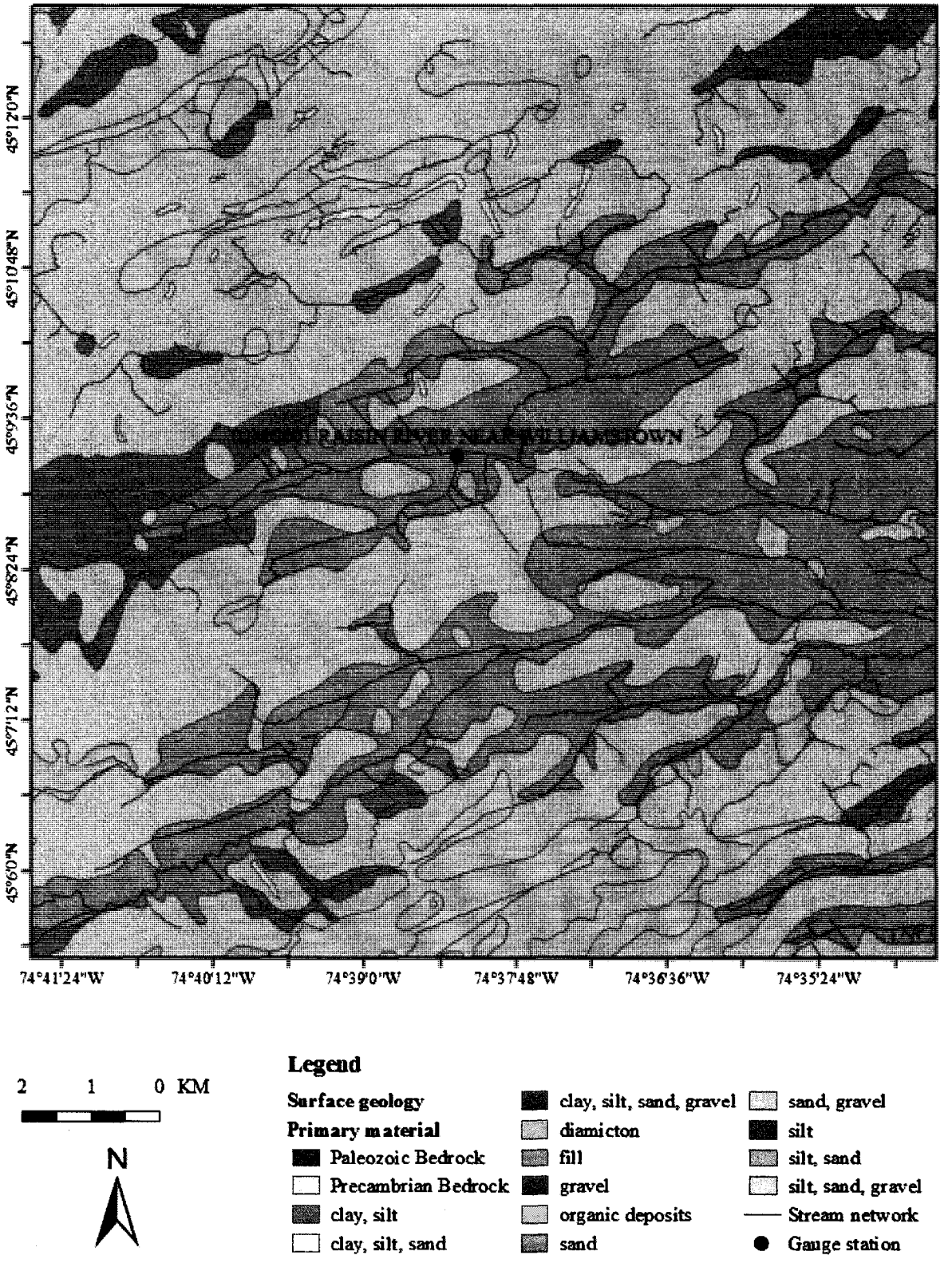

Figure 3.3 Primary material surface geology map at Raisin River study reach

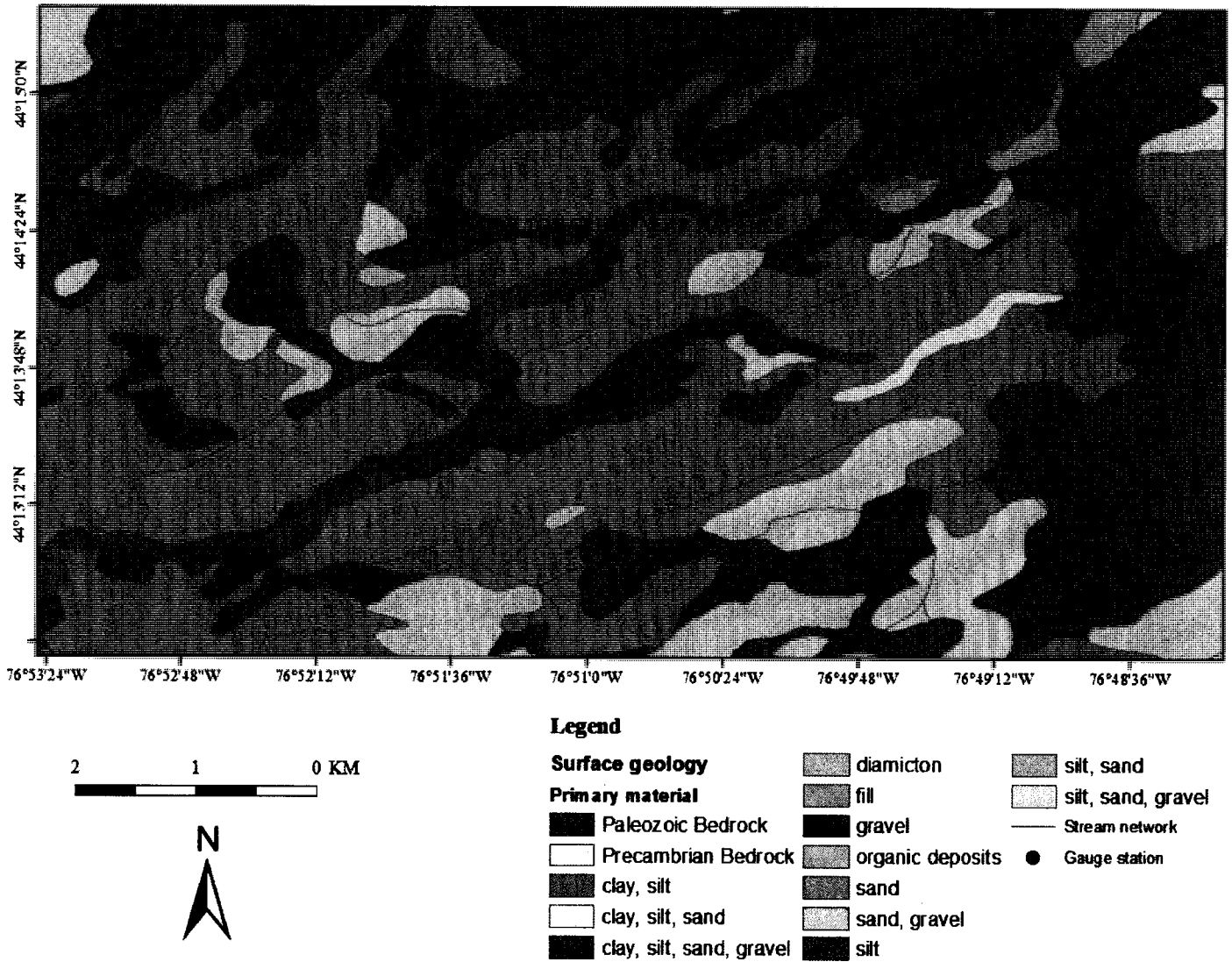

Figure 3.4 Primary material surface geology map at Wilton Creek study reach

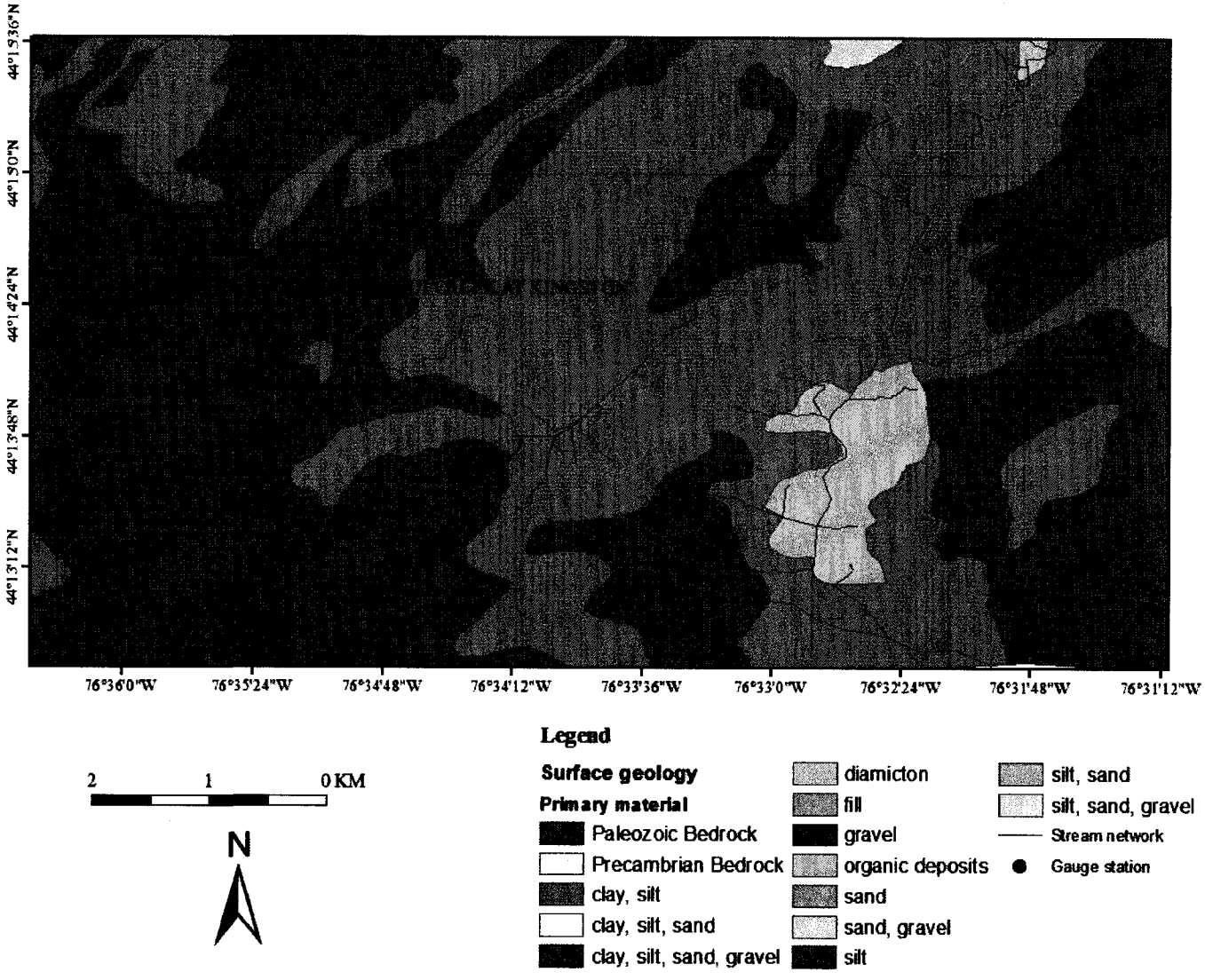

Figure 3.5 Primary material surface geology map at West Branch Little Cataraqui Creek study reach

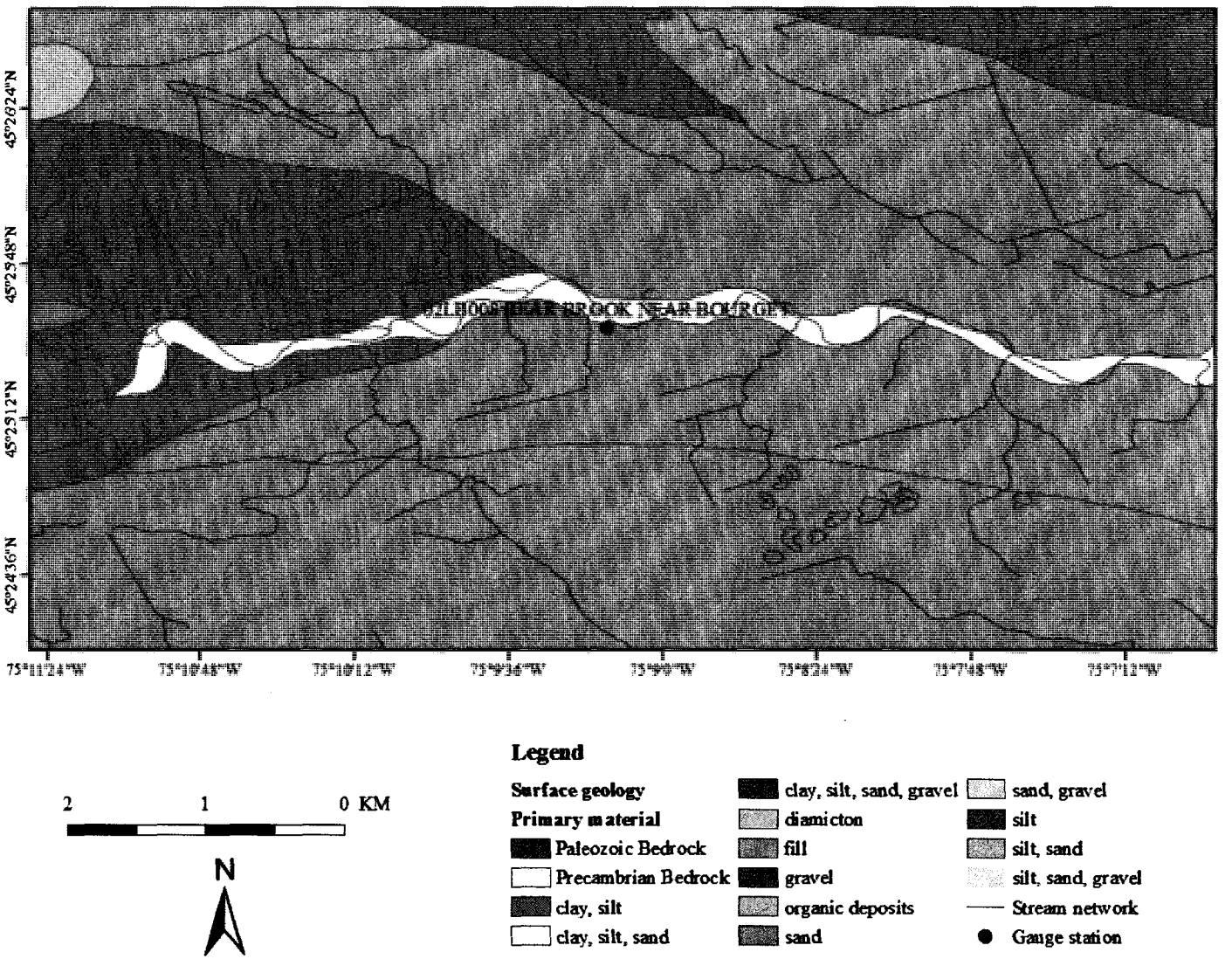

Figure 3.6 Primary material surface geology map at Bear Brook River study reach

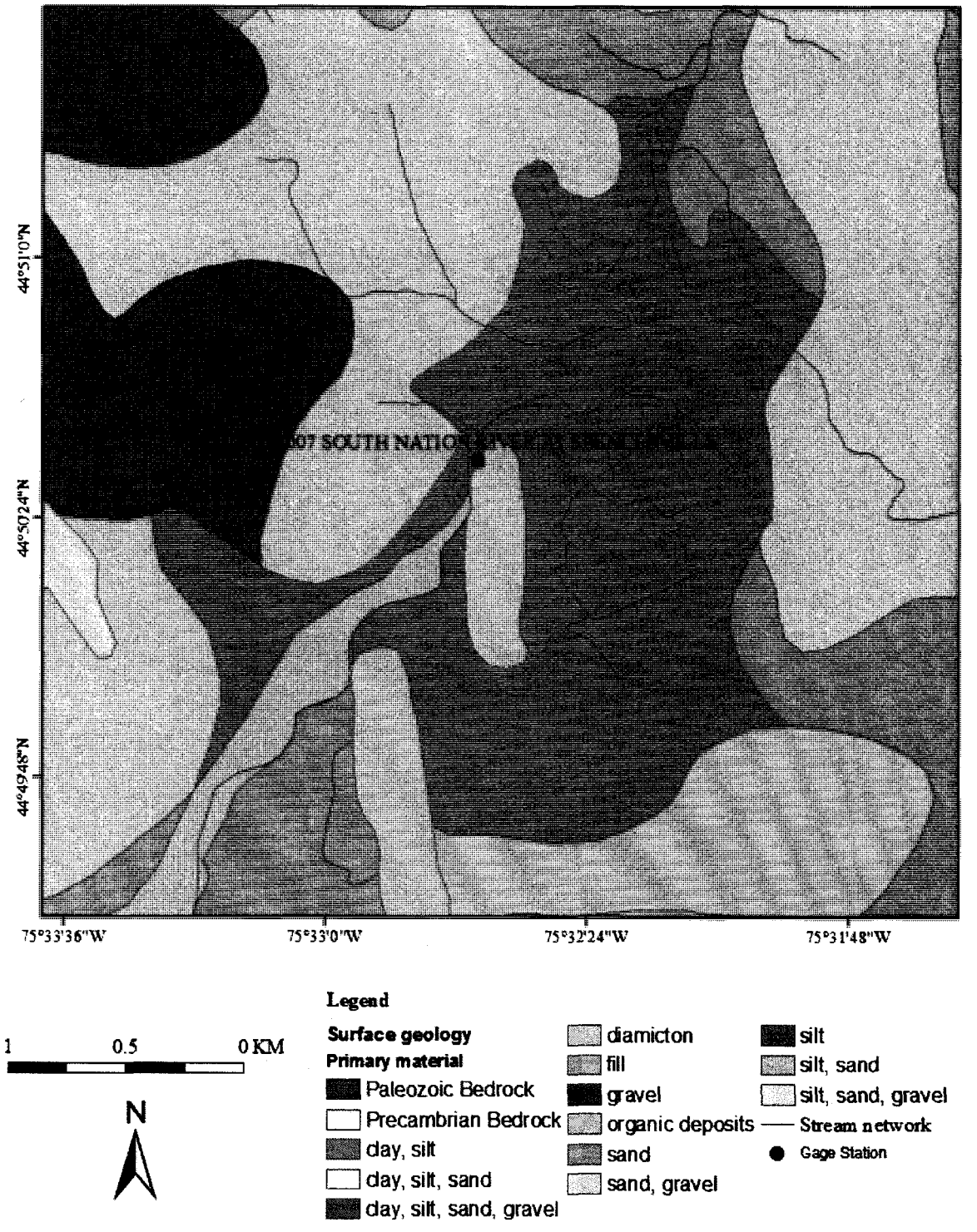

Figure 3.7 Primary material surface geology map at South Nation River study reach

3.2 Data Collection

3.2.1 Major Instruments Deployed

3.2.1.1 Acoustic Doppler Current Profiler (ADCP)

Acoustic Doppler Current Profiler (ADCP) is a relatively new instrument capable of measuring depth, flow velocity, and discharge in open channels such as natural rivers. It measures water velocity or current using the Doppler effect. An ADCP sends sound (ping) at a constant frequency and receives the reflected sound (ping) from scatterers (suspended particles) moving with the water. Since scatterers are moving either away or toward the ADCP, the transmitted sound waves perceived by scatterers and the reflected sound waves received by ADCP transducers are Doppler shifted (Fig. 3.8). Doppler shift is the difference in frequency between the sound waves that are transmitted and received due to relative motion between source and receiver. Thus ADCP uses these Doppler shifts to calculate the velocity of the scatterers (suspended particles) parallel to the beam. The scatterers are assumed to have the same velocity as the water (3.1).

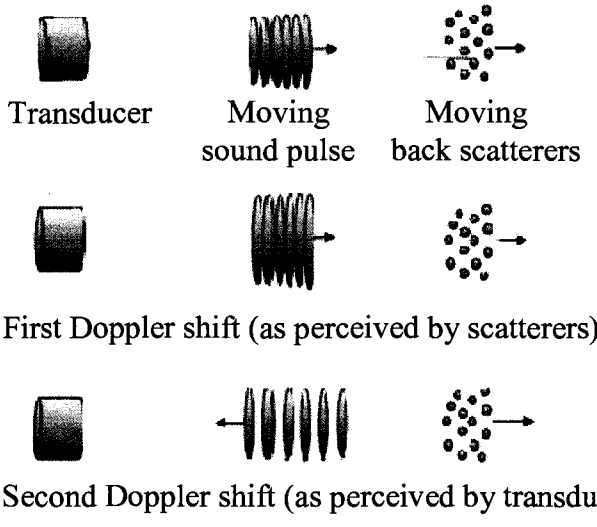

Figure 3.8 Reflected pulses showing two Doppler shifts (adapted from Simpson, 2001)

$$Fd = 2 \cdot Fc \cdot \left(\frac{v}{C}\right) \qquad (3.1)$$

Where, v is the velocity of the scatters relative to the ADCP in the direction parallel to the beam, C is the speed of sound, F_d is the change in the received frequency at the receiver (i.e., the Doppler shift), and F_s is the frequency of the transmitted sound.

Because usually ADCP is mounted on a moving frame of reference such as a boat, corrections for boat velocity are made to determine absolute water velocities (water velocity relative to the Earth) either by bottom tracking or by use of differential global positioning system (DGPS) data (see Section 3.2.1.2). Bottom tracking involves measurement of the Doppler shift in the frequency of sound pulses reflecting back from the bed. The bottom-track pulse is somewhat longer than the water tracking pulse to properly illuminate the bottom (Simpson, 2001). The bottom tracking ping is also used to measure profiled depth range (total depth) from each beam.

ADCPs are comprised of either three or four beams. An ADCP computes a single component of velocity along each beam at a large number of points (depth cells, they are usually called bins) by range-gating the back-scattered signal in time (Boiten, 2000). Because the beams are positioned orthogonally to one another and at a known angle from the vertical, trigonometric relations can be used to compute three dimensional flow velocity vectors from the three or four beam velocity components measured at equivalent depth cells. The fourth beam provides a redundant vertical velocity, which is useful for assessing errors and data quality. Each depth cell is comparable to a single current meter. Therefore an ADCP velocity profile is like a string of current meters uniformly spaced (Fig. 3.10). Hence the following definitions can be made by analogy (RD Instruments, 1996).

- ✓ Depth cell (bin) size = distance between current meters
- ✓ Number of depth cells (bins) = number of current meters

A single crossing of the stream from one side to the other (moving vessel-mounted ADCP either from left bank to right bank or vice versa) during measurement is referred to as a transect, which is a collection of many ensembles (verticals) (Fig. 3.9).

Discharge measurement in rivers using ADCP has many advantages compared with other traditional point velocity measuring devices such as propeller current meters. A few of the prime advantages and differences (RD Instruments, 1996; Oberg, et al., 2005) are:

- ✓ Less time is required to complete measurements
- ✓ ADCP profiles are always uniformly spaced while current meters can be spaced at irregular intervals. Regular spacing of velocity data over the profile makes it easier to process and interpret the measured data.
- ✓ ADCP allows for continuous data collection throughout most of the water column and cross section rather than at discrete points (Fig. 3.10).
- ✓ Reduces chance of being snagged by debris.
- ✓ It can be boat-mounted, thus, eliminates the installation, maintenance, and liability of costly manned cableways.
- ✓ Many parameters are available for analyzing measurement quality.

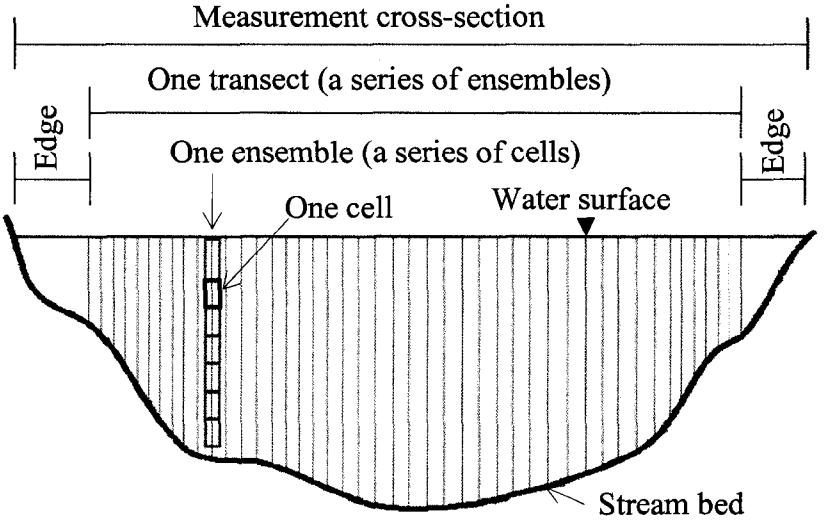

Figure 3.9 Typical layout of components of ADCP measurement along river cross-section

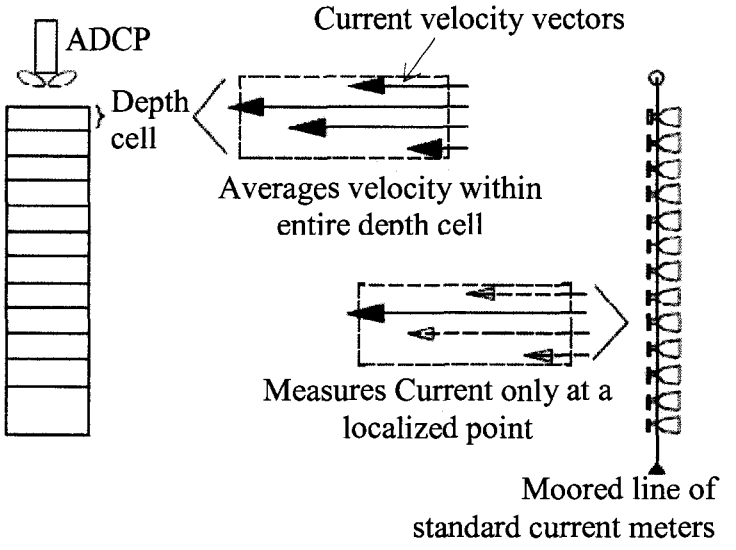

Figure 3.10 ADCP depth cells compared with conventional current meter (Adapted from RD instruments, 1996)

The main instruments used for ADCP surveys of this study are: a four beam 1200 KHz Workhorse RDI 'Rio Grande" broadband ADCP, ADCP mounting assembly, RTK-DGPS and communication radios, field computer which has serial ports and with appropriate software (WinRiver and RDI tools). The instruments were deployed for surveying larger rivers which were too deep to wade. A small river (West Branch Little Cataraqui Creek) was surveyed by wading with a conventional propeller meter.

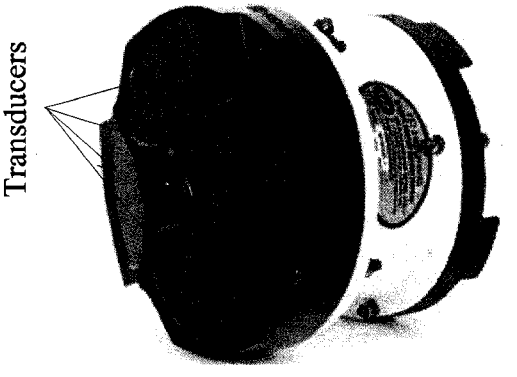

Figure 3.11 A four beam 1200 KHz Workhorse Rio Grande ADCP

3.2.1.2 Real Time Kinematic Differential Global Positioning System (RTK-DGPS)

Global Positioning System (GPS) is a passive, all-weather, 24-hour global navigation satellite system operated and maintained by the U.S. Department of Defense (DoD); it consists of a nominal constellation of 24 satellites orbiting the earth at a very high altitude (USACE, 2003). A Global Positioning System (GPS) works with a receiver that acquires signal from satellites in order to locate its position geographically. Each satellite broadcasts two carrier waves in microwave L-band (L1 and L2) that travel to earth at the speed of light. The GPS receiver computes the distance to the satellites by measuring the travel time of the signals transmitted from the satellites and multiplying it by the velocity (= speed of light). The carrier waves are coded with a Pseudo Random Code (PRC), which facilitates estimation of travel time through calculation of the phase shift between the measured and expected PRC. In order to get a 3 dimensional position (latitude, longitude and altitude) by triangulation from satellite positions at least four satellites are needed within signal range. Some of the most common sources of errors that affect the accuracy of GPS observations are (USACE, 2003):

- ✓ The geometric effect of the spatial relationship of satellites relative to the receiver — Geometric Dilution of Precision (GDOP). GDOP is a measure of the strength of the geometry of the satellite configuration
- ✓ Satellite and receiver clock errors — time difference as recorded by the satellite clock and that recorded by receiver (satellite atomic clock accuracy >> GPS receiver clock accuracy)
- ✓ Satellite characteristics — frequency, stability
- ✓ Atmospheric conditions — signal propagation delays in ionosphere and troposphere due to dispersion and refraction.
- ✓ Multipath conditions at receivers — signals arrive at receivers from more than one path usually due to a reflection on other nearby objects.

Differential GPS (DGPS) is a technique used to improve positioning accuracy by determining the positioning error at a known reference location and subsequently incorporating a corrective factor (by real-time transmission of corrections or by post-

processing) into the position calculations of another receiver operating in the same area and simultaneously measuring/observing the same satellite code ranges and/or carrier phases from the NAVSTAR GPS satellite constellation (USACE, 2003; B C Guidelines For RTK GPS Surveys, 2005). The basic principle is that the absolute positioning errors at the two receiver points will be approximately the same for a given instant in time.

Real Time Kinematic DGPS (RTK-DGPS) uses a local static GPS (base) receiver as a reference station located at a known point (reference point) and a rover GPS receiver which can move and survey any points of interest. Signals from a GPS Reference Station are transmitted instantaneously to a rover receiver during the survey (i.e., in "real time"). The rover receiver uses the signals from the base receiver together with its own and computes accurately its position relative to the position of the base receiver. Importantly, the phase shift in the carrier wave, as opposed to phase shift in the PRC, is used to estimate distance to each satellite. The wavelength of the carrier wave is much smaller than the wavelength of the PRC, which greatly increases precision. Even greater accuracy and precision is achieved if both L1 and L2 signals are processed simultaneously. The errors listed above and many other errors inherent to the absolute positioning system are effectively minimised or removed using the RTK-DGPS, especially when short baseline distances are observed (>10km) with high quality dual-frequency carrier phase receivers.

The NovAtel ProPak-LBplus dual-frequency carrier phase receivers (Fig. 3.12) were used together with the ADCP to survey three rivers which are too deep to wade. NovAtel dual-frequency GPS receivers can provide 2 cm nominal accuracy RTK-performance. Positioning Data Link (PDL) communication products (radio system) from Pacific Crest Corporation have been utilized to provide the communication link between the base and rover receivers. RTK-DGPS has become widely used for accurate engineering and construction surveys, including topographic site plan mapping, setting project control, construction stake out (lots, roads, levees, culverts, grades etc), construction equipment location, and hydrographic (accurate river depth and cross-section measurement, over bank and flood plain topography) survey (USACE, 2003).

A)

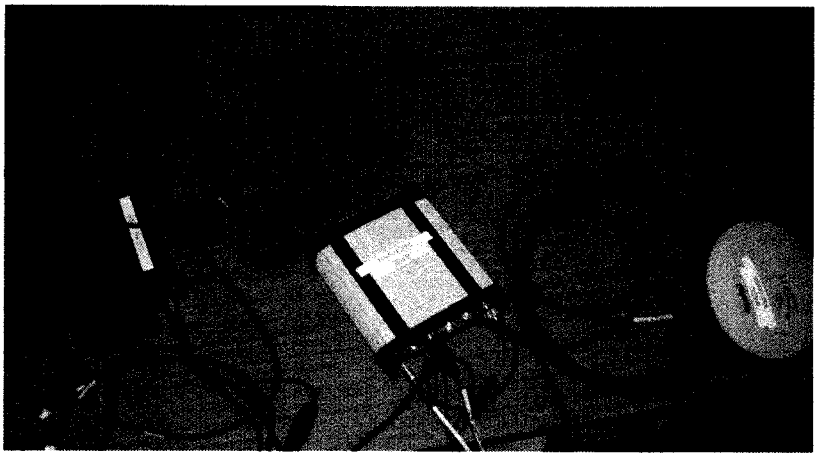

B)

Figure 3.12 Base (A) and Rover (B) GPS Components

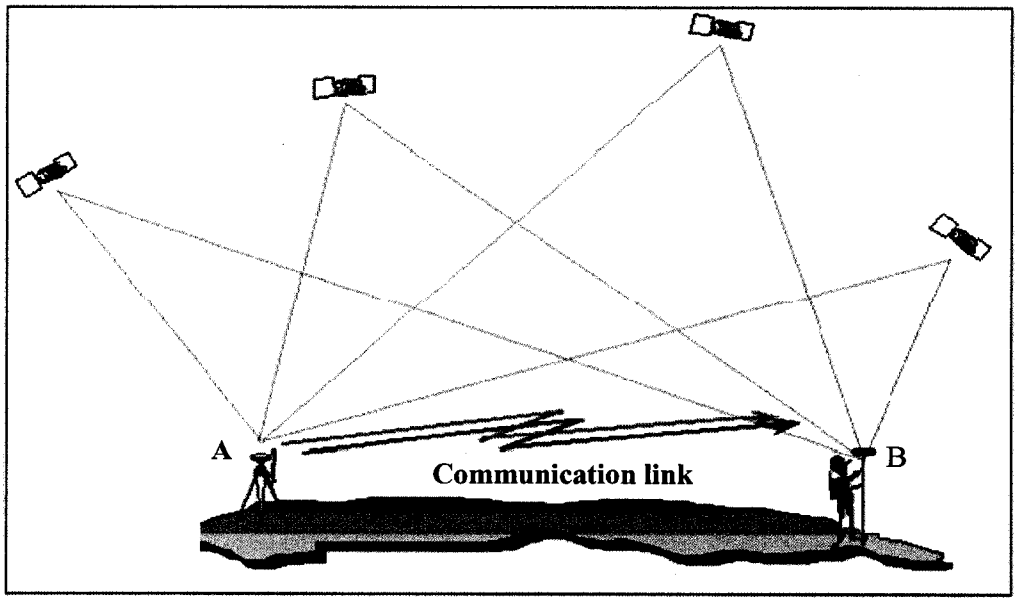

Figure 3.13: Classic RTK system diagram; A is RTK Base Station, B is RTK rover (Adapted from B C Guidelines for RTK-GPS Surveys, 2005)

3.2.1.3 Electronic Total Station (ETS)

Electronic Total station is an electronic theodolite combined with an Electronic Distance Measurement (EDM) and an electronic data collector capable of measuring and recording horizontal and vertical distances and angles and then computing east (E), north (N) and elevation (Z). TOPCON Electronic Total Station, GTS-220 series (Fig. 3.14) was deployed to survey all study rivers. The three major components for total station survey are Electronic Total Station, reflector prism and tripod. For big rivers, the floodplain and channel margins of each cross-section were surveyed by Electronic Total Station. In small wadable rivers, the entire cross-sectional profile can be fully surveyed by Electronic Total Station.

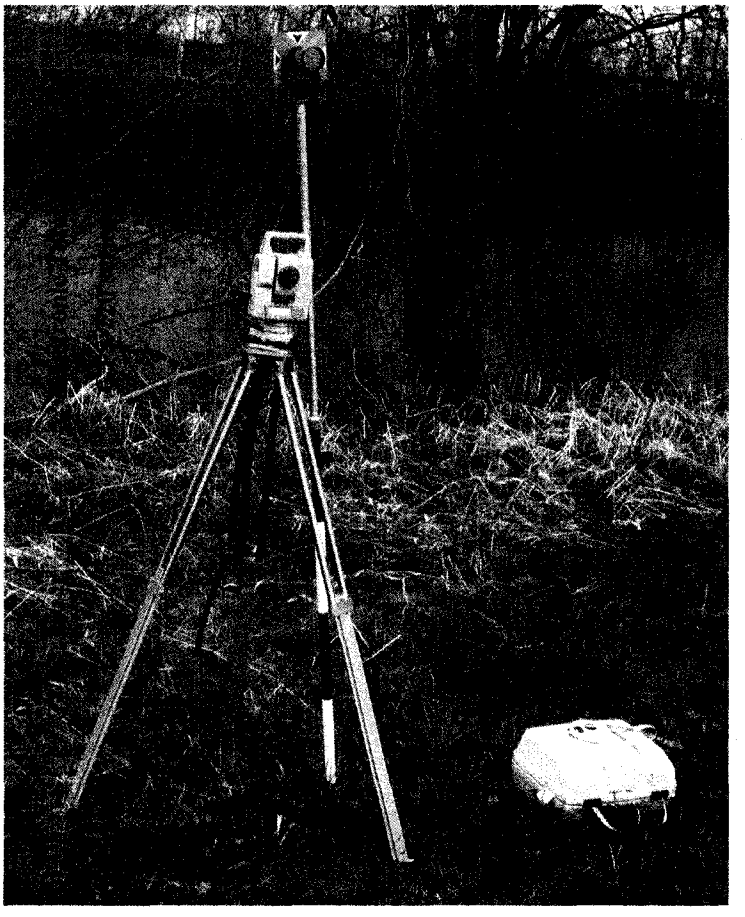

Figure 3.14 TOPCON Electronic Total Station, GTS-220 series

3.2.1.4 Propeller Current Meter

Current meters are devices for measuring velocity at a point of a water column. The current meter propeller turns as the water particle passes along. The number of revolutions measured during a certain time interval is related to velocity of water according to the calibration formula of the propeller. The number of revolutions of the propeller is counted either by a person who conducts the measurement or with a counter device. The general calibration equation of a current meter has the following form:

$$v = \lambda \cdot nr + \Delta \qquad (3.2)$$

Where: v is flow velocity (m/s), nr is propeller revolutions (s^{-1}), λ is hydraulic pitch of the propeller (m) and Δ is characteristic meter constant (m/s).

Propeller current meters are used to measure flow velocity of creeks which are too shallow or narrow to deploy ADCP survey. Point velocities are measured at a constant interval across the cross-section along with the corresponding total station survey of bed below each point. Therefore, the geometric data from the total station and the velocity data from propeller current meter can be used to calculate discharge of the creek.

Current meters used for this study:

1) Model 1205 "Mini" Current meter (Fig. 3.15).
   Calibration equation: $v = 0.977 \cdot nr + 0.00853$
2) Model 1-081B (Source: Mr. Rob Waring (Technician), Water survey Canada personnel)
   $v = 0.6744 \cdot nr + 0.0108$

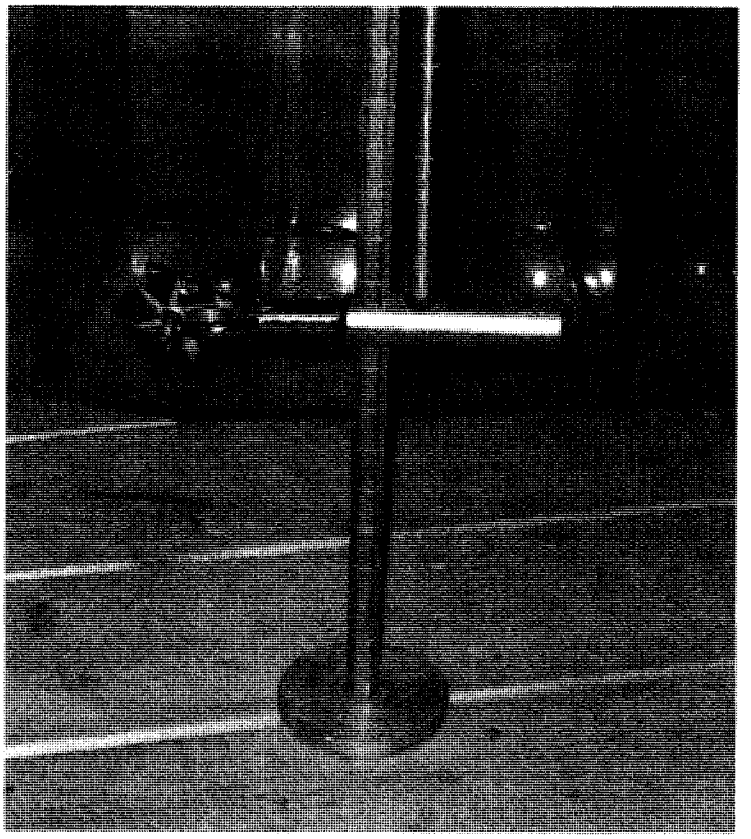

Figure 3.15 Model 1205 "Mini" Current meter

3.2.2 Measurement Methods

3.2.2.1 ADCP and RTK-DGPS Measurement

ADCP and RTK - DGPS were used to survey three rivers: South Nation, Jock and Raisin during the spring freshet, in April, 2007. The combination of the two instruments has been used for precise measurement of cross-sectional hydraulic data (depth, width and velocity) and discharge on each river. ADCP and RTK-DGPS have a unique capacity to continuously collect flow velocity profile, depth profile, and position coordinates (latitude, longitude and altitude) with outstanding accuracy. This unique capacity of the two instruments was utilised for detail measurements on three rivers of the study. The measurement was deployed from a manned boat (Fig. 3.16 and 3.17). Summary of major instrument setups and procedures are presented below:

3.2.2.2 ADCP Setup

- ✓ Mounting ADCP on side of manned boat in such a way that it is free and clear of a boat. The ADCP mount used was adjustable and at the same time capable of holding ADCP in a fixed and vertical position (Fig. 3.17B).
- ✓ Connecting ADCP to a power supply (12 Volt battery) and a field computer equipped with appropriate software (WinRiver and RDI tools software).
- ✓ Checking a communication link between ADCP and field computer

3.2.2.3 RTK-GPS Setup (Base and Rover)

- ✓ Selection of a control point (i.e., GPS base station) unobstructed from view of the sky and close to the survey location; the control point for each survey reach was made permanent for future use by installing a tagged metal rod.
- ✓ Installing base GPS antenna on tripod directly above the control point (Fig. 3.17 A) and document its height above the control point.
- ✓ Connecting GPS receiver to power supply, GPS antenna, radio and radio antenna.
- ✓ Waiting till the base GPS fixes its position coordinates (latitude, longitude and altitude) and then recording them properly.
- ✓ Placing the rover GPS antenna directly above ADCP so that the velocity of the antenna and ADCP would be the same in all directions during the whole measurement.
- ✓ Connecting Rover GPS receiver to power supply, field computer, rover GPS antenna and communication radio antenna.
- ✓ Checking a communication link between rover GPS and field computer as well as radio communication between base GPS receiver and rover GPS receiver.

3.2.2.4 Pre-Measurement Procedure

1) Selection of appropriate location for cross-sectional survey

Every survey reach was selected where it is apparent that its channel bed material is cohesive and as much as possible close to the gage site. Measurement section

selection was accomplished before instrument setup. For all rivers, there was no tributary between measurement site and gage station. Reaches with obvious secondary currents, highly turbulent flow, or a possibility of considerable blockage of signals from satellites were avoided as much as possible.

2) Acoustic Doppler Current Profiler (ADCP) configuration

Configuration of ADCP was made step by step using the configuration wizard of the WinRiver software. Although the WinRiver default configuration is generally supposed to be acceptable for most flow measurement situations, site specific parameters were carefully input to supplement it. ADCP frequency, ADCP depth, maximum water depth (profiling range), maximum water speed, bed material type, salinity, water temperature, boat speed (approximate), magnetic variations of the site, and extrapolation method for the top and bottom unmeasured zones are important parameters required to be specified before starting measurement on each study river. Site specific environmental conditions such as maximum depth, maximum velocity, bed material type and instrument frequency are used to generate commands of configuration such as optimal water mode, bottom mode, depth cell size and number of depth cells.

The depth of ADCP which is the vertical distance from water surface to the center of transducer faces was determined by measurement for each site (Table 3.2). Profiling range which is maximum expected river depth as well as maximum water speed were estimated from a trial transect. An ADCP cannot measure near the water surface, near the river bed and near the left and right edges of water, thus WinRiver requires selection of an appropriate extrapolation method (usually the default one-sixth power law) to estimate near-surface and near-bed discharges, as well as measurement or first-class estimate of edge distances from the start and end of the measurement point to estimate near-shore discharges. Water measurement modes manage different lag distances, pulse lengths, code element combinations, and adaptive schemes to measure water velocity under many hydrologic conditions (Simpson, 2001).

Appropriate bottom truck mode is useful to determine the speed of ADCP relative to river channel bottom.

Table 3.2 Some important field configuration data for ADCP survey

River Name	ADCP Depth (m)	Maximum River Depth (m)	WM	BM
South Nation	0.23	2.1 - 2.2	11/12	7
Raisin	0.21	4.4 - 4.5	12	5
Jock	0.21	5.5 - 5.6	12	5

3) Compass calibration and evaluation

Acoustic Doppler Current profiler (ADCP) internal compass calibration is a mandatory step if a RTK-DGPS unit is used for tracking the position and instrument velocity of the ADCP. Calibration of internal ADCP compass heading data for local magnetic variation and for one-cycle deviation errors helps to reconcile the magnetic coordinate system of the ADCP with the GPS true earth coordinate system (Teledyne RD Instruments, 2007). Local magnetic variation correction was estimated by referring to a chart of the local area, therefore for all rivers it has been referred from a Natural Resources Canada, Geomagnetism (Magnetic declination calculator); webpage: http://www.geolab.nrcan.gc.ca/geomag/apps/mdcal_e.php. The one-cycle deviation error was corrected in *situ* in accordance with the method stated in WinRiver II manual: driving the ADCP vessel (boat) in continuous, small complete circles and evaluating the deviation errors.

4) Moving bed test

When a moving bed condition is present, both boat and ADCP velocity measurements using bottom tracking will be biased and can cause significant error in discharge computation. Therefore, a moving bed test is also a necessary step before starting discharge measurement, using bottom tracking. Although RTK-DFGPS, which is not affected by moving bed condition, has been deployed, a moving bed test was performed for all study rivers surveyed by ADCP. It was performed at least

twice on each river by keeping the boat (i.e., ADCP) in a steady position for at least 10 minutes at the region of maximum velocity while the ADCP recorded data. The moving bed effect is considered significant when there is perceived upstream displacement of the boat relative to bed. Moving bed conditions were not observed in any of the three rivers surveyed.

5) Discharge and position coordinates data collection

Generally, the main purpose of ADCP is discharge measurement. However, for this study ADCP with RTK-DGPS was deployed not only for discharge measurement but also for collection of depth and position coordinates data at each ensemble (vertical), from which a cross-sectional bed profile could be generated. Four or more transects were measured in reciprocal fashion at each section. For discharge measurements using ADCP, precision of boat-manoeuvring techniques are not required by the transect software. However, for this study maximum possible effort was made to keep the boat's route at right angles to the flow direction, because position coordinates and depth data were to be used for generating cross-sectional bed profile data.

Measurements on two rivers (Jock and Raisin) were made when their flows were greater than their bankfull discharges and one river (South Nation) had a flow less than but close to its bankfull discharge. The measurement time was intentionally scheduled to during spring freshet when rivers carry high flow or close to their bankfull discharge. The closer the measured discharge to bankfull discharge, the better is the accuracy of the estimation of the latter from the former. Position coordinates (north, east and altitude above reference datum) of the channel bank and parts of the cross-section not surveyed by ADCP were surveyed using Electronic Total Station (Fig. 3.16), from start and end points of ADCP measurement to the edges of left and right banks. This was only possible where water depth was sufficiently shallow for wading.

3.2.3 Propeller Current Meter and Electronic Total Station Measurement

The setup of a propeller current meter is straightforward and it involves connecting the propeller to both a small graduated adjustable wading rode which has a bottom plate (Fig. 3.15) and a sensor which gives signal per every complete revolution of the propeller. Electronic Total Station setup involves placing the total station on the top of the tripod tightly and levelling, setting horizontal and vertical angles, setting and inputting instrument occupied point coordinates (north, east and altitude), measuring and inputting height of instrument above occupied point and height of reflector prism, and inputting weather data such as temperature and pressure (Fig. 3.14).

The flow velocity measurement of West Branch Little Cataraqui Creek has been performed by wading (Fig. 3.18). Discharge of Wilton creek has been measured by Environment Canada Water Survey Technicians on the same day the creek was surveyed. Geometric data of cross-sections (bed profile, depth, and width), as well as water surface elevations, of both creeks were collected using the Electronic Total Station.

Figure 3.16 Typical field setup of ADCP, RTK-DGPS and ETS on field survey

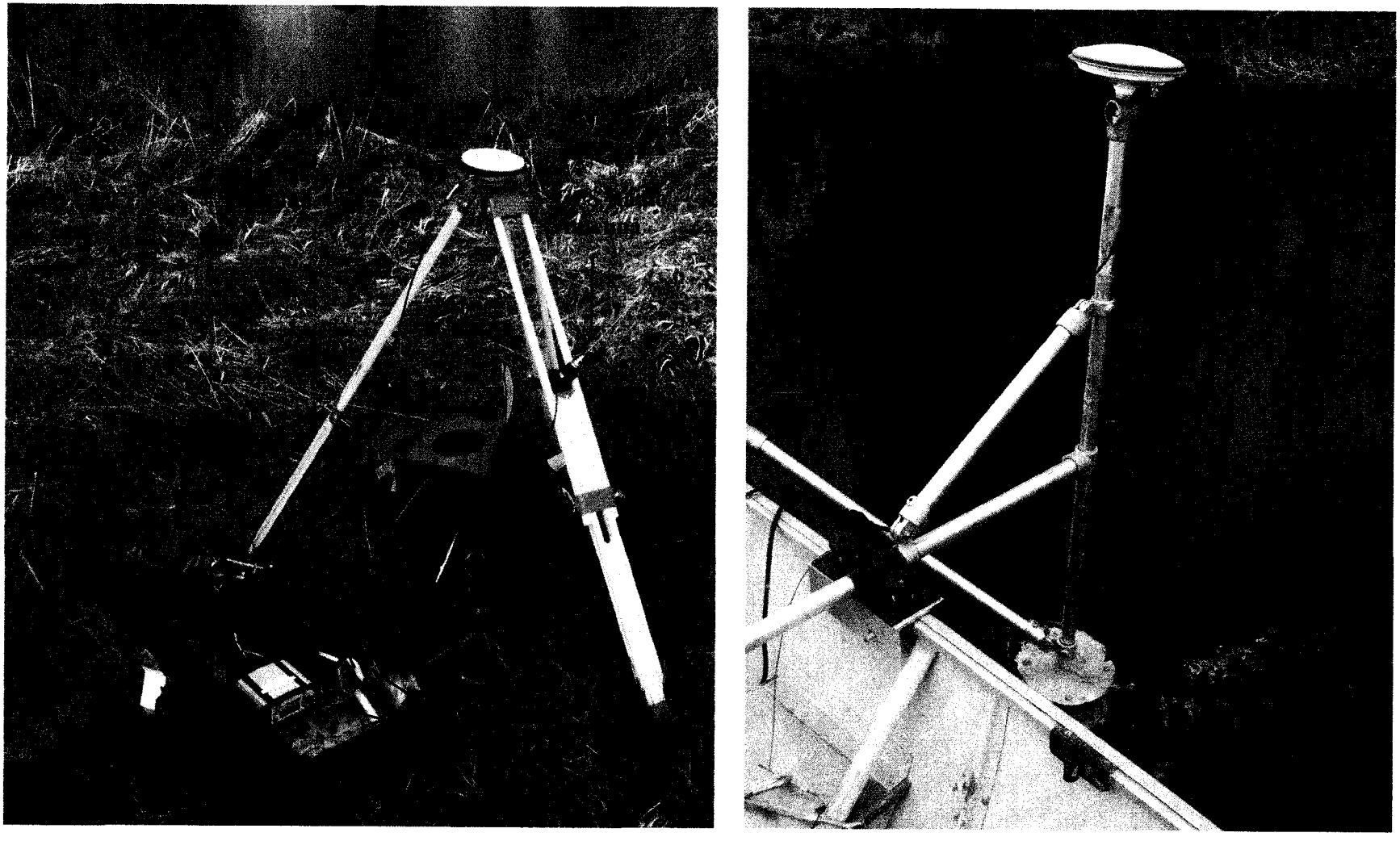

A) B)

Figure 3.17 View of base station GPS (A) and rover GPS and ADCP (B) in operation

Figure 3.18 Measuring flow velocity using propeller current meter, West Branch Little Cataraqui Creek

3.3 Extraction of Discharge and Cross-Sectional Profile Data

3.3.1 Measured Discharge

Discharge in three rivers such as Jock, Raisin and South-Nation were measured by Acoustic Doppler Current Profiler (ADCP) using both bottom tracking and GPS references. Discharge measurements were carried out on two of the rivers (Jock and Raisin) when their flow exceeded bankfull and on the third river (South Nation) when its flow was less than but close to its bankfull discharge. Four or more transects have been used in reciprocal fashion to perform the measurements. The WinRiver software can process each transect to calculate discharge based on either bottom tracking or GPS references. To compute the total discharge during the time of measurement WinRiver estimates the discharge in the unmeasured regions of the cross-section (top, bottom and left and right edges) using configuration data (ADCP depth, extrapolation methods, etc) and inputs during measurement (edge distances) and adds to the measured discharge from the ADCP (middle Q) (Fig.3.19).

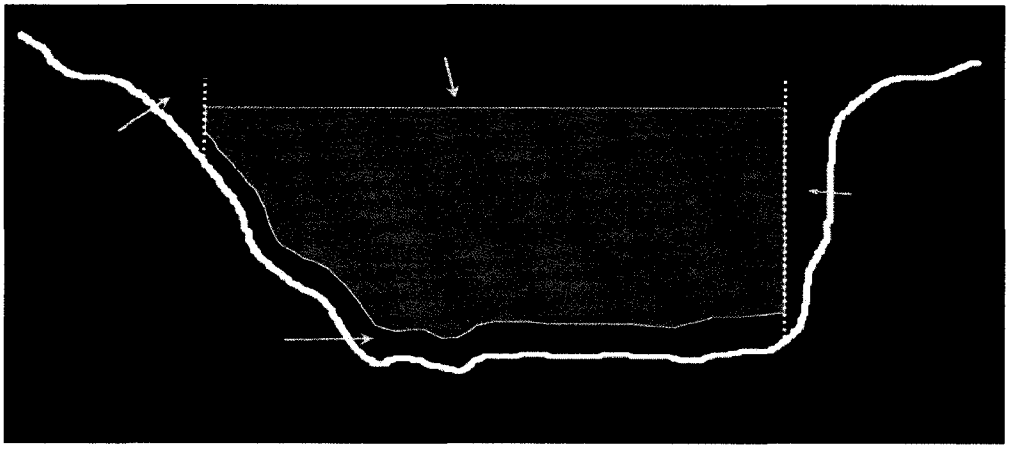

Total Q = Middle Q + Top Q +Bottom Q + Left Q + Right Q

Figure 3.19 Calculation of total discharge at the time of measurement using WinRiver (Adapted from Environment Canada, 2004)

Although moving bed tests did not indicate significant moving bed conditions on any of the three rivers, transect discharges calculated based on bottom tracking reference deviated significantly from one-another or their average for Jock and South Nation rivers. However, transect discharges calculated based on GPS (GGA) references were consistently close to one another and each one of them deviated by less than 5% from their average for all of the three rivers. Hence, for all of the three rivers (Jock, Raisin and South Nation) the average of transect discharges calculated based on GGA reference was adopted (Table 3.3).

Table 3.3 Transect discharges of ADCP measurement from WinRiver

River Name	Transect	Transect Discharges			
		BT[⊗]		GPS (GGA)[⊕]	
		Q_B	$\left(\frac{Q_{BAve}-Q_B}{Q_{BAve}}\right)\cdot 100$	Q_G	$\left(\frac{Q_{BAve}-Q_G}{Q_{GAve}}\right)\cdot 100$
		(m^3/s)	%	(m^3/s)	%
South Nation	16 (L_R)	19.988	-9.1	17.578	-1.8
	17 (R_L)	18.481	-0.9	17.739	-2.7
	18 (L_R)	16.497	10.0	16.784	2.5
	19 (R_L)	18.319	0.0	16.903	1.9
	Average	18.321	0.0	**17.251**	0.0
Jock	1 (R_L)	55.446	7.0	56.488	4.6
	4 (L_R)	62.268	-4.5	61.644	-4.1
	5 (R_L)	59.452	0.3	60.368	-1.9
	6 (L_R)	61.293	-2.8	58.376	1.4
	Average	59.615	0.0	**59.219**	0.0
Raisin	1 (R_L)	41.706	-2.5	41.029	2.3
	2 (L_R)	39.919	1.9	41.842	0.4
	3 (R_L)	39.854	2.1	43.426	-3.4
	4 (L_R)	41.345	-1.6	41.713	0.7
	Average	40.706	0.0	**42.003**	0.0

[⊗]: Q_B is BT discharge of each transects and Q_{BAve} is average BT discharge of all transects

[⊕]: Q_G is GGA discharge of each transects and Q_{GAve} is average GGA discharges of all transects

Discharge on the two creeks such as Wilton and Cataraqui was calculated from velocity measurement carried out using propeller current meter and channel cross-section surveyed with Electronic Total Station (ETS). Cross-sections are regarded as being made up of a number panels or sub-sections, each bordered by two adjacent verticals (Fig. 3.20). To calculate the discharge through each sub-section the average of average velocities and depths at the borders and the width of the sub-section (panel) were used (Eq. 3.3) and the total discharge is the summation of discharges through all sub-sections (Eq. 3.4). The average measured discharges of Wilton and Cataraqui creeks have been calculated to be 5.391 and 0.281 m^3/s respectively.

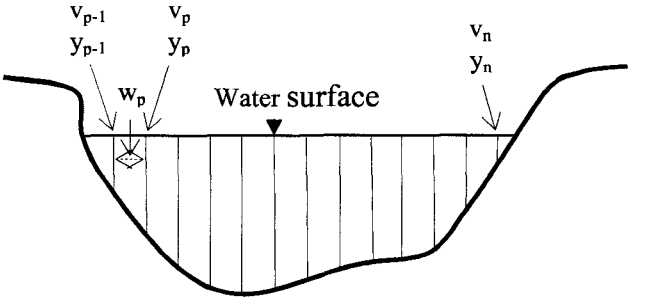

Figure 3.20 Calculation of discharge from propeller current meter and ETS survey

$$Q_p = \left(\frac{v_{p-1} + v_p}{2}\right) \cdot \left(\frac{y_{p-1} + y_p}{2}\right) \cdot w_p \tag{3.3}$$

$$Q_{Total} = \sum_{p=1}^{n} Q_p \tag{3.4}$$

Where:

Q_p is discharge (m^3/sec) through p sub-section

v_{p-1} and v_p are flow velocities (m/sec) at left and right border of p sub-section respectively

y_{p-1} and y_p are depths (m) at left and right border of p sub-section respectively

w_p is width (m) of p subsection (distance between left and right borders of sub-section)

p is an index of channel sub-sections and n is total number of sub-sections

3.3.2 Geometric Data of Cross-Sections

One of the main purposes of the surveys carried out using ADCP and RTK-DGPS supplemented by ETS was to obtain accurate cross-sectional profile data of the river channels. This study utilized the unique capability of ADCP in measuring river depth and RTK-DGPS in collecting three dimensional position coordinates at each ensemble with accuracy level of one to two centimeters to survey the cross-sectional profiles of three rivers (South Nation, Jock and Raisin). ETS were deployed to collect the position coordinates of the edges of river cross-sections where ADCP and RTK-DGPS survey were not possible. The position coordinates of left and right bank benchmarks were surveyed using both RTK-DGPS and ETS, so that the coordinate systems of both instruments can be related to each other. Concurrent position coordinates data from both GPS and ETS are required for at least two points to change the ETS position coordinates of other points to its GPS coordinates or vice versa. Moreover, at some benchmarks where GPS quality was poor, the position coordinates of the benchmarks from ETS can be used to obtain the equivalent good quality GPS position coordinates.

For each cross-section of a river at least four transects were used to extract the channel geometry of a cross-section. While taking a transect measurement with a boat mounted ADCP and GPS, the ideal path would be at right angles to the flow direction of a river and exactly on the same path for all transects. However, in practice this is hardly attainable due to currents and wind which forces the boat not to stay along the desired path. Hence, transect lines are arbitrarily located around the ideal cross-sectional route (Fig. 3.21A). To extract the position coordinates at the measured cross-section along the path perpendicular to the river flow direction the following step-by-step data processing procedure was carried out for all rivers surveyed by ADCP and RTK-GPS.

1) Extraction of GPS position coordinates and transducer depths

Position coordinates (latitude, longitude and altitude) of ensembles of each transect and each transducer depth (i.e., a river depth measured by a transducer) were extracted together with other variables such as ensemble number, coordinated universal time

(UTC), GPS data quality indicator, number of satellites, and GPS Horizontal Dilution of Position (HDOP) from the raw ADCP data file (*.pd0) of each transect. The extraction has been carried out using a binary matlab code written by David S. Mueller (2007) of U.S. Geological Survey, Office of Surface Water and ASCII file output of WinRiver II software.

For all rivers position coordinates with best GPS quality indicator 4 (= Real Time Kinematic; System used in RTK mode with fixed integers, that is, dual frequency measurements) and very good quality HDOP (1-3) were extracted. Position coordinates which had the next best GPS quality indicator 5 (= Float Real Time Kinematic; Satellite system used in RTK mode, floating integers, that is, single frequency measurements) were excluded because up to 3.8 m discrepancy in altitude between the data which had GPS quality indicator 4 and GPS Quality indicator 5 was observed. The river depth below the ADCP transducer at each ensemble of transects was determined by taking an average of the depths measured by four transducers. Ensembles which did not have valid depth measurements (greater than zero) from three or four transducers were excluded.

2) Computing position coordinates of river bed for all transects

Position coordinates of river bed corresponding to each ensemble of all transects was derived from GPS antenna position coordinates directly above each ensemble and river depth at each ensemble.

River depth at an ensemble	=	Depth from water surface to center of ADCP transducers	+	Average depth below transducers

River bed altitude at an ensemble	=	GPS antenna altitude	-	Height of GPS antenna above water surface	-	River depth at an ensemble

3) Generating river bed position coordinates along the path perpendicular to the flow direction

Generation of a cross-sectional profile involved the following analyses:

- ✓ River bed position coordinates of all transects were plotted using ArcGIS software to observe the arrangements of the paths of all transects relative to one another and the flow direction (Fig. 3.21A). The coordinates were projected using UTC projection method, that is, geographic coordinates (latitude (degree) and longitude (degree)) changed to projected coordinates (east (m) and north (m)).
- ✓ Point kriging interpolation method was used to generate grids from the projected transect data using Surfer 8 software.
- ✓ The generated grids were mapped again using ArcGIS software. The position coordinates of benchmarks collected using both GPS (projected) and ETS (digitized) were checked for their accuracy and mapped with the generated grids (Fig. 3.21B)
- ✓ All grid points which fell on the path at right angles to the flow direction and the center of the grid block (i.e., along the line connecting the right and left bench marks) were extracted (Fig. 3.21C).
- ✓ The position coordinates collected using ETS were also digitized and combined with the extracted grids (Fig. 3.21D). Then the cross-sectional profile data (length from left to right and depth) of the surveyed section was calculated from coordinates of the extracted GPS grid points and ETS points. The extracted grid points were presented in Appendix C (Table C.1 – C.5)

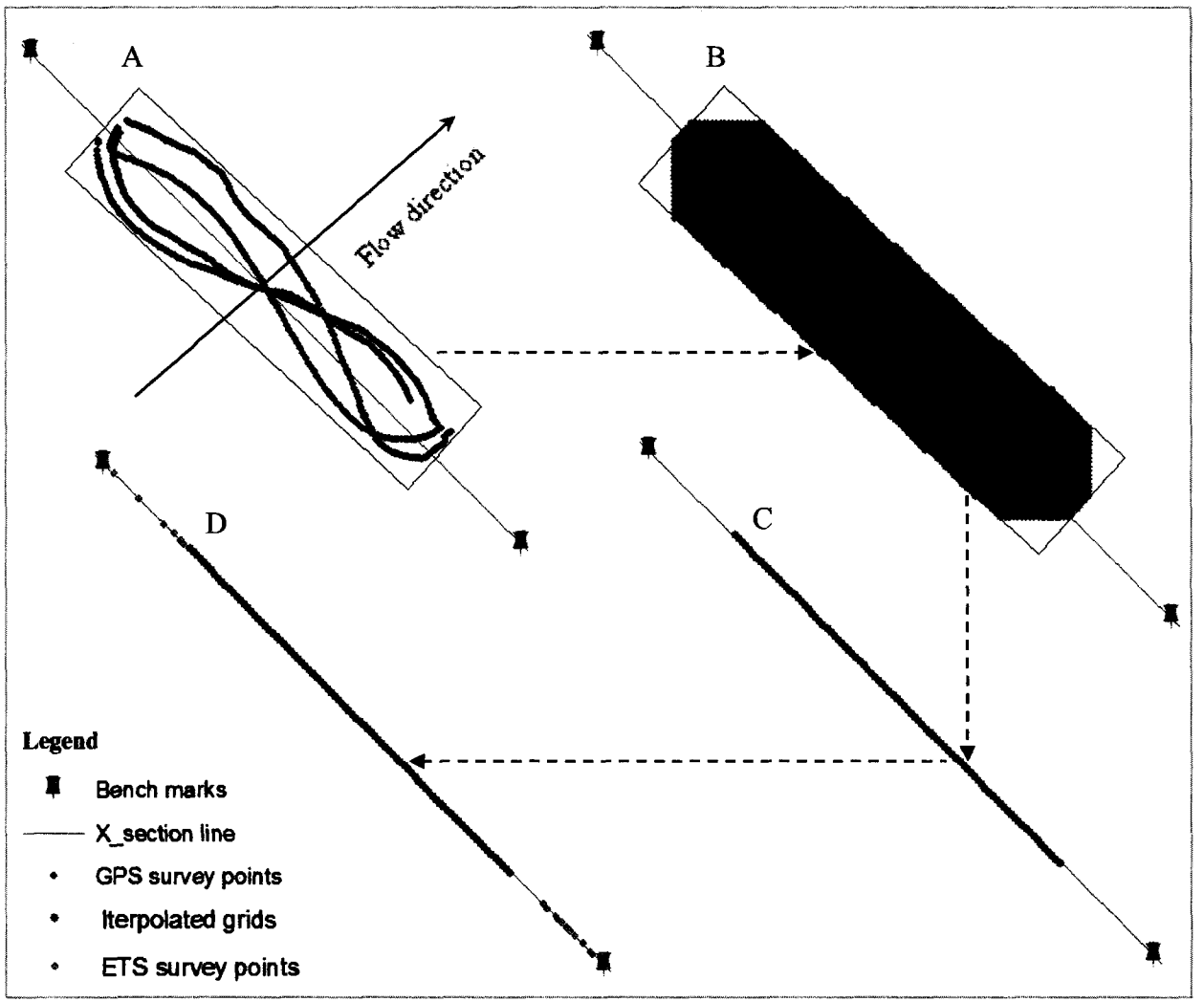

Figure 3.21 Typical steps carried out to extract position coordinates from ADCP, GPS and ETS data (Jock River)
A) Raw GPS survey points of river bed; B) Grids generated from projected GPS survey points
C) GPS grids along the line Perpendicular to flow direction; D) GPS and ETS grids for river cross-section

3.4 Study Streams Bed Material

Bed material samples were collected in each study reach during the 2007 spring freshet field survey in order to classify the bed material. Bed material in rivers that were not surveyed in detail was determined during careful on-site-assessment during summer low flow in the previous year (2006). From rivers such as South Nation, Raisin and Jock, on which boat surveying was deployed, surficial bed material samples were collected from the boat by dragging an Environment Canada bed-material sampler along the river bed. Unfortunately, samples collected by this method may not fully reflect the channel bed material of the reach, because the sampler may not have capable of breaking into and picking up the stable bed material. Furthermore, during the sampling there was also the possibility of trapping material transported as bed-load and deposited on the bed surface. The bed-load transported from upstream may differ in particle characteristics from the consolidated glacial origin silt and clay bed. This is the nature of semi-alluvial rivers. Wilton creek was too narrow to deploy the available boat for field survey as well as too deep to wade in, therefore, its bed material sample was not collected. Bed material samples from the measurement reach on West Branch Little Cataraqui Creek were collected by direct sampling of the stream bed with a knife.

The sieve analysis of the bed material samples indicated that for West Branch Little Cataraqui Creek, about 75% of the particles had the size within the range of silt-clay (i.e., passed through sieve # 200). Jock and Raisin revealed that 47.2% and 45% of the bed surface particles were within the range of silt-clay (i.e., passed through sieve # 200), respectively. Although direct sampling of the bed materials for those two rivers was not possible due to high depth with the instrument used, the high percentages of silt-clay content of their surficial bed material samples indicate the dominant particles of bed material were silt-clay. The silt-clay content of surficial bed material samples from South Nation River was 5%. Although it was not possible to confirm by sieve analysis of the samples, the surficial geology at the study reach of South Nation River undoubtedly suggest the presence of glacial deposit with high silt-clay content (Fig. 3.7). In summary, it was concluded that the dominant bed material of all study reaches was silt-clay.

Chapter Four

4 Analysis and Results

4.1 Peak Discharge Magnitude and Frequency

The peak discharge frequency analysis of all rivers and creeks of this study was performed using the latest version (2005) of USGS PeakFQ program, based on annual maximum series flow data. Program PeakFQ performs statistical flood-frequency analyses of annual maximum flows (annual peaks) following procedures recommended in Bulletin 17B of the Interagency Advisory Committee on Water Data (1982) (Flynn et al., 2006). It uses the method of moments to fit the logarithm of annual peaks of the flow data to the Log-Pearson Type III distribution. The Pearson Type III distribution with log transformation of the flood data (Log-Pearson Type III) is recommended as the basic distribution for defining the annual flood series (Interagency Advisory Committee on Water Data, 1982). Program PeakFQ estimates the parameters of the log-Pearson Type III frequency distribution from the logarithmic sample moments (mean, standard deviation, and coefficient of skewness) of the record of annual peak flows, with adjustments for low outliers, high outliers, historic peaks, and generalized skew (if available). In fact, there were no data such as historical peak and generalized skew for eastern Ontario river data, thus only systematic records (annual maximum flow data) and station skew estimated from the systematic record were used to perform the analysis (Eq..4.1). The Weibull plotting position formula is used for approximating the recurrence interval (T) for the annual maximum series (Interagency Advisory Committee on Water Data, 1982). The results of frequency analysis, such as discharges corresponding to return periods of 1.01, 1.11, 1.25, 1.5, 2, 2.33, 5 and 10 years, are summarised in Table 4.1.

The recurrence intervals of bankfull discharges derived from field measurement and rating curve data (section 4.2) of all study rivers were determined by interpolation. The resulting recurrence intervals for all study rivers appeared to be greater than one year and, hence, frequency analysis based annual maximum series was mathematically capable of

estimating at least up to the morphologically most significant discharge (bankfull) for all rivers.

The Log-Pearson Type III distribution equation:

$$\mathrm{LogQ} = \overline{\mathrm{X}} + \mathrm{K} \cdot \mathrm{SD} \tag{4.1}$$

$$\mathrm{T} = \frac{\mathrm{N}+1}{\mathrm{M}} \tag{4.2}$$

Where:

Q is annual maximum flow data

$\overline{X}$ is mean of the logarithm of annual maximum flow

SD is the standard deviation of the logarithm of annual maximum flow

G is the skew coefficient of the logarithm of annual maximum flow

K is frequency factor — a function of selected frequency (RI) and the skew coefficient (G); tabulated values are available from statistics books.

T is recurrence interval

M = the ordered sequence of flood events with the largest flood equal to 1

N = the total number of flood events (samples) in the data set.

Table 4-1 Recurrence interval discharge (Q_T) data estimated by Log Pearson III flood frequency analysis

Gage Station ID - River Name	Q_T (m^3/s)							
	$Q_{1.01}$	$Q_{1.11}$	$Q_{1.25}$	$Q_{1.5}$	Q_2	$Q_{2.33}$	Q_5	Q_{10}
02LA007- Jock River near Richmond, EON	30.60	49.50	59.90	71.10	84.60	90.70	116.50	136.40
02MC001 – Raisin River near Williams Town, EON	27.80	44.40	53.00	61.80	72.00	76.40	94.00	106.40
02HM009 – West Branch Little Cataraqui Creek at Kingston, EON	0.70	0.90	1.00	1.10	1.20	1.30	1.50	1.70
02HM004 – Wilton Creek near Napanee, EON	7.80	11.60	13.70	15.90	18.50	19.70	24.80	28.80
02GG009 – Bear Creek below Brigden, EON	10.40	28.80	41.70	57.10	77.00	86.30	126.70	157.60
4216875 – Little Tonawanda Creek Tributary near Bativia, NY	2.15	4.45	6.36	9.14	13.79	16.51	33.92	57.17
12331700 – Edwards Gulph at Drummond, MT	0.03	0.10	0.19	0.32	0.56	0.71	1.64	2.83
6307740 – Otter Creek at Ashland, MT	0.05	0.19	0.35	0.61	1.10	1.39	3.38	6.05
6308400 – Pumpkin Creek at mouth, near Miles City, MT	0.52	2.57	4.84	8.54	15.16	19.09	43.55	73.11
02LB007-South Nation River near Spencerville, EON	15.50	24.70	29.80	35.50	42.30	45.50	59.10	70.00

Q_T: Discharge (Q) of T years return period

4.2 Bankfull Discharge from Measured and Rating Data

As it was explained in chapter three, of the five study streams from Eastern Ontario, measurements such as discharge and cross-sectional geometries of three rivers (South Nation, Raisin and Jock) were performed using ADCP, RTK-DGPS and ETS instruments, and on two creeks (Wilton and West Branch Little Cataraqui) using propeller current meter and ETS. Rating data such as stage-discharge relations for all study rivers were obtained from Environment Canada. Discharge measurements of all Study Rivers were made when their flow levels were close to the widely accepted bankfull reference level (top of active flood plain). When discharge measurement on Jock and Raisin rivers were carried out, flow levels were higher than their top of active flood plain. But the flow level of the other three study rivers and creeks (South Nation, Wilton and West Branch Cataraqui) were lower than the level of their bankfull indicators. For three rivers and one creek (South Nation, Raisin, Jock and Wilton) field measurement and rating data were utilised to determine their bankfull discharges. For West Branch Little Cataraqui creek, since the channel geometry at the gauge site and the measurement site do not have similar morphological conditions, bankfull discharge was estimated using field measurement data and flow formula (Manning's equation).

4.2.1 Procedures for estimating bankfull discharge based on rating data

The following procedures were carried out to derive bankfull discharge from field measurements (discharge, water level and bankfull level) and rating data:

1) Calculating change in depth between measured flow water level and bankfull level of a river. Both altitude of water surface during measurement (H_m) and altitude of bankfull level (H_{bf}) were determined based on the same temporary datum established near the measurement section (Fig. 4.1A). Hence, difference of the two levels (δH) was calculated as: $\delta H = H_m - H_{bf}$. The value of δH could be either negative or positive, depending on the water level during measurement relative to bankfull level.

2) Using the rating data (stage-discharge curve or table) of the stream from gauge station at or close to the measurement reach, the stage (H_{mr}) corresponding to the measured discharge (Chapter 3) was determined.
3) Adding the difference of measured water level and bankfull level (δH) from step 1 to measured water level from stage discharge data (H_{mr}) from step 2, the bankfull level based on stage discharge data (H_{bfr}) was determined (Fig. 4.1B). Hence, $H_{bfr} = H_{mr} + \delta H$; the magnitude of H_{bfr} could be greater or equal or less than H_{mr} depending on the magnitude and sign of δH.
4) Therefore, bankfull discharge corresponding to the bankfull level on stage discharge data could be read (Fig. 4.1B).

The above steps were followed to determine the bankfull discharges of South Nation, Jock and Raisin rivers as well as Wilton creek. Their measured discharges and bankfull discharges were summarised in Table 4.2.

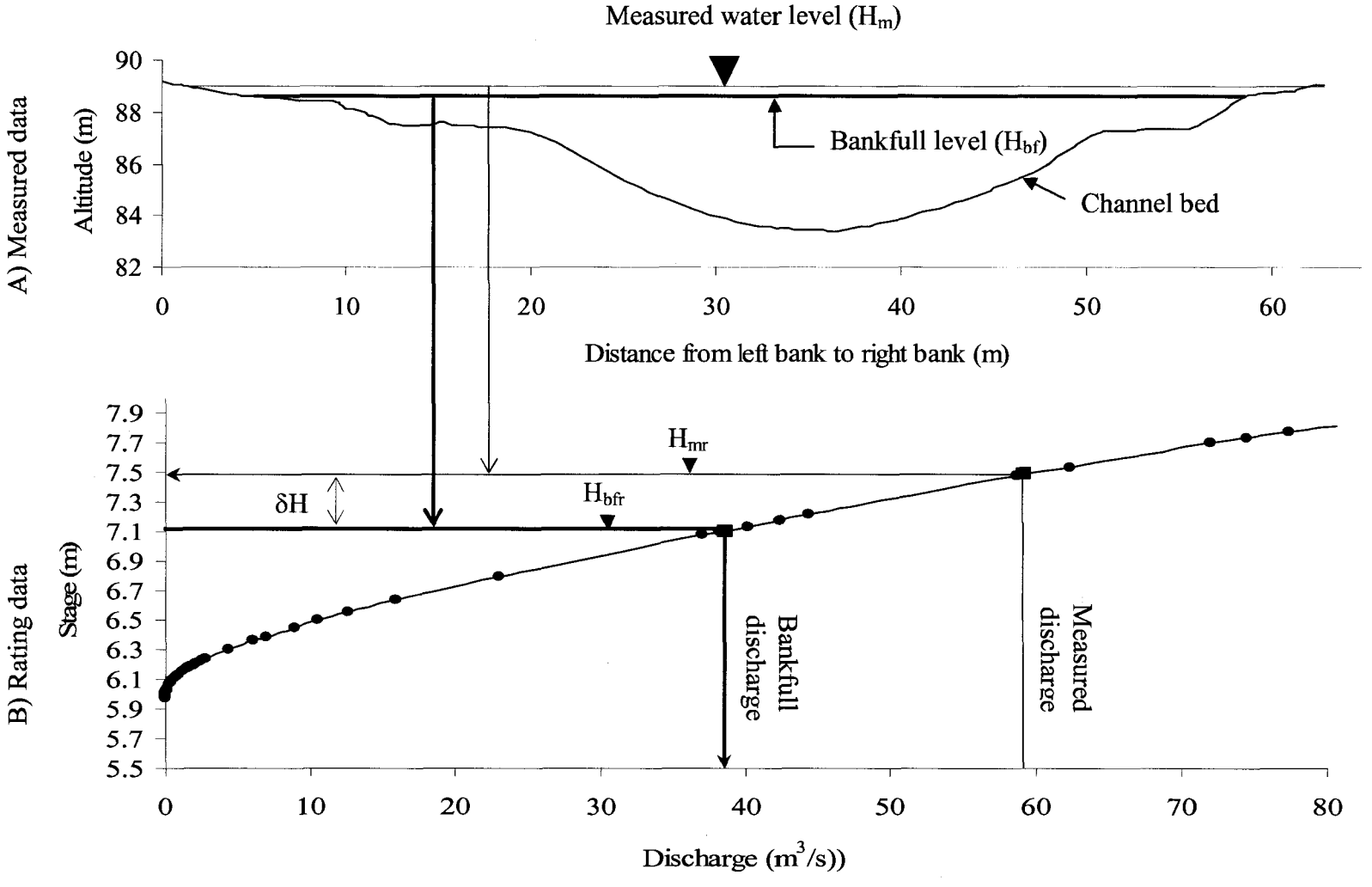

Figure 4.1 Typical diagram showing estimation of bankfull discharge from measured and rating data (Jock River)

4.2.2 Estimating bankfull discharge based on flow equation

Manning's flow formula (Eq. 4.3) and measured discharge data (Chapter Three) have been used to estimate the bankfull discharge of West Branch Little Cataraqui creek. The Manning's roughness, n = 0.06 which is the roughness of similar channel reported in Hicks and Mason (1998), were used. Therefore, using flow variables (discharge, cross-section area, width, hydraulic depth) generated from the survey data, slope for the flow condition during measurement were estimated. During measurement, West Branch Cataraqui creek was carrying a discharge less than its bankfull flow. Therefore, to estimate the bankfull discharge of the creek it was assumed that Manning's roughness and slope would be the same for the measured flow and bankfull flow condition. Measured and estimated bankfull discharges of the creek were incorporated in Table 4.2.

$$Q = \frac{1}{n} \cdot A \cdot D^{2/3} \cdot S^{1/2} \qquad (4.3)$$

Where: Q is discharge (m^3/sec); A is cross –sectional area (m^2); D is hydraulic depth (m) and S is slope (m/m) in and n is Manning's roughness (sec/$m^{1/3}$).

4.3 Derivation of Downstream Hydraulic Geometry Relations

One of the primary objectives of this thesis is to develop a downstream hydraulic geometry (≈ scaling relationship between discharge and hydraulic variables) for clay-dominated cohesive bed rivers and creeks. As it was explained in more detail in the introduction section of this thesis, downstream hydraulic geometry relates haydraulic variables such as bankfull width, mean bankfull depth and mean bankfull velocity to bankfull water and sediment discharge. All hydraulic variables of the study rivers and creeks were generated from field measurement data.

4.3.1 Bankfull Hydraulic Variables

- ✓ Bankfull discharges were generated from field survey data and rating data or flow formula using the method outlined in section 4.2.
- ✓ Bankfull cross-sectional area (A_{bf}) and bankfull top width (w_{bf}) of creeks surveyed only by propeller current meter and ETS were calculated from ETS data using the method explained in section 3.3.1. A similar approach has been also used to calculate the bankfull cross-sectional areas of rivers surveyed using ADCP, RTK_DGPS and ETS. Cross-sections are considered as being made up of a number of sub-sections, each bordered by two adjacent verticals through geometric data points derived from RTK_DGPS and/or ETS position coordinate data (section 3.3.2). Distance between verticals and bankfull width (cumulative of distances between verticals from left to right bankfull level indicators) were calculated using position coordinates from left bank to right bank. The area of the section is calculated through piecewise integration. The area of each sub-section is calculated from the average depth at the borders and the width of the sub-section (distance between left and right borders of a sub-section) (Eq 4.4) and the total cross-sectional area is the cumulative area of the sub-sections (Eq. 4.5).
- ✓ Bankfull mean depth or hydraulic depth (D_{bf}) was calculated by dividing total bankfull cross-sectional area to bankfull top width (Eq. 4.6)
- ✓ Bankfull mean velocity (v_{bf}) was calculated by dividing bankfull discharge to bankfull cross-sectional area (Eq. 4.7).

$$A_p = w_p \cdot \left(\frac{y_{p-1} + y_p}{2} \right) \tag{4.4}$$

$$A_{bf} = \sum_{p=1}^{n} A_p \tag{4.5}$$

$$D_{bf} = \frac{A_{bf}}{w_{bf}} \tag{4.6}$$

$$v_{bf} = \frac{Q_{bf}}{A_{bf}} \tag{4.7}$$

Where:

A_p and w_p area (m^2) and width (m) of p sub-section respectively

y_{p-1} and y_p are bankfull depth (m) at left and right borders of p sub-section respectively

p is order number of sub sections from left to right and n is total number of sub-sections

Q_{bf}, A_{bf}, w_{bf}, D_{bf} and v_{bf} are bankfull discharge (m^3/sec), area (m^2), water surface width (m), mean depth (m) and flow velocity (m/s) respectively.

In addition, hydraulic variables and discharge data from previous studies of cohesive bed rivers in similar physiographic regions were collected to increase the data set for derivation of downstream hydraulic geometry equations, which relate bankfull hydraulic variables (top width, mean depth and mean velocity) to the corresponding bankfull water and sediment discharge. Five other suitable creeks from neighbouring geographic regions were found in the literature: one creek is from southern Ontario, Canada (Annable, 1996), three creeks are from Montana, USA (Lawlor, 2004; Chase, 2004) and one creek is from Hydrologic Region 6 of New York, USA (Mulvihill et al., 2005). All of those creeks have channel bed material that have a characteristic grain size (D_{50}) of less or equal to 0.06 mm. Their bankfull hydraulic variables and bankfull discharges are summarised in Table 4.2.

Table 4-2 Discharges and hydraulic variables of clay-dominated cohesive bed rivers

Gage Station ID - River Name	Discharge		Bankfull Hydraulic Variables				BFD-RI
	Q_M	Q_{bf}	w_{bf}	D_{bf}	v_{bf}	A_{bf}	
	(m^3/s)	(m^3/s)	(m)	(m)	(m/s)	(m^2)	(year)
02LA007- Jock River near Richmond, EON	59.22	38.58	53.50	2.53	0.28	135.39	1.04
02MC001 – Raisin River near Williams Town, EON	42.00	26.55	39.18	2.58	0.26	101.00	1.01
02HM009 – West Branch Little Cataraqui Creek at Kingston, EON	0.28	1.14	5.08	0.57	0.39	2.90	1.69
02HM004 – Wilton Creek near Napanee, EON	5.93	12.63	13.98	1.27	0.71	17.78	1.18
02GG009 – Bear Creek below Brigden, EON	NA	27.94	25.67	2.38	0.46	61.09	1.10
4216875 – Little Tonawanda Creek Tributary near Bativia, NY	NA	1.13	6.69	0.22	0.77	1.46	1.03
12331700 – Edwards Gulph at Drummond, MT	NA	0.40	1.86	0.24	0.88	0.46	1.64
6307740 – Otter Creek at Ashland, MT	NA	0.71	5.79	0.43	0.28	2.51	1.60
6308400 – Pumpkin Creek at mouth, near Miles City, MT	NA	1.84	9.75	0.70	0.28	6.69	1.1
02LB007-South Nation River near Spencerville, EON	17.25	19.66	37.15	1.25	0.43	46.31	1.04

Q_{bf}, w_{bf}, D_{bf}, v_{bf}, A_{bf} are bankfull discharge, width, mean depth and mean velocity respectively; BFD-RI is bankfull discharge recurrence interval

Q_m is measured discharge; NA is not applicable

As described in Chapter 2, Leoopold and Maddock (1953) were the first to introduce the concept of hydraulic geometry, relating hydraulic variables and water and sediment discharge in the form of power equations. Since then, numerous workers followed this concept, and demonstrated that indeed the logarithmic linear (power) relationship is the most suitable approach to describe hydraulic geometry of natural river channels. Linear regression of the logarithm of bankfull discharge versus logarithm of hydraulic variables such as bankfull width, mean depth, mean velocity and area was used to derive downstream hydraulic geometry exponents and coefficients.

Log-linear form of hydraulic geometry (fitting a power curve) may not be always the best to describe the hydraulic geometry of stable river channels (Richrad, 1973 cited in Knighton, 1977). Other forms of equations such as linear, semi-log linear, exponential and polynomial were also fitted to the data and the resulting equations were compared to the result of the log linear regression based on coefficient of determination (r^2). Their respective coefficient of determination (r^2) indicated that indeed, in general, fitting power equations (log-linear) showed better results. In fact, the coefficient of determination value of linear regression also depicted very reasonable fit. The coefficient of determinations obtained by fitting linear curve for width, mean depth, mean velocity and cross-sectional area were 0.90, 0.92, 0.15 and 0.91 respectively.

The resulting power equations are:

$$w_{bf} = 5.07 \cdot Q_{bf}^{0.57} \qquad r^2 = 0.91 \tag{4.8}$$

$$D_{bf} = 0.40 \cdot Q_{bf}^{0.52} \qquad r^2 = 0.91 \tag{4.9}$$

$$v_{bf} = 0.49 \cdot Q_{bf}^{-0.09} \qquad r^2 = 0.11 \tag{4.10}$$

$$A_{bf} = 2.13 \cdot Q_{bf}^{1.09} \qquad r^2 = 0.95 \tag{4.11}$$

Table 4-3 95% confidence interval of the exponents and coefficients

Confidence interval	Exponents			Coefficients		
	b	f	m	a	c	k
Lower 95%	0.41	0.37	-0.32	3.56	0.29	0.30
Upper 95%	0.73	0.67	0.14	7.23	0.56	0.80

The regression result curves were also presented in Figs. 4.2 - 4.5. The sum of the exponents (a, c and k) and the product of the coefficients (b, f and m) of hydraulic geometry of bankfull width, mean depth and mean velocity must be unity (Eq. 1.5 and 1.6) in order to satisfy continuity (Eq. 1.4). The coefficients, a, c and k are equal to 5.07, 0.40 and 0.49 respectively and their product is approximately 1; the exponents, b, f, and m are 0.57, 0.52 and -0.09 respectively and their sum is 1. The upper and lower 95% confidence intervals of regression analysis for all exponents (b, f and m) and coefficients (a, c and k) are indicated in Table 4.3. Furthermore, a step by step regression analysis, which leaves one variable out at each step, was used for validation and the results are discussed in Appendix F.

$$a \cdot c \cdot k = 5.07 \times 0.40 \times 0.49 \approx 0.994 \tag{4.12}$$

$$b + f + m = 0.57 + 0.52 + (-0.09) = 1.0 \tag{4.13}$$

The result indicates that 91% of the variation of the bankfull width and the bankfull mean depth of clay-dominated cohesive bed river channels are explained by the magnitude of discharge. According to these results, the variation of bankfull mean flow velocity of clay-dominated cohesive bed river channels is poorly explained by their bankfull discharge. However, the variation of bankfull cross-sectional area is dictated by water discharge more than any other hydraulic parameters considered in the above analysis. About 95% of the bankfull cross-sectional area variation is the result of discharge that the clay-dominated cohesive bed river can accommodate within the section up to top of bank level. The plots of cross-sectional profiles that indicate water surface level during measurement and estimated bankfull stage, and pictures taken from the surveyed reaches of all study rivers in eastern Ontario were indicated in Figs. 4.6 to 4.10.

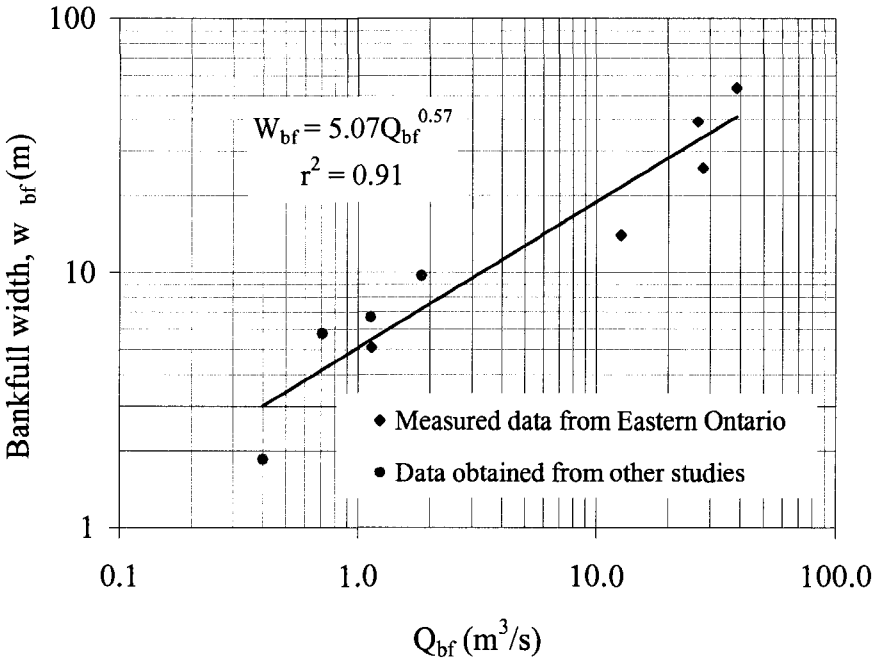

Figure 4.2 Downstream hydraulic geometry of bankfull width

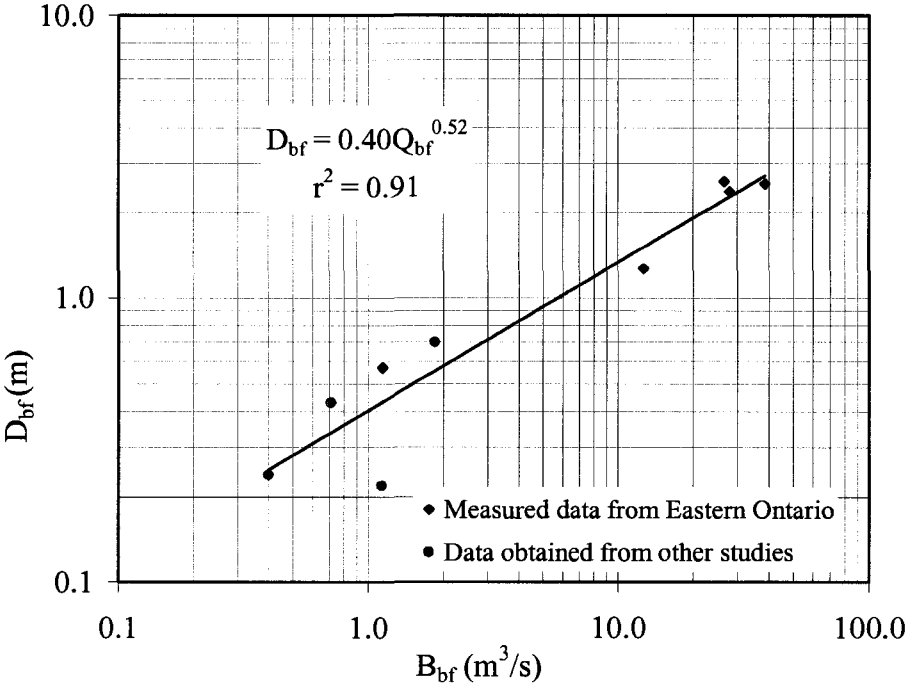

Figure 4.3 Downstream hydraulic geometry of bankfull mean depth

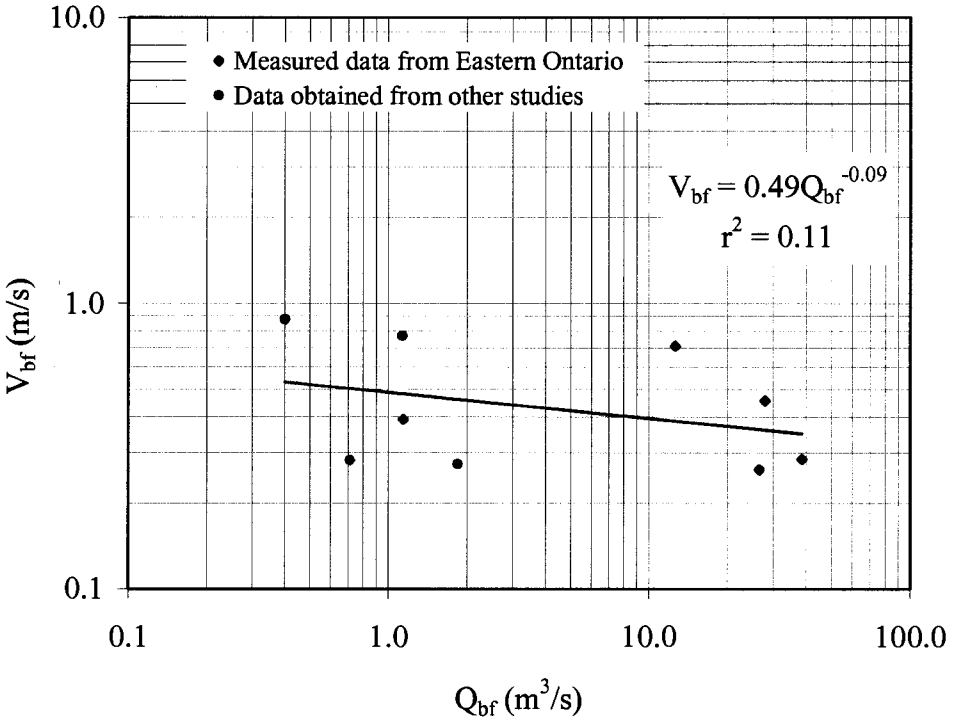

Figure 4.4 Downstream hydraulic geometry of bankfull mean velocity

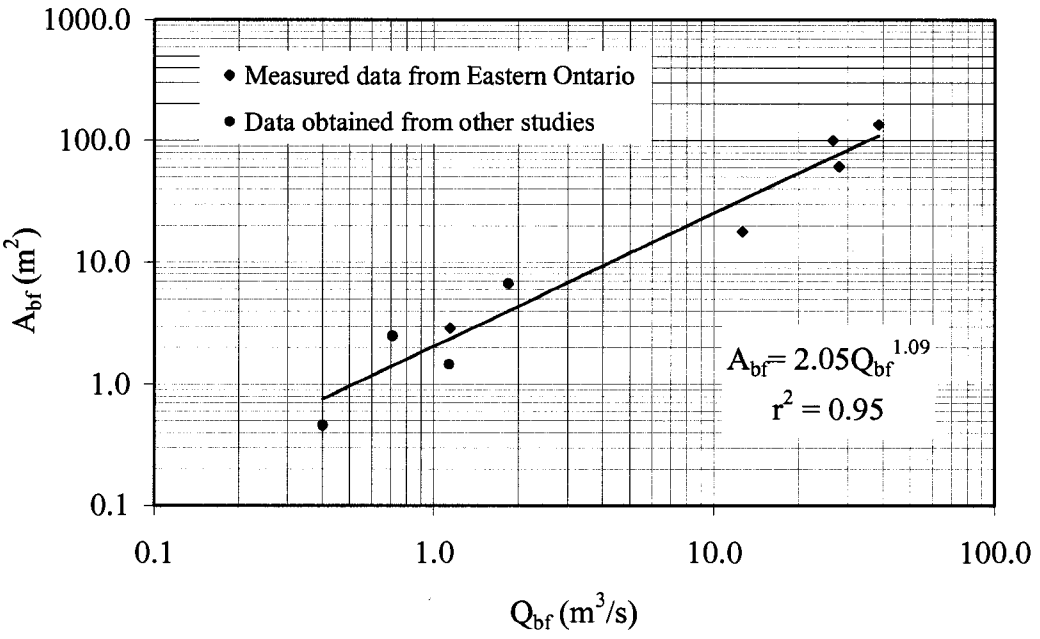

Figure 4.5 Downstream hydraulic geometry of bankfull area

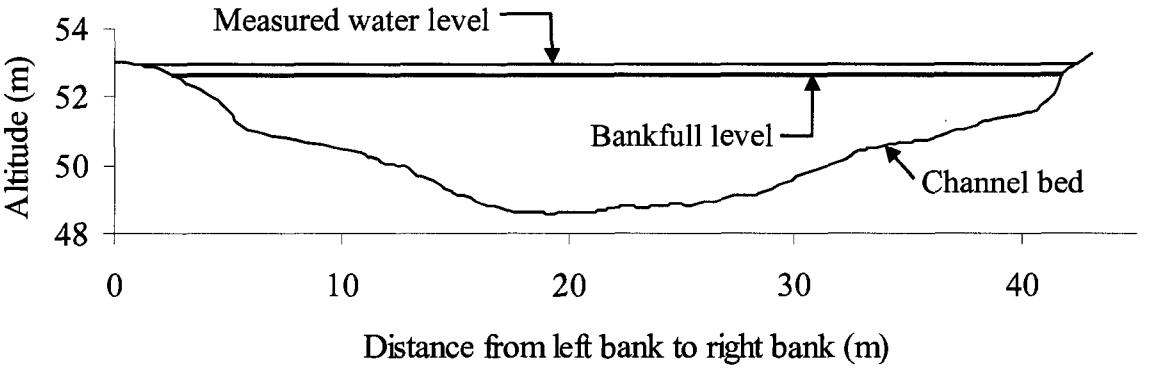

Figure 4.6 Cross-sectional profile of Raisin River

Figure 4.7 Raisin River study reach on measurement day

Figure 4.8 Raisin River study reach indicating left bank channel morphology

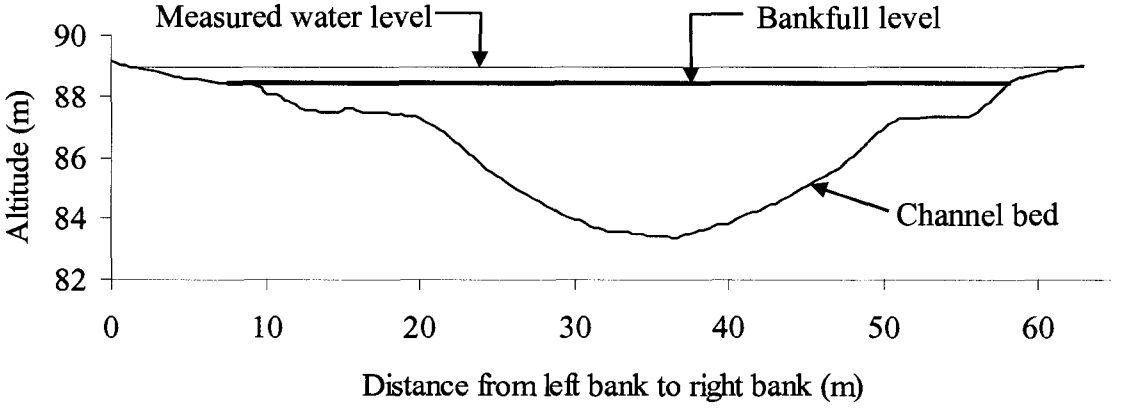

Figure 4.9 Cross-sectional profile of Jock River

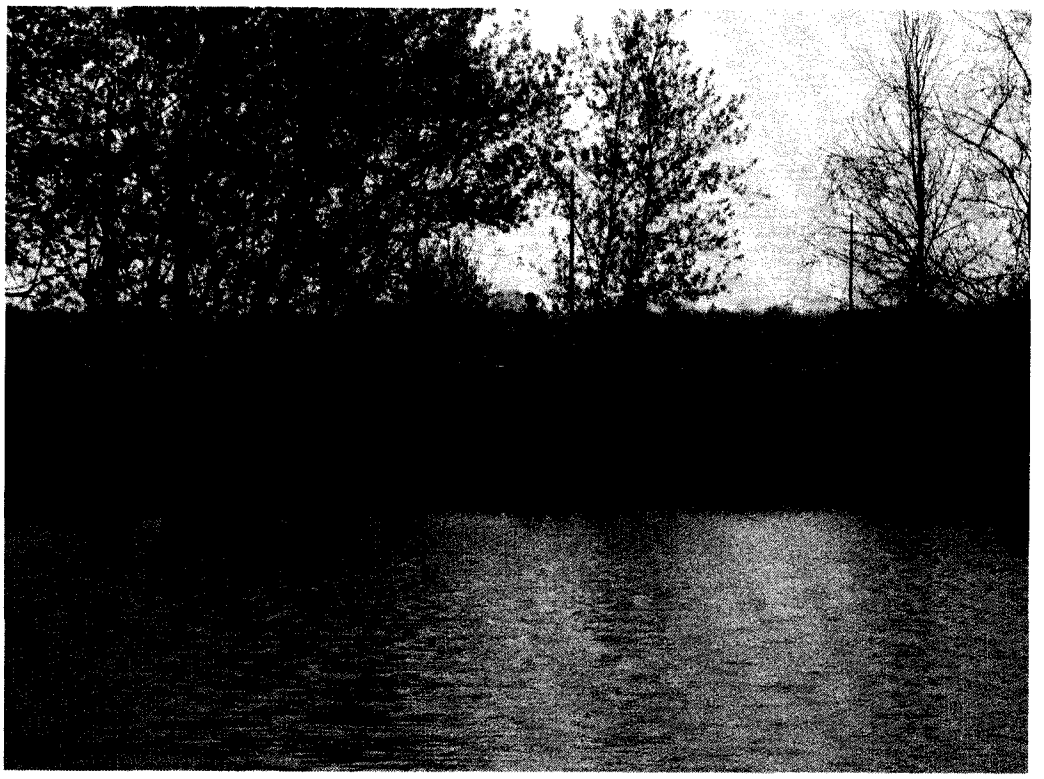

Figure 4.10 Jock River (right bank)

Figure 4.11 Jock River (left bank)

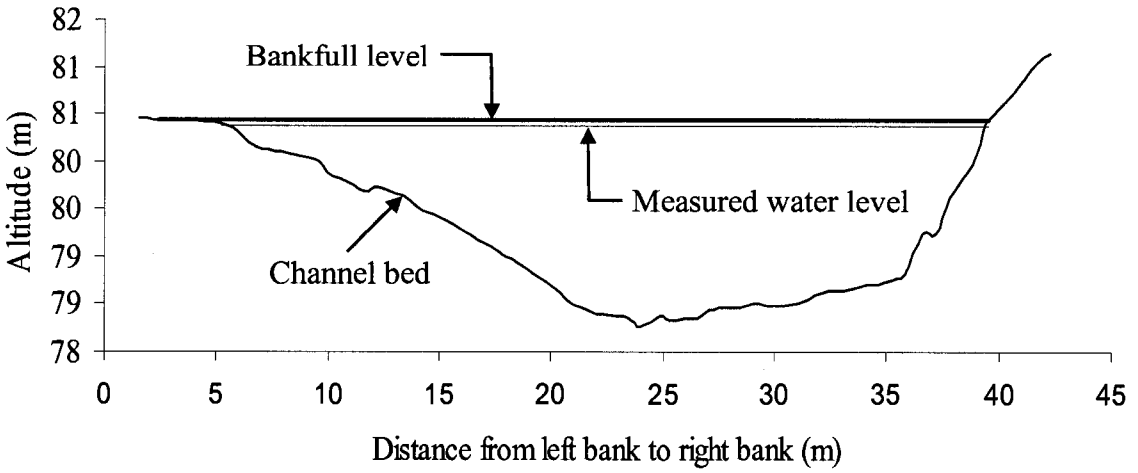

Figure 4.12 South Nation River cross-section

Figure 4.13 South Nation River study reach on measurement day

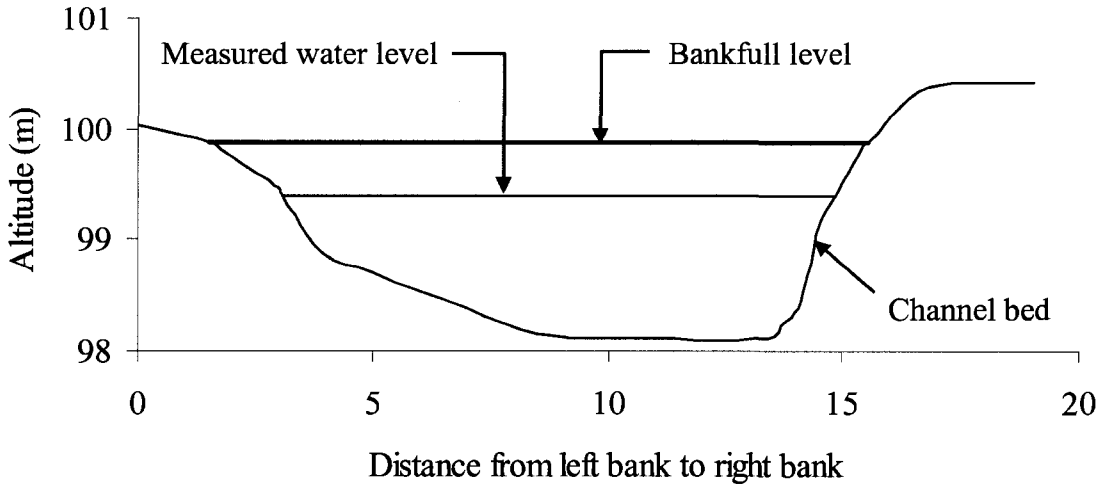

Figure 4.14 Cross-sectional profile of Wilton Creek

Figure 4.15 Wilton Creek study reach on measurement day

Figure 4.16 WiltonCreek study reach during low flow (Summer 2006)

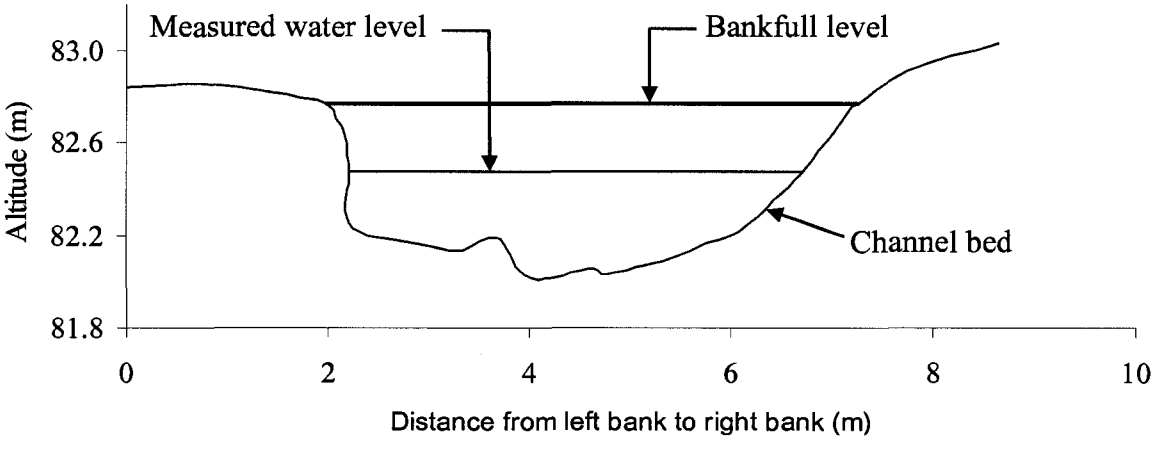

Figure 4.17 Cross-sectional profile West Brach Little Cataraqui Creek

Figure 4.18 West Branch Little Cataraqui Creek study reach

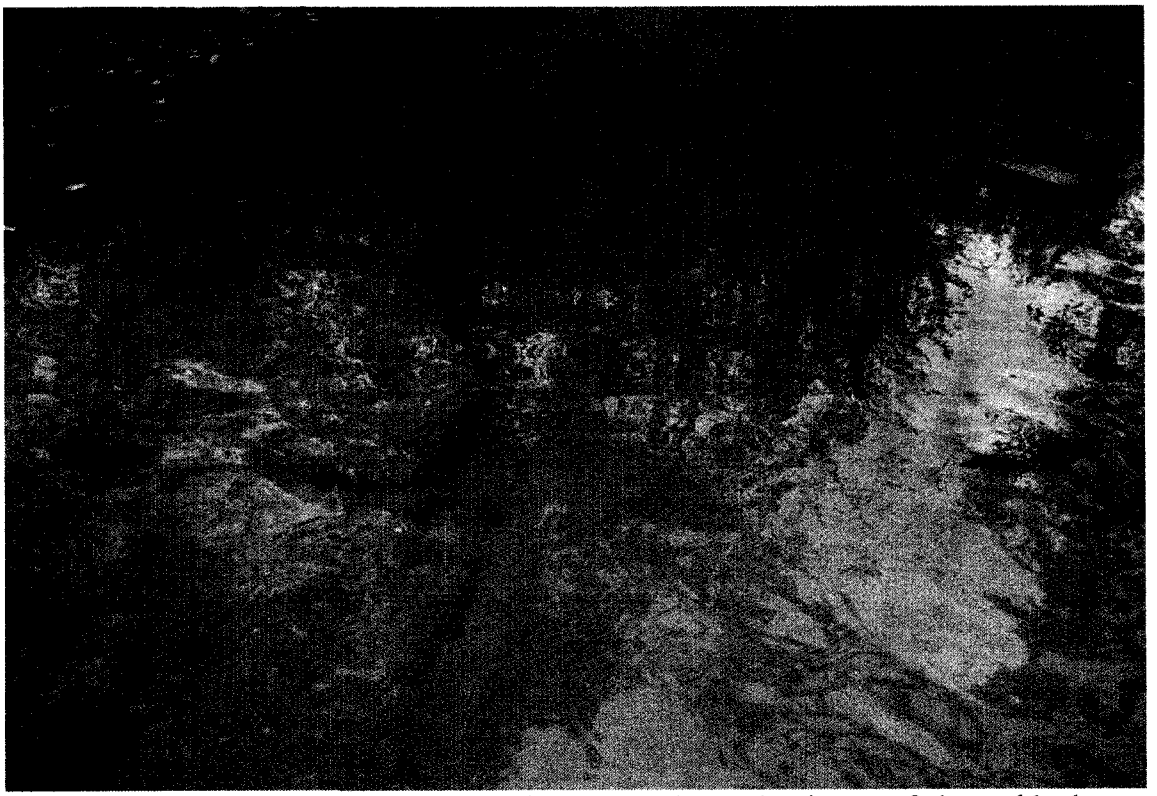

Figure 4.19 West Branch Little Cataraqui Creek study reach, picture of channel bed.

Chapter Five

5 Discussion

5.1 The Challenge and Importance of Estimating Bankfull Discharge

Discharge is one of the most important driving forces for the formation and adjustment of stream channel morphology, through scouring of banks and bed and transport and deposition of sediment. Hence, discharge is a key parameter to understand the past, assess the present, and forecast the future morphological changes in a fluvial system. Furthermore, it is a major reference for assessing the suitability of streams as aquatic habitat, and in fact it is the most reliable independent variable in the study of hydraulic geometry relations. Therefore, the dependability of all kinds of studies in the fluvial system primarily depends on the accuracy of discharge measurement.

Accurate discharge measurement is a challenging task for hydrologists, engineers and geomorphologts. The majority of channel morphology researchers believe that bankfull discharge is a single reference discharge that reasonably represents the channel forming discharge (dominant discharge). The three most commonly used methods of determining bankfull discharge in natural streams are: 1) estimating from field survey data, 2) computing as effective discharge from bed-load data and flow-duration data, and 3) as recurrence interval discharge, commonly the 1.5 year return period discharge. However, previous studies have indicated that effective discharge method generally underestimates bankfull discharge (Pickup and Warner, 1976; Whiting et al., 1999; Copeland et al., 2005). Furthermore, the return period of bankfull discharge can be significantly different from 1.5 years. Hence, bankfull discharges for the study rivers of this research were estimated from field survey data.

Discharge measurements were made when the flow level in the rivers was close to bankfull level to increase the accuracy of the estimation of bankfull discharges. Surveys on two creeks were made with the traditional propeller current meter and Electronic Total Station. However, the three larger rivers (South Nation, Raisin and Jock) were too deep to

wade across and conduct measurements with the traditional propeller current meter. To overcome the accessibility problem and carry out accurate discharge measurement and cross-section survey, Acoustic Doppler Current Profiler (ADCP) and Real Time Kinematic Differential Global Positioning System (RTK-DGPS) were deployed from a boat. This study is the first to deploy a relatively modern method of stream survey using ADCP and RTK-DGPS to accurately collect cross-sectional data and measure discharges on such lower depth rivers for the purpose of bankfull discharge computation and downstream hydraulic geometry study.

The discharge readings from the gage stations which have real-time hydrometric data (Jock and Raisin) on the same day, at about the same time as the time of measurement indicated very small difference from the measured discharges. For Jock River the difference was only 3.08 m^3/s and for Raisin River it was 5.39 m^3/s. These represent approximately 5% and 11% differences, respectively. There are several possible explanations for these discrepancies. First, ADCP discharge measurements require extrapolation of measured velocities for unmeasured areas (see Chapter 3). Similarly, traditional gauging methods with propeller meters employ measurement of velocity at several verticals across the section, and sectional integration of these profiles. Thus, discharge estimation with either technique requires some approximation to translate velocity measurements to discharge. Second, it is possible that the Environment Canada rating curves were outdated due to morphological change in the cross-section due to sediment transport. Finally, the measurements occurred on the falling limb of the hydrograph. It is possible that discharge was changing during the period of measurement (approximately one hour for four repeat transects on each river). However, this is difficult to verify from the gauge records, which were recorded every 15 minutes, and the ADCP data do not display a decreasing trend in discharge with time. For all rivers, the ADCP data displayed less than 5% variation in measured discharge between transects and their average, which is the criterion employed by Environment Canada to verify good discharge measurement.

In addition to the difficulties of discharge measurement, field determination of bankfull level, which is key factor for accurate computation of bankfull discharge by the field survey method, is very challenging for river morphology researchers. Typical methods of defining bankfull level were reviewed in Chapter Two.

The elevation of active flood plain (top of flood plain) is the most commonly used and reliable definition of bankfull level for perennial or intermittent streams of humid regions. Top of Active flood plain can be considered as the most morphologically significant level because it is the transition point from the main river channel to its floodplain. After conducting careful assessments of evident bankfull indicators at the survey reaches of the study rivers and creeks (Raisin, Jock, Wilton, and West Branch Little Cataraqui), elevation of active flood plain was the most noticeable and reliable indicator to define the bankfull level. Where apparent identification of active flood plain was difficult, change in bank slope was used to estimate the bankfull level. For West Branch Little Cataraqui Creek both top of active flood plain and permanent vegetation such as grasses and shrubs, led to the same bankfull level. However, for Jock and Raisin rivers, the lower limit of perennial vegetation (mostly trees) and top of active flood plain were substantially different. Although trees on both banks of those rivers appeared to play locally bank stabilizing roles, their lower limits were not sufficiently consistent throughout the reaches to be considered as a reasonable bankfull level indicator. In most cases their lower limit level was far below the top of active flood plain of both left and right banks. Futhermore, the lower vegetation limit level at left and right banks of a single cross-section was inconsistent, as well as on one bank within the reach. Riley (1972) downgraded the usefulness of vegetation for defining bankfull level for similar reasons: "trees often delineate banks of larger streams, but they are not reliable indicators of bankfull since they frequently occur at irregular elevations on the banks."

Unfortunately, there were also elevation differences between the identified left and right bank top of active flood plain on both rivers (Jock and Raisin). The right bank indicators (top of active flood plain) were taken as bankfull level of the channel sections on both rivers since they were more evident than the left top of active flood plain and the flows

corresponding to the right bank level were well within the reasonable range of the theoretical bankfull discharges based on annual frequency analysis. On South Nation River, perennial vegetation (trees and shrubs) were reasonable bankfull level indicators. Their lower limit led to the same conclusion on both left and right banks and coincided with the slope changes of both left and right banks.

Bankfull level identified by field survey, discharge measured during field survey and the rating data obtained from Environment Canada were used to compute the bankfull discharge for each study river (refer to Chapter 4). The recurrence intervals of the bankfull discharges of all study rivers were computed using log-Pearson Type III distribution frequency analysis based on annual maximum series flow data. The recurrence intervals of bankfull discharges of all study rivers (see Table 4.2) were within the range of 1 to 2 years, which is the range of the typical recurrence interval for bankfull discharge in natural streams from humid regions. The result is in good agreement with the recurrence intervals of the bankfull discharges of streams in the neighbouring regions with similar climatic condition. Almost all of the 43 streams from Southern Ontario investigated by Annable (1996) had bankfull discharges with recurrence intervals ranging from 1 to 2 years. Bankfull discharge recurrence interval for five snowmelt-dominated rivers in the northern Rocky Mountains, USA ranged from 1.5 to 1.7 (Emmet and Wolman, 2001) and for Yampa River Basin fell between 1.18 and 1.40 years (Andrew, 1980). For 16 streams in central New York, 14 streams in southern Tier New York, and 10 streams in western New York (region 7 adjacent to Eastern Ontario) bankfull discharge recurrence interval ranged from 1.11 to 3.40, 1.01 to 2.35, and 1.05 to 3.60 years, respectively (Westergard et al, 2004; Muluihill et al., 2005, 2006). Miller and Davis (2003) reported the average bankfull discharge recurrence intervals ranged from 1.2 to 2.7 years for three other hydrologic regions of New York State.

The concept of bankfull discharge (channel forming) was generally assumed to be applicable only for alluvial stable streams. Alluvial streams are free to adjust their shape and dimensions, such as width, depth and slope, in response to changes in discharge and watershed sediment (US-FISRWG, 1998; Trenhaile, 2005). Four of the five study rivers

of this research have erosion resistant consolidated cohesive (clay-silt) bed, i.e., they possess semi-alluvial channels. However, the recurrence intervals of their bankfull discharges were within the range of the classical 1 to 2 years and hence comparable to that of most alluvial rivers. Therefore, the result of this study indicated that the applicability of the concept of channel forming (bankfull) discharge is not limited to alluvial stable channels and can be extended to semi-alluvial channels.

5.2 Discussion on Downstream Hydraulic Geometry Relations

Rivers adjust their hydraulic and geometric channel variables to accommodate the variation of discharge both at a single cross section and/or spatially along their course in the downstream direction. Downstream hydraulic geometry is used to describe the relation between the spatial variation of discharges with hydraulic and/or geometric variables on a single river system in the downstream direction and/or on multiple rivers usually from similar physiographic regions. The concept can be applied to almost all hydraulic and geometric variables of streams. However, the results of the majority of extant hydraulic geometry studies indicate that rivers accommodate the spatial variation of discharge for the most part by adjusting their width and depth.

Bed and bank materials of the stream channels are one of the primary factors which influence the responses of streams to the variation of water and sediment discharge. In nature, the materials through which the streams make their channel are seldom the same from the head water region (beginning) to the lowland region (mouth). In addition to the variation of stream channel materials due to the general trend of fining in downstream direction, channel materials reflect the local or regional variations of the geology of the area. Likewise, the adjustments of a river channel to the changes of discharge along its course are expected to be variable due to the geological variation. Coarse (gravels, cobbles, and boulders) or cohesive channel materials have high resistance to the scouring effect of the discharges that the streams carry.

If the cohesiveness of channel bed material is very high (i.e., high percent of silt-clay) it possesses high resistance to erosion and the channel will be narrow, but if the channel bed

material has less or no cohesive materials (i.e. small percent of or no silt-clay) it is less resistant to erosion and the channel will generally be wide (Shumm, 1960; Ostertkamp and Hedman, 1982). The cohesiveness of silt-clay provides resistance to erosion due to the electrochemical properties of their particles (Knighton, 1998). Alluvial river channels which have sand as a dominant channel material are wide and highly susceptible to erosive and deposition effects of flows (Knighton, 1998). If the dominant channel material is coarse (much greater than 2 mm), there will be a possibility of the formation of armour layer (coarser surface layer) which plays a bed stabilizing role by providing shear resistance to flow at the bed (Kellerhals 1967; Montgomery and MacDonald, 2002; Ostertkamp and Hedman, 1982).

The analysis of surface geology maps of eastern Ontario (Ontario Geological Survey, 2003), indicates that glacially derived sediments such as tills and glaciomarine and glaciolacustrine silts and clays are widespread in eastern Ontario. There are also many streams across the region which cut their channel into those deposits. Stream channels with bed materials from consolidated glaciomarine and glaciolacustrine sediment deposits are cohesive as their dominant particles are within the range of silt-clay. From the study streams of this research which have beds from consolidated glaciolacustrine sediment deposits, appropriate sampling of bed material was possible only for one (West Branch Little Cataraqui creek); for the rest due to high depth flow, direct sampling of their bed material was impossible. For West Branch Little Cataraqui, about 75% of the particles had the size within the range of silt-clay (i.e., passed through the standard sieve # 200). The sieve analysis results of the surficial bed material from Jock and Raisin revealed that 47.2% and 45% of the bed surface particles were within the range of silt-clay (i.e., passed through standard sieve # 200) respectively. This high percentage of silt-clay content of surficial bed material samples indicates the dominant particles of bed material are silt-clay.

Review of extant downstream hydraulic geometry studies indicated that works done so far on the hydraulic geometry study of natural rivers with cohesive bed (semi-alluvial) channels are very limited in comparison to alluvial channels with coarser bed materials (sand, gravel and cobles). The author and his supervisor are not aware of any previous

downstream hydraulic geometry study on cohesive bed natural streams; more specifically on streams which have clay dominated cohesive bed. The phrase 'Clay dominated cohesive bed' is used to represent semi-alluvial channel bed materials from consolidated glaciomarine and glaciolacustrine sediment deposits or cohesive bed materials with median particle size (D_{50}) less than or equal to 0.06mm. One possible reason for less work done on natural rivers with cohesive channels is the relative scarcity of this type of river, particularly in a homogeneous climatic and physiographic region, and the consequent insufficiency of data to conduct reliable hydraulic geometry analysis. Other possible reasons might be: many researchers consider that the concept of bankfull discharge as well as hydraulic geometry is applicable only for alluvial river channels; the complex physical and chemical properties inherent in cohesive materials, which complicate defining threshold values such as threshold discharge or velocity or critical shear stress; and, the absence of gauging facilities at cohesive bed reaches. Furthermore, cohesive channels have accessibility problems due to narrow channels with steep, slippery banks and abundant vegetation conditions which impedes morphological survey. In the present research, poor accessibility prevented detailed morphological survey on Bear Brook River reach at Bourget during high flow conditions (i.e., a flow depth close to bankfull discharge).

Simons and Albertson (1963) applied a regime theory in order to derive an empirical equation similar to downstream hydraulic geometry approach from a wide range of channel data (cohesive to non-cohesive) of Indian and United States sources. However, out of 24 channel reaches data from the United States, used by Simons and Albertsons (1963) only one reach fulfills the criteria used in this study to define cohesive (clay/silt) bed — median grain size (D_{50}) should be less or equal to 0.06mm. Thus, their bed material is predominantly sand. Moreover, the channels were canals conveying regulated flows and sediments, which make them quite different from the natural and unregulated river systems of the present research. Osterkamp et al. (1982) conducted channel geometry study on several streams with a wide range of bed material from high silt-clay bed to cobble bed. Channel geometry is similar to the hydraulic geometry concept, except it uses discharge as the dependent variable and geometric parameters such as width and

depth as independent variables, and it is used as a method of indirectly estimating discharge characteristics at ungaged channel sites (Osterkamp et al., 1983 and 1982). They divided channel type based on the dominant particles of the bed material and derived channel geometry which related characteristic discharge to active channel width of river channels with high cohesive bed (61 to 100% silt-clay).

However, Osterkamp et al. (1982) did not use bankfull channel variables and bankfull discharge, instead they related different discharge characteristics such as mean annual discharge and discharges with recurrence intervals of 2, 5, 10, 25, 50 and 100 to width at active channel reference level. Hence, their results can not be compared to the results of this research. Active channel reference level is the lower limit of perennial vegetation for perennial and intermittent streams (Osterkamp et al., 1983) or in Montgomery and MacDonald (2003) it was defined as a reference to the largely unvegetated portion of the channel, at least for some portion of the year, and inundated at times of high discharge

Hydraulic geometry relations derived from different bed and bank materials were included in Table 5.1 for comparison purpose although their bed is not from cohesive material. Streams from the Bollin-Dean basin, U.K (Knighton, 1974) have cohesive banks but beds composed of largely pebbles. The pebble beds may have been armoured, thus the beds are expected to have similar competence to that of clay dominated cohesive beds in resisting erosion. Knighton (1974) related 2 years recurrence interval discharge to bankfull hydraulic parameters. The bank materials of channel data collected from Brandywine creek and tributaries were predominately cohesive, but the bed materials were also composed largely of gravel with bed material D_{50} ranging from 18 mm to 104 mm (Wolman, 1955). Hydraulic geometry of gravel-bed rivers from Emmet (1975) and Hey and Thorne (1986) were also included for the same reason. Hydraulic geometry relations derived from sand bed canals studied by Simons and Albertson (1963) and sand-bed natural river channels data (mean depth $\geq$ 1.5m) collected from several literatures are also incorporated for comparison purpose.

Table 5.1 Some downstream hydraulic geometry data taken from literature for comparison with the results of this study

Source	b	f	m	a	c	k	Note
This study	0.57	0.52	-0.09	5.07	0.40	0.49	Cohesive bed river
A) Simons and Albertson (1963)	0.5	0.36	--	5.23	0.69	--	Sandy banks and bed
B) Simons and Albertson (1963)	0.5	0.36	--	2.55	0.45	--	Cohesive banks and sandy bed; large load
C) Simons and Albertson (1963)	0.5	0.36	--	3.93	0.58	--	Cohesive banks and sandy bed; small load
Osterkamp et al. (1982)	0.47[1]	--	--	5.14[2]	--	--	Cohesive bed river
Emmett (1975)	0.54	0.34	0.12	2.86	0.28		Gravel bed
Hey and Thorne (1986)	0.45	0.35	--	3.67	0.33	--	Gravel bed
Knighton (1974)	0.61	0.31	0.08	--	--	--	Pebble bed river
Wolman (1955)	0.42	0.45	0.05	--	--	--	D_{50} = 18 – 104 mm
Cited in Singh (2003) from Ponton (1972)	0.60	0.40	-0.01	--	--	--	Green river
	0.80	0.44	-0.23	--	--	--	Birkenhood River
Natural sand bed rivers	0.60	0.23	0.17	2.68	0.93	0.40	Depth ≥ 1.5m

$w = aQ^b$, $d = cQ^f$, $v = kQ^m$; --: not available; [1, 2]: Deduced from Channel geometry relations

w, d, v and *Q* are width, mean depth, mean velocity and discharge respectively.

b, f, m, a, c, and *k* are constants.

The absence of extant hydraulic geometry studies conducted specifically on clay dominated cohesive bed streams, limits comparison of the findings of this study to

previous research. However, the high correlations (a good fit) between major channel parameters (bankfull width and depth) and bankfull discharge indicated the applicability of the concept of downstream hydraulic geometry for clay dominated cohesive (semi-alluvial) channels analogous to fully alluvial natural streams. In fact, the exponent of width (b) is within the range of the exponents reported for previous studies (see Table 5.1 and Table 2.2 of Chapter 2). Furthermore, the relatively higher value of the exponent (b) and coefficient (a) of the width equation suggests the prevailing means of accommodating increased discharge for cohesive bed streams is through lateral (width) adjustment.

However, the depth exponent was greater in these clay-bed channels than for typical gravel-bed rivers, thus it appears that cohesive clay-bed channels have width to depth ratios that are intermediate between less erodible gravel-bed and highly erodible sand-bed channels. Analysis of width:depth ratio relations (Fig. 5.1) shows that sand-bed channels are relatively narrow and deep. Large clay-bed channels in the present study were also narrower and deeper than gravel-bed channels with the same conveyance capacity, but small clay-bed channels were actually wider and shallower than respective gravel-bed channels. The width to depth ratio of a channel should depend on the relative erodibility of the bed and banks. Relatively erodible banks will result in wider and shallower channels, and relatively erodible beds will result in deeper and narrower channels. Clay-bed channels with clay banks should have bed and bank materials with comparable erodibility, whereas sand-bed channels with relatively fine bank materials that display some cohesion likely have beds that are more erodible than banks. Thus, sand-bed channels should be more likely to develop relatively deeper and narrower channels than the stiff clay-bed channels of this study. Gravel-bed channels, on the other hand, have relatively resistant bed material, and thus develop relatively wider and shallower channels. It is worth noting that the findings of this study are somewhat contrary to conventional wisdom that clay channels are narrower than both sand-bed and gravel-bed channels for a given discharge (Church 1992). It appears that the consolidated stiff clay of the channels in this research had beds that were relatively resistant to erosion.

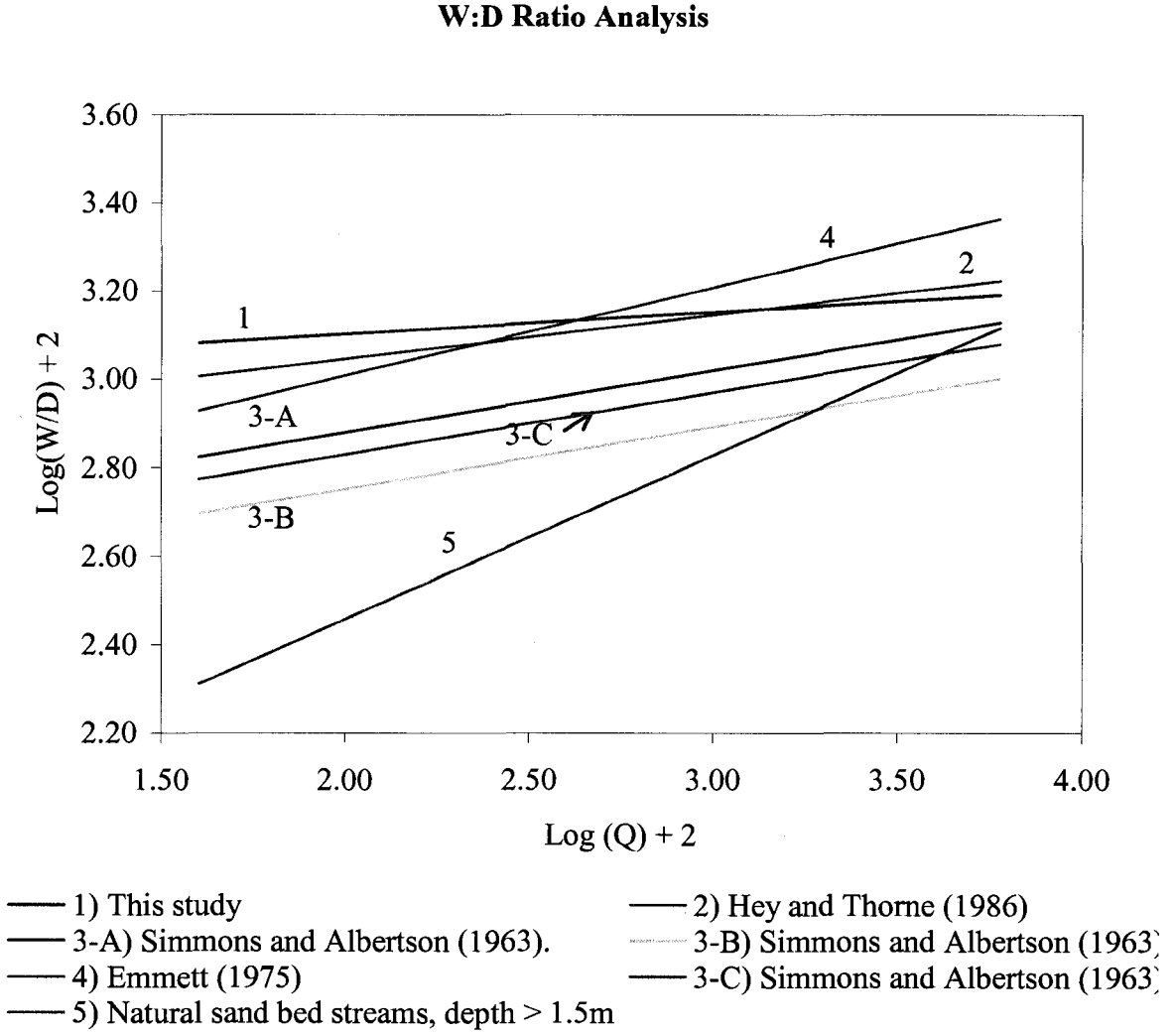

Figure 5.1 Comparison of width to depth ratio versus discharge plot of this study to others (The dominant bed material of channels from which each hydraulic geometry relation derived was indicated in Table 5.1)

The regression of bankfull area and bankfull discharge indicated the highest coefficient of determination (r^2 = 0.95). This means about 95% of the changes in bankfull cross-sectional area can be attributed to change in bankfull discharge. This implies that when width increases or decreases from the predicted value, depth responds in the opposite direction (i.e. flow area = width × depth remains near the predicted value). Hence, flow area would be the most reliable in predictions of bankfull discharge (Emmett, 1975).

The regression of bankfull mean velocity showed the lowest coefficient of determination ($r^2 = 0.11$). The poor correlation of mean velocity to discharge in downstream hydraulic geometry is fairly consistent with the results of the majority of the previous studies. However, the negative exponent that is a decrease of velocity moving down stream along the same river or among different size streams was contrary to the majority of the previous downstream hydraulic geometry (scaling) relations. But it is worth noting that, the regression was not significant as the 95% confidence interval of exponent (-0.32 to 0.14) was very wide, and not significantly different from zero. In fact, there is only about 60% confidence (-0.178 to 0.005) that the velocity exponent was less than or equal to zero.

Since slope decreases in downstream direction, it was believed that velocity also decreases before Leopold and Maddock (1953) challenged this classic geomorphic concept by showing that velocity increases in downstream direction (Carlston, 1969; Ledger, 1981). In fact, almost all previous hydraulic geometry studies reviewed indicated that velocity either slightly increases or approximately remains constant in comparison to considerable increase of the two major geometric channel variables (width and depth) in the downstream direction (see Table 2.2 of Chapter 2).

Wolman (1955) showed that at no stage does the mean velocity decrease downstream; during low flow conditions mean velocity increases and during higher flow conditions it apparently remains constant in downstream direction. Leopold (1953) used stream-gaging data on 20 rivers from Yellow Stone River Basin and also found a constant downstream velocity during both the 5 year and 50 year floods. Ledger (1981) also used velocity measurement at fourteen hydrometric stations in the Tweed basin, Scotland and concluded that at low flows velocity increases but at higher flows (i.e., greater than mean flood and 10 year flood levels) it is reasonable to assume constant velocity in the downstream direction. However, some workers such as Carlston (1969) challenged the absolute conclusion of only an increase or a constant velocity in downstream direction: "*My own studies and the studies by Brush in the Susquehanna River basin show that the number of streams with a downstream velocity increase are balanced by an equal number of streams with either a constant velocity or downstream decrease in velocity. In these studies the*

modal exponent for velocity in downstream direction is zero". Furthermore, three of the 16 streams in central Pennsylvania that Brush (1961) used to derive downstream hydraulic geometry relations had a negative velocity exponent (m); although, the velocity exponent of the equation derived from basin-wide data (using data from all 16 streams) was positive (0.09).

Singh (2003) stated that "*Ponton (1972) found the hydraulic geometry of the Green and Birkenhood River basins in British Columbia, Canada, to significantly depart from the previous works, and attributed the departure to the recent glaciation in the area and the strong control which glacial features* exercise *on streams. He concluded that the equilibrium throughout the stream was not established. Many reaches within each system may have reached a quasi-equilibrium, as indicated by the at-a-station hydraulic geometry. However, these reaches were not yet adjusted to each other because of glacial features which separate them."* The hydraulic geometry relation of the most dominant channel variable (width) of this study fairly agrees with the findings of pervious studies. Ponton's (1972) conclusion could perhaps be one of the possible postulations for the departure of depth and velocity exponents of this study. However, to validate and/or provide further speculation for the sources these departures, extensive data from rivers which have glacial origin bed material (glaciomarine and glaciolacustrine silts and clays) are required.

Downstream hydraulic geometry relations can be used for preliminary design and evaluation of river channels, preliminary assessment of stream restoration projects, and suitability assessment of streams by using as an initial estimation of hydraulic variables such as width, depth and velocity given discharge or vice versa. Surface geology map of Canada indicates that glacial origin deposits with high silt-clay are wide spread across Canada, particularly in Manitoba, Saskatchewan, South-eastern Ontario, South-western Quebec and some in Alberta. This indicates that the clay-silt deposits of glacial origin are very common across the Canadian fluvial system and particularly in eastern Ontario, streams which have incised their channel through them are also very common. The results of this study can be useful for preliminary assessment of cohesive bed streams.

Furthermore, it can be used as a tool to estimate the initial dimension of stable clay channels for other purposes, such as design of stable irrigation channels. The author believes that the findings of this research can be used as a good start and reference for future hydraulic geometry research in the region or elsewhere on semi-alluvial (clay dominated cohesive bed) streams. However, since the data used for this study are very few in number, more data are required to validate or improve the findings of this study so that it can be used confidently for practical applications such as design and assessment of cohesive bed channels.

Chapter Six

6 Conclusion

Numerous downstream hydraulic geometry studies have been conducted worldwide on natural stable stream channels since the concept was first introduced by Leopold and Maddock (1953). The majority of the previous studies focussed on alluvial stream channels. Stream channels are classified as alluvial, semi-alluvial and non-alluvial based on the type of bank and bed materials as well as sediment load being transported by the streams. Streams are classified as alluvial when their channels are formed from materials once transported and/or deposited by the streams themselves and usually free to adjust their shape and dimensions to accommodate changes in discharge. However, semi-alluvial channels have at least either one of their banks or a bed composed of a material resistant to erosion and slightly or fully different from sediment that the river transports for most flow conditions.

Surface geology map of eastern Ontario indicates that glacial origin deposits, glaciomarine and glaciolacustrine silts and clays are wide spread across the region. There are also many streams which cut into those deposits. As these deposits are consolidated and stiff cohesive materials, they are highly resistant to erosion and streams which flow over these deposits are semi-alluvial. To the author's knowledge, no hydraulic geometry relations have been derived previously from semi-alluvial channels, specifically channels which have bed materials such as from glaciolacustrine silts and clay deposits.

ADCP and RTK-DGPS were deployed to collect position data and measure discharges of half of the study rivers. This study showed that a field surveying method which deploys ADCP and RTK-DGPS can be used to simultaneously measure discharge and collect data required to compute cross-sectional geometry with reasonable accuracy. This surveying method has tremendous advantages in that it can be deployed when flows are high (i.e., close to or at bankfull level) and therefore, can be used to avoid the prerequisite of gauging facility for streams to be considered for hydraulic geometry study. Moreover, it is

the best solution to the problems associated with the usage of traditional propeller current meter and other instruments which usually necessitate wading across the streams.

Bankfull discharges of five streams from eastern Ontario were computed and their recurrence intervals were also determined using log-Pearson Type III distribution frequency analysis based on annual maximum series flow data. Downstream hydraulic geometry equations which related bankfull width, mean depth and mean velocity to bankfull discharge were derived for semi-alluvial (clay dominated cohesive bed) channels using the data from four streams in eastern Ontario region and five other suitable creeks from neighbouring geographic regions found in the literature. Based on the results obtained the following conclusions can be made:

1) The frequencies of bankfull discharges of semi-alluvial streams of eastern Ontario region are with in the range of 1 to 2 years, which falls within the worldwide typical range of recurrence interval of bankfull discharge for humid region natural streams. This indicates that bankfull discharge is a single morphologically significant reference flow to represent channel forming discharge and the applicability of the bankfull discharge concept to streams which cut into erosion resistant semi-alluvial (clay-dominated cohesive deposits) bed material.
2) The correlations of major channel parameters (bankfull width and depth) to bankfull discharge were very high. The width exponent (b) was within the range reported in many of the previous studies. Bankfull width shows one of the strongest and dependable basin scale relationships when it is related to bankfull discharge (Annable, 1996; Ellis and Church, 2005). This fact illustrates the applicability of the concept of downstream hydraulic geometry for clay dominated cohesive (semi-alluvial) channels analogous to fully alluvial natural streams.
3) The exponent (b) of width equation was high. Therefore it is reasonable to conclude the prevailing means of accommodating varying discharge for cohesive bed streams is through lateral (i.e. width) adjustment. Assessment of width:depth ratio suggests that the clay-bed channels in this study were wider than typical sand-bed rivers, and similar in shape to gravel-bed rivers. Large channels were narrower and narrower than

comparable gravel-bed channels, but small channels were actually wider and shallower than typical gravel-bed rivers. This can likely be attributed to the resistance of stiff and consolidated cohesive bed to erosive effects of more frequent flows.

4) The correlation of bankfull area to bankfull discharge had the highest coefficient of determination ($r^2 \approx 0.95$). The overall variations of the two major channel parameters (width and depth) were explained better by the variation of discharge when combined in the form of area than when considered independently.
5) The poor correlation of mean velocity to discharge in downstream hydraulic geometry is fairly consistent with the results of the majority of the previous studies. However, the negative exponent i.e., a decrease of velocity moving downstream along the same river, or from small to large among different size streams, was contrary to the majority of the previous downstream hydraulic geometry (scaling) relations.

Canada has very diverse climate and physiographic regions from west cost to east cost and from north to south. The climatic, geologic and topographic variations either locally or regionally influence morphological characteristics of stream channels. Therefore, downstream hydraulic geometry equations which take in to account specifically the geological origin of channel materials are very essential when their application to specific channel formation is required. Of the many previous morphological studies reported in the Canadian fluvial environment, high calibre works include Annable (1996) who conducted extensive study to compile a database of morphological characteristics of watercourses in Southern Ontario, and Kellerhals et al. (1972) who compiled detailed hydraulic and geomorphic characteristics of rivers in Alberta.

The hydraulic geometry equations derived in this study is for channels with specific bed material (clay dominated cohesive); therefore, these equations are expected to be reliable for practical applications such as morphological assessment or design of semi-alluvial channels with similar bed material. However, since the data used to generate the equations are very limited, more data or future extensive studies are required to validate them. This study proved that ADCP and RTK-DGPS complemented with ETS can be successfully applied to collect data with reasonable accuracy for hydraulic geometry study. Especially,

if they are deployed when flows are high (i.e., close to or at bankfull level), it will be possible to avoid the requirement of gauging facility for streams to be considered for hydraulic geometry study. Therefore, the author recommends that other ungauged local rivers be surveyed using ADCP and RTK-DGPS to extend the data set. Furthermore, the author is confident that the results of this research can be used as a good start and reference for the future hydraulic geometry research on semi-alluvial (clay dominated cohesive bed) streams.

References

Allen, P.M, Arnold, J.G. and Byars, B.W., 1994. Downstream Channel Geometry for use in Planning-level Models. Journal of Water Resources Bulletin, Vol. 30: 663-971.

Anderson, R.J. Bledsoe, B.P., and Hession, W.C., 2004. Width of Streams and Rivers in Response to Vegetation, Bank Material, and Other Factors. Journal of the American Water Resources Association (JAWRA) 40(5):1159-1172.

Andrews, E. D., 1980. Effective and Bankfull Discharges of Streams in the Yampa Basin, Colorado and Wyoming. Journal of Hydrology, 46: 311-330.

Andrews, E. D., 1984. Bed Material Entrainment and Hydraulic Geometry of Gravel Bed Rivers in Colorado. Geological Society of America Bulletin, 95: 371-378.

Annable, W.K., 1996. Database of Morphological Characteristics of Watercourses in Southern Ontario. Ministry of Natural Resources, Ontario, 212 p.

Annable, W.K., 1996. Morphologic Relationships of Rural Watercourses in Southern Ontario and Selected Field Methods in Fluvial Geomorphology. Toronto, Ontario Ministry of Natural Resources, 92 p.

Bagnold, R.W., 1960. Sediment Discharge and Stream Power: A Preliminary Announcement. Geological Survey Circular 421, US Geological Survey, Washington, 22 p.

BC Guidelines of RTK GPS Surveys, 2005. British Columbia Guidelines For GPS RTK surveys, including operating within a Municipal Active Control System area (BC ACSm) – Release 1.0. Ministry of Sustainable Resource Management Base mapping and Geomatic Services Branch, 43 p.

Bedient, P.B. and Huber, W.C., 1992. Hydrology and Flood Plain Analysis, Second Edition. Addison-Wesley Publishing Company, 692 p.

Beyer, P.J., 2006. Variability in Channel form in a Free-flowing Dry-land River. River Research and Application, 22: 203–217.

Biedenharn, D.S., Copeland, R.R. and Fischenic, J.C., 2000. Channel-Forming Discharge. U.S. Army Engineer, Technical Note, ERDC/CHL CHETN-VIII-5, 10 p.

Boiten, W., 2000. Hydrometry. A.A. Balkema, Rotterdam, Netherlands, 245 p.

Brush, L.M., 1961. Drainage Basins, Channels and Flow characteristics of Selected streams in central Pennsylvania. United States Geological Survey Professional Paper 282 –F, 44 p.

Burns, M.M, 1998. Limitations of Hydraulic Geometry Techniques in Stream Restoration Design: Engineering Approaches to Ecosystem Restoration. Wetlands Engineering and River Restoration Conference 1998, Editor: Donald F. Hayes , Denver, Colorado, USA, 7 p.

Burns, M.M., 2004. Limitations of Hydraulic Geometry Techniques in Stream Restoration Design. ASCE, 9 p.

Carlton, C.W., 1969. Dounstream Variations in the Hydraulic Geometry of Streams: Special Emphasis on Mean Velocity. American Journal of Science, Vol. 267: 499-509.

Chang, H. H., 1979A. Geometry of Rivers in Regime. Journal of hydraulics Division, Vol. 105, No. HY6: 691-705.

Chang, H. H., 1979B. Minimum Stream Power and River Channel Patterns. Journal of hydrology, Vol. 41: 303-327.

Chase, K.J., 2004. Channel-Morphology Data for the Tongue River and Selected Tributaries, South eastern Montana, 2001-02. U.S. Geological Survey, Reston, Virginia, Open File Report:1260, 79 p.

Cheema, M. N., Marino, M. A. and de Vries, J. J., 1997. Stable Width of an Alluvial Channel. Journal of Irrigation and Drainage Engineering, Vol. 123, No. 1: 55-61.

Church, M. 1992. Channel Morphology and Typology. In Calow, P. and Petts, G.E., editors. The rivers handbook, Vol. 1, Oxford, Blackwell Science: 126-143.

Copeland, R., Soar, P. and Thorne, C., 2005. Channel-forming Discharge and Hydraulic Geometry width Predictors in Meandering Sand-bed Rivers. World Water Congress; Impact of Global Climate Change, World Water and Environmental Resources Congress; ASCE: 1-12.

Copeland, R.R., Biedenharn, D.S., and Fischenich, J.C., 2000. Channel-Forming Discharge. US Army Corps of Engineers, ERDC/CHL CHETN-VIII-5, 9 p.

Crowder, D.W. and Knapp, H.V., 2005. Effective Discharge Recurrence Intervals of Illinois Streams. Journal of Geomorphology, Vol. 64: 167-184.

Dalrymple, T., 1960. Flood-Frequency Analyses: Manual of Hydrology: Part 3, Flood-Flow Techniques. Geological Survey Water-Supply Paper: 1543-A, Washington, 85 p.

Davis, T.R. and Sutherland, A.J., 1980. Short Communications: Resistance to Flow Past Deformable Boundaries. Journal of Earth Surface Process, Vol. 5: 175-179.

Davis, T.R.H. and Sutherland, A.J, 1983. Extremal Hypothesis for River Behavoir. Journal of Water Resources Research, Vol. 19, No. 1: 141-148.

Dosselman, E., 2004. Discussion: "Hydraulic Geometry of Straight Alluvial Channels and the Principles of Least Action by H.Q. Huang, G.C. Nanson and S.D. Fagan", Journal of Hydraulic Research, Vol. 42, No 2: 219-222.

Doyle, M.W., Shields, D., Boyd, K.F., Skidemore, P.B. and Dominick, D., 2007. Channel-Forming Discharge Selection in River Restoration Design. Journal of Hydraulic Engineering, Vol. 133, No.7: 831-837.

Dudley, R.W., 2004. Hydraulic-Geometry Relations for Rivers in Costal and Central Maine. U.S Department of Interior and U.S. Geological Survey, Scientific Investigation Report 2004-5042, 30 p.

Dury, G.H., 1976. Discharge Prediction, Present and Former, Form Channel Dimensions. Journal of Hydrolgy, Vol. 30: 219-245.

Ebisa-Fola, M., 2006. Hydraulic Gemmetry Study of Semi-Alluvial Rivers in Eastern Ontario. CVG6108 Directed Study Report, Course Supervisor: Professor Colin D. Rennie, 119 p.

Ellis, E. R., and Church, M., 2005. Hydraulic Geometry of Secondary Channels of Lower Fraser River, British Columbia, from Acoustic Doppler Profiling. Journal of Water Resources Research, Vol. 41: 1-15.

Emmett, W.W., 1975. The Channels and Waters of the Upper Salmon River, Idaho., United States Geological Survey, Professional Paper 870-A Washington, DC, 116 p.

Emmett, W.W., 2004. A Historical Perspective on Regional Channel Geometry Curves. USDA Forest Services; Stream Systems Technology Center, Stream Notes, downloaded in January, 2006 at URL: http://stream.fs.fed.us/news/streamnt/pdf/jan04.pdf: 5 - 6.

Emmett, W.W., and Leopold, L.B., 1964. Discussion: Geometry of River Channels, by W.B. Langbein, ASCE Proceedings, Vol. 90, HY5: 277-285

Emmett, W.W., and Wolman, M.G., 2001. Effective Discharge and Gravel-bed Rivers: Earth Surface Processes and Landforms, Vol. 26: 1369-1380.

Environment Canada, 2004. Procedures for Conducting ADCP Discharge Measurements. Water Survey of Canada, Hydrometric Operations Division, SOP001-2004, 25 p.

Flynn, K.M., Kirby, W.H., and Hummel, P.R., 2006. User's Manual for Program PeakFQ Annual Flood-Frequency Analysis Using Bulletin 17B Guidelines: U.S. Geological Survey, Techniques and Methods Book 4, Chapter B4, 42 p.

Forest Practices Board Manual (FPBM), 2004. Section 2: Standard Methods For Identifying Bankfull Channel Features and Channel Migration Zones. Washington State Department of Natural Resources, Forest Practice division, Board Mannual 11/2004: M2-2 to M2-69.

Goodwin, P., 2004. Analytical Solutions for Estimating Effective Discharge. Journal of Hydraulic Engineering, Vol. 130, No. 8: 729-738.

Harman, W.H., 1999. Bankfull Hydraulic Geometry Relationships for North Carolina Streams. AWRA Wildland Hydrology Symposium Proceedings. Edited By: D.S. Olsen and J.P. Potyondy. AWRA Summer Symposium, Bozeman, Montana, 32 p.

Harrelson, C.C., Rawlins, C.L. and Potyondy, J.P., 1994. Stream Channel Reference Sites: An Illustrated Guide to Field Technique. General Technical Report RM-245. Fort Collins, CO: U.S. Department of Agriculture, Forest Service, Rocky Mountain Forest and Range Experiment Station, 61 p.

Harvey, A. M, 1969. Channel Capacity and the Adjustment of Streams to Hydrologic Regime. Journal of Hydrology, Vol. 8: 82-98.

Heil, T.M. and Johnson, P.A., 1995. Uncertainity of Bankfull Discharge Estimations. Proceedings of ISUMA-NAFPS, 95: 340-345.

Henderson, F.M., 1966. Open Channel Flow. Macmillan, New York, 522 p.

Hey, R.D., 1978. Determinate Hydraulic Geometry of River Channels. Journal of the Hydraulics Division, ASCE, Vol. 104: 869-884.

Hicks, D.M. and Mason, P.D., 1999. Roughness Characteristics of New Zealand Rivers. National institute of Water and Atmospheric Research Ltd, Christchurch, New Zealand, 329 p.

Horel, G., 2006. Defining Active Fluvial Units. Ostapowich Engineering Services Ltd, downloaded in June 2006 at URL http://www.coastforestconservationinitiative.com/uploaded_files/Defining%20Active%20Fluvial%20Units%20-%20April%201,%202006.pdf, 5 p.

Huang, H.Q. and Nanson, G.C., 2000. Hydraulic Geometry and Maximum Flow Efficiency as Products of the Principle of Least action. Earth Surface Processes and Land Forms, Vol. 25: 1-16.

Huang, H.Q., Nanson, G.C. and Fagan, S.D., 2002. Hydraulic Geometry of Straight Channels and Principle of Least Action. Journal of Hydraulic Research, Vol. 40, Issue. 2: 153-160

Interagency Advisory Committee on Water Data, 1982. Guidelines for Determining Flood flow Frequency: Water Resources Council Bulletin 17B, 194 p.

Jaquith, S. and Kline, M., 2001.Vermont Regional Hydraulic Geometry Curves. Waterbury, VT, Vermont Water Quality Division, downloaded in June 2006 at URL: http://www.anr.state.vt.us/dec/waterq/ rivers/docs/rv_hydraulicgeocurves.pdf.

Jia, Y., 1990. Minimum Froude Number and the Equilibrium of Alluvial Sand Rivers. Earth Surface Processes and Land Forms, Vol. 15: 199-209

Jiongxin, X., 2004. Comparison of Hydraulic Geometry Between Sand and Gravel Bed Rivers in Relation to Channel Pattern Discrimination. Earth Surface and Process Landforms, 29: 645–657.

Jowett, I. G., 1998. Hydraulic geometry of New Zealand Rivers and Its Use as a Preliminary Method of Habitat Assessment. Regulated Rivers: Research & Management, 14: 451-466.

Kellerhals, R., 1967. Stable Channels with Gravel-paved Beds. Journal Waterways Harbors Division, American Society of Civil Engineers, Vol., 97: 1165-1180.

Kellerhals, R., Neill, C.R. and Bray, D.I., 1972. Hydraulic and Geomorphic Characteristics of Rivers in Alberta. Research Council of Alberta, River Engineering and Surface Hydrology Report 72-1, 52 p.

Knighton, A.D., 1974.Variation in Width-discharge Relation and Some Implications for Hydraulic geometry, Geological Society of American Bulletin, 85: 1069– 1076.

Knighton, A.D., 1977. Alternative Derivation of Minimum Variance Hypothesis. Geological Society of American Bulletin, Vol. 88: 364-366.

Knighton, D., 1998. Fluvial Forms and Processes: a New Perspective. Arnold, a member of the Hodder Headline Group, London; John Wiley & Sons Inc., New York, 383 p.

Kolberg, F.J. and Howard, A.D., 1995. Active Channel Geometry and Discharge Relations of U.S. Piedmont and Midwestern Streams: The Variable Exponent Model Revisited. Water Resources Research, Vol. 31, No. 9: 2353-2365.

Langbein, W.B. and Leopold, L.B, 1964. Quasi-Equilibrium States in Channel Morphology. American Journal of Science, Vol., 262: 782-794.

Langbein, W.B. and Leopold, L.B, 1966. River Meanders—Theory of Minimum Variance: Physiographic and Hydraulic Studies of Rivers. Geological Survey Professional Paper 422-H, Washington, 15 p.

Langbein, W.B., 1964. Geometry of River Channels. Journal of the Hydraulics Division, ASCE, Vol. 90, HY2: 301–312.

Lawer, S.M., 2004. Determination of Channel-Morphology Characteristics, Bankfull Discharge, and Various Design-peak Discharge in Western Montana. U.S Department of Interior and U.S. Geological Survey, Scientific Investigation Report 2004-5263, 19 p.

Ledger, D.C., 1981. The Velocity of the River Tweed and its Tributaries. Blackwell Scientific Publications Edinburgh, Freshwater Biology, 11, 10 p.

Lee, J. and Julien, P.Y., 2006. Downstream Hydraulic Geometry of Alluvial Channels. Journal of Hydraulic Engineering, Vol. 132, No.12: 1347-1352.

Leopold, L.B. and Maddock, T., 1953. The Hydraulic Geometry and Some Physiographic Implications. US Geological Survey Professional Paper, No. 252, p. 56.

Leopold, L.B. and Skibitze, H.E., 1967. Observations on Unmeasured Rivers. Geografiska Annaler, Vol. 49A 2-4: 247-255.

Leopold, L.B., 1992. Sediment Size that Determines Channel Morphology. Dynamics of Gravel Bed Rivers. Edited by. P. Billi, R.D. Hey, C.R. Thorne, & P. Tacconi, Eds. John Wiley & Sons Ltd.: 297-311.

Leopold, L.B., Wolman, M.G, and. Miller, J.P, 1964. Fluvial Processes in Geomorphology.W.H. Freeman and Company. San Francisco, CA. 511 p.

Leopold, L.M., 1953. Downstream Change of Velocity in Rivers. American Journal of Science, Vol. 251: 606 – 624.

McCandless, T. L. and. Everett, R. A. 2002. Maryland Stream Survey: Bankfull Discharge and Channel Characteristics of Streams in the Piedmont Hydrologic Region. U.S. Fish & Wildlife Service: CBFO-S02-01, 40 P.

McCandless, T. L., 2003. Maryland Stream Survey: Bankfull Discharge and Channel Characteristics of Streams in the Allegheny Plateau and the Valley and Ridge Hydrologic Regions. Report CBFO-S03-01, U.S. Fish and Wildlife Service, Chesapeake Bay Field Office, 33 p.

McCuen, R.H, 1998. Hydrologic Analysis and Design. Prentice Hall, Inc, Upper Saddle River New Jersey, USA, 814 p.

Millar, R.G., 2005. Theoretical Regime Equations for Mobile Gravel-bed Rivers with Stable Banks. Science Direct, Journal of Geomorphology, Vol. 64: 207-220.

Miller, S.J. and Davis, D., 2003. Optimizing Catskill Mountain Regional Bankfull Discharge and Hydraulic Geometry Relationships: Proceedings of the American Water Resources Association, 2003 International Congress, Watershed management for water supply systems, New York City, N.Y.: 10 p.

Molar,P. and Ramirez, J.A., 2002. On Downstream Hydraulic Geometry Study and Optimal Energy Expenditure: Case Study of the Ashley and Taieri Rivers. Journal of Hydrology, 259: 105-115.

Montgomery, D.R. and MacDonald, L.H, 2002. Diagnostic Approach to Stream Channel Assessment and Monitoring. Journal of American Water Resources Association, Vol. 38, No.1, 1-15 p.

Moody, J.A. and Troutman, B. M., 2002. Characterization of the Spatial Variability of Channel morphology. Wiley InterScience, Earth Surface Processes Landforms 27: 1251-1266.

Mosselman, E., 2004. Discussion: Hydraulic Geometry of Straight Channels and Principle of Least action. Journal of Hydraulic research, Vol. 42, No. 2: 219-222.

Mueller, D.S., 2007. Matlab code (pd0wr2.m): Read RDI PD0 File Format (WinRiver). U.S. Geological Survey Office of Surface Water.

Mulvihill, C.I., Ernst, A.G., and Baldigo, B.P., 2005. Regionalized Equations for Bankfull Discharge and Channel Characteristics of Streams in New York State: Hydrologic Region 6 in the Southern Tier of New York: U.S. Geological Survey Scientific Investigations Report 2005-5100, 14 p.

Mulvihill, C.I., Ernst, A.G., and Baldigo, B.P., 2006. Regionalized Equations for Bankfull-Discharge and Channel Characteristics of Streams in New York State: Hydrologic Region 7 in Western New York: U.S. Geological Survey Scientific Investigations Report 2006-5075, 14 p.

Natural Resources Canada, Geomagnetism Webpage: http://www.geolab.nrcan.gc.ca/geomag/apps/mdcal_e.php; accessed in March, 2007.

Navratil, O., Albert, M-B., Herouin, E. and Gresillon, J-M., 2005. Determination of Bankfull Discharge Magnitude and Frequency: Comparison of Methods on 16 Gravel-bed River reaches. Earth Surface Processes and Landforms, Vol. 31: 1345–1363.

Norris, J. M., 2002. Office of Surface Water Technical Memorandaum No. 2002.01: Configuration of Acoustic Profilers (RD Instruments) for Measurement of Streamflow. US Geological Survey, Office of Surface Water, Mail Stop 415, 6 p.

NovAtel, 2005. OEM4 Family Installation and Operation User Manual (for NovAtel GPSolution, ProPak, RT-20 and RT-2). NovAtel Inc, Publication Number: OM-20000046, Revision level 19, 119 p.

Oberg, K.A., Morlock, S.E., and Caldwell, W.S., 2005. Quality-Assurance Plan for Discharge Measurements Using Acoustic Doppler Current Profilers. U.S. Geological Survey Scientific Investigations Report 2005-5183, 35 p.

Ontario Geological Survey, 2003. Surficial Geology of Southern Ontario; Ontario Geological Survey, Miscellaneous Release Data: 128, 52 p.

Osterkamp, W.R, Lane, L.J., and Foster, G.R., 1983. An analytical Treatment of Channel-Morphology Relations. U.S. Geological Survey Professional Paper 1288, 21 p.

Osterkamp, W.R. and Hedman, E.R., 1982. Perennial-Streamfiow Characteristics Related to Channel Geometry and Sediment in the Missouri River Basin. U.S. Geological Survey Professional Paper 1242, 37 p.

Park, C.C., 1977. Wold-wide Variations in Hydraulic Geometry Exponents of Stream Channels: an Analysis and Some Observations. Journal of Hydrology 33: 133–146.

Parker, G., 1979. Hydraulic Geometry of Active Gravel Rivers. ASCE Journal of Hydraulic Division 105: 1185–1201.

Parrett, C. and Johnson, D.R., 2004. Methods for Estimating Flood Frequency in Montana Based on Data through Water Year 1998. U.S. Department of the Interior and U.S. Geological Survey, Water-Resources Investigations Report 03-4308, 101 p.

Pettit. F. and Pauet A., 1997. Bankfull Discharge Recurrence Interval in Gravel Bed Rivers. Earth Surface Processes and Landforms, Vol. 22: 685-693.

Phillips, J.D, 1990. The Instability of Hydraulic Geometry. Journal of Water Resources Research, Vol. 26, No. 4: 739-744.

Pickup, G. and Warner, R.F., 1976. Effects of Hydrologic Regime on Magnitude and Frequency of Dominant Discharge. Journal of Hydrology, Vol. 29: 51-75.

Powell, R.O, Miller, S.J., Westergard, B.E.,. Mulvihill, C.I. Baldigo, B.P., Gallagher, A.S. and. Starr, R.R., 2004. Guidelines for Surveying Bankfull Channel Geometry and Developing Regional Hydraulic-Geometry Relations for Streams of New York State. U.S. Geological Survey Open-File Report 03-92, 20 p.

Powell, R.O., Miller S.J., Westergard, B. E., Mulvihill, C.I., Baldigo B.P., Gallagher, A.S., and. Starr, R.R., 2004. Guidelines for Surveying Bankfull Channel Geometry and Developing Regional Hydraulic-Geometry Relations for Streams of New York State. U.S. Geological Survey, Open-File Report 03-92, 20 p.

Pyrce, R.S., 2003. Field Measurement of Bankfull Stage and Discharge. Waterpower Project Science Transfer Report 2.0, Ontario Ministry of Natural Resources, 17 p.

Radecki-Pawlik, A., 2002. Bankfull Discharge in Mountain Streams: Theory and Practice. Earth Surface Process and Landforms, Vol. 27: 115-123.

Rasid, H., Phillips, B.A.M. and Osterveld, M., 1985. Morphologic Effects of Canalization: the case Study of Neebing-McItyre Floodway, Thunder Bay, Ontario, Canada. Environmental Management, Vol. 9, No. 5: 399-416.

RD Instruments, 1996. Acoustic Doppler Current Profiler Principles of Operation: A Practical Primer, Second Edition for Broadband ADCPs. RD Instruments, San Diego, California, P/N 951-6069-00, 57 P.

RD Instruments, 2003. WinRiver User's Guide USGS Version, 158 p.

Rhodes, D. D., 1977. The b-f-m Diagram: Graphical Representation and Interpretation of At-A Station Hydraulic Geometry: American Journal of Science, Vol. 277: 73-96.

Rhodes, D. D., 1978. Discussion: World-Wide Variations in Hydraulic Geometry Exponents of Stream Channels: An Analysis and Some Observations-Comments: Journal Hydrology, Vol. 39: 193-197.

Rhodes, D.D., 1987. The b-f-m Diagram for downstream Hydraulic Geometry. Geografiska Annaler, Vol. 69: 147-161.

Rosgen, D.L., 1994. A Classification of Natural Rivers. Catena, 22: 169-199.

Schumm, S.A., 1960. The Shape of Alluvial Channels in Relation to Sediment Type. U.S. Geoligical Survey Professional Paper 352-B, U.S. Government Printing Office, Washington, DC: 17-30.

Sherwood, J.M., and Huitger, C.A., 2005, Bankfull Characteristics of Ohio Streams and their Relation to Peak Stream-flows: U.S. Geological Survey Scientific Investigations Report 2005–5153, 38 p.

Simpson, M.R., 2001. Discharge Measurements Using a Broad-Band Acoustic Doppler Current Profiler, United States Geological Survey Open-File Report 01-1, 123 p.

Singh, V.P., 2003. On the Theories of Hydraulic Geometry. International Journal of Sediment Research, Vol. 18, No. 3: 196-218.

Singh, V.P., C.T. Yang, and. Deng, Z.Q., 2003. Downstream Hydraulic Geometry Relations: 1. Theoretical Development, Water Resources Research, Vol. 39 No. 12, 1337, 15 P.

Singh, V.P., C.T. Yang, and. Deng, Z.Q., 2003. Downstream Hydraulic Geometry Relations: 2. Calibration and Testing, Water Resources Research, Vol. 39 No. 12, 1338, 10 p.

Smith, T.R, 1974. A derivation of the Hydraulic Geometry of Steady-state Channels from Conservation Principles and Sediment Transport Law. Journal of Geology, Vol. 82: 98-104.

Song, C.C.S. and Yang, T.C., 1980. Minimum Stream Power: Theory. Journal of the Hydraulics Division, Proceedings of the ASCE, Vol. 106, No. HY9: 1477-1486.

Soong, D.T., Ishii, A.L., Sharpe, J.B., and Avery, C.F., 2004. Estimating Flood-Peak Discharge Magnitudes and Frequencies for Rural Streams in Illinois. U.S. Geological Survey, Reston, Virginia, Scientific Investigations Report: 5103, 148 p.

Speight, J.G., 1965. Flow and Channel Characteristics of the Angabunga River, Papua. Journal of Hydrology, Vol.3: 16-36.

Stevens, M.A. and Nordin, C.F., 1987. Critique of the Regime Theory for Alluvial Channels. Journal of Hydraulic Engineering , Vol. 113, No. 11: 1359-1380.

Stewardson, M., DeRose, R., and Harman, C., 2005. Regional Models of Stream Channel Metrics. Technical Report 05/16, Cooperative Research Centre for Catchment Hydrology, Australia, 52 p.

Stewardson. M., 2005. Hydraulic geometry of stream reaches. Journal of Hydrology 306: 97–111.

Sweet, W.V. and Geratz, J.W., 2003. Bankfull Hydraulic Geometry Relationships and Recurrence Intervals for North Carolina's Coastal Plain. Jouranl of the American Water Resources Association (JAWRA), Vol. 39, No. 4: 861-871.

Swift, L.W.Jr. and Ledford, E.S., 1993. Riparian Ecosystems in the Humid US: functions, values and management. National association of conservation districts, Washington: 306 – 311.

Tabata, K.K. and Hickin E.J., 2003. Interchannel Hydraulic Geometry and Hydraulic Efficiency of the Anastomosing Columbia River, southern British Columbia, Canada. Earth Surface Processes and Landforms 28: 837–852

Teledyne RD Instruments, 2007. WinRiver II Software Version 1.01 Help File. Teledyne RD Instruments, California, USA.

Todd, H., Lewis, A. Ohlson, D. and Bradford, M., 2003. Development of Instream Thresholds as Guidelines for Reviewing Proposed Water Uses. British Columbia Ministry of Sustainable Management, and British Columbia Ministry of Water and Air Protection, Victoria BC, 88 p

Trenhaile, A.S., 2004. Geomorphology: a Canadian Perspective. Oxford University Press, Ontario, Canada, 440 p.

United States Federal Interagency Stream Restoration Working Group (FISRWG), 1998. Stream Corridor Restoration: Principles, Processes, and Practices: accessed in June 2006 at URL: http://www.usda.gov/ stream_restoration/.

USACE, 2003. Engineering Manual: NAVSTAR Global Positioning System Surveying. Department of the Army, US Army of Corps of Engineers, Washington, EM 110-1-2003, 469 p.

USFWS, 2002. Maryland Stream Survey: Bankfull Discharge and Channel Characteristics of Streams in the Piedmont Hydrologic Region. CBFO-S01-01, US Fish & Wildlife Service Cheasapeake Bay Field Office, Annapolis, MD.

Westergard, B.E., Mulvihill, C.I., Ernst, A.G., and Baldigo, B.P., 2005. Regionalized Equations for Bankfull-Discharge and Channel Characteristics of Streams in New York State – Hydrologic Region 5 in Central New York: U.S. Geological Survey Scientific Investigations Report 2004-5247, 16 p.

Westergard, B.E., Mulvihill, C.I., Ernst, A.G., and Baldigo, B.P., 2004. Regionalized Equations for Bankfull-Discharge and Channel Characteristics of Streams in New York State – Hydrologic Region 5 in Central New York: U.S. Geological Survey Scientific Investigations Report 2004-5247, 16 p.

White, W.R., Bettess, R., and Paris, E., 1982. Analytical Approach to River Regime. Journal of the Hydraulics Division, ASCE, Vol. 108: 1179-1193.

Whiting, P.J., Stamm, J.F. Moog, D.B. and Orndorff, R.L., 1999. Sediment-Transporting Flows in Headwater Streams. GSA Bulletin, Vol. 111; No. 3: 450–466.

Wiley, J.B., Atkins, J.T, and Newell, D.A., 2002. Estimating the Magnitude of Annual Peak Discharges with Recurrence Intervals between 1.1 and 3.0 Years for Rural, Unregulated Streams in West Virginia. U.S. Department of the Interior and U.S. Geological Survey: Water-Resources Investigations Report 02-4164, 73 P.

Williams, G.P., 1978a. Hydraulic geometry of river cross-sections—Theory of minimum variance. U.S. Geological Survey, Washington, D.C. Professional paper 1029, 47 p.

Williams, G.P., 1978b. Bankfull Discharge of Rivers. Journal of Water Resources Research, Vol. 14: 1141-1154.

Wohl, E., 2004. Limits of Downstream Hydraulic Geometry. Geological Society of America, Vol. 32: 897-900

Wohl, E., Kuzma, J.N. and Brown, N.E., 2004. Reach-Scale Channel Geometry of a Mountain River. Earth Surface Processes and Landforms, 29: 969–981.

Wohl, E.E. and Wilcox, A., 2005. Channel Geometry of Mountain Streams in New Zealand. Journal of Hydrology, Vol. 300: 252-266.

Wolman, M.G. – Miller, J.P., 1960. Magnitude and Frequency of Forces in Geomorphic Process. Journal of Geology, Vol. 68, No. 1: 54-74.

Wolman, M.G., 1955. The natural Channel of Brandywine Creek, Pennsylvania. U.S. Geological Survey Professional Paper, 271, 56 p.

Woodyer, K.D, 1968. Bankfull Frequency in Rivers. Journal of Hydrology, 6:114-142.

Yang, T.C. and Molinas, A., 1982. Sediment Transport and Unit Stream Power Function. Journal of the Hydraulics Division, Proceedings of the ASCE, Vol. 108, No. HY6: 774-793.

Yang, T.C., 1972. Unit Stream Power Function and Sediment Transport. Journal of the Hydraulics Division, Proceedings of the ASCE, Vol. 98, No. HY10: 1805-1826.

Yang, T.C., Song, C.C.S. and Woldenberg, M.J., 1981. Hydraulic Geometry and Minimum rate of Energy Dissipation. Watter Resources Research, Vol. 17, No. 4: 1014-1018.

Appendix A

A Flood Frequency Analysis Based on PDS

Frequency analysis based on annual maximum series (AMS) is the most commonly applied approach for estimating discharges and their corresponding recurrence intervals using the available annual maximum flood data. However, it is applicable only for discharge magnitude which has a recurrence interval of greater than one year. Frequency analysis based on annual maximum series is mathematically incapable of estimating discharges which have a recurrence interval of less than one year. In fact, knowledge about the more frequent floods is needed in many types of problems, such as environmental studies for the protection and restoration of stream channels, aquatic habitats, and floodplains; non-point source pollution analyses, channel erosion analyses, fishery management etc (Soong et al., 2004, McCuen, 1998).

Moreover, the recurrence interval of the morphologically significant discharge (bankfull) is not always greater than one year. Particularly, bankfull discharge may recur more than once in a year in many urban and perhaps some rural streams. In these streams, it is not possible to estimate bankfull discharge based on annual maximum flood series. For instance, Navratil et al. (2006) estimated the magnitude and frequency of bankfull discharge of 16 gravel bed river reaches of three river basins in France by applying different methods; they confirmed that annual maximum series analysis is mathematically incapable of providing appropriate solutions, as top of bank discharge occurred several times per year in most of their surveyed reaches

Therefore, another approach that is capable of estimating discharges that recur more than once per year must be considered. Flood frequency analysis based on partial duration series (PDS) is an approach applied to estimate discharges that recur more frequently than once per year. Flood frequency analysis based on the annual maximum flood (AMF) uses one peak flood from each year, but for frequency analysis based on PDS more than one flood event per year can be considered in the analysis. Frequency analysis based on PDS uses all measured discharges above a certain threshold or base discharge of interest.

The concept of a return period for PDS is not the same as it is applied for AMS. In annual flood series the recurrence interval is the average interval in which a flood of a given magnitude will recur as an annual maximum. In the partial duration series, the recurrence interval is the average time between floods of a given magnitude regardless of their relation to the year or any other period of time (Dalrymple, 1960; McCuen, 1998). Soong et al. (2004) presented a method to estimate the yearly based recurrence interval of PDS. Similar to the approach for AMS that uses the Weibull formula to approximate the recurrence intervals of systematic data, the Weibull formula for PDS recurrence interval (T_{PDS}) can be expressed in the form of Eq. A.1

$$T_{pds} = \frac{N+1}{M \cdot r} \tag{A.1}$$

T_{PDS} is PDS recurrence interval.
M is the ordered sequence of PDS peaks with the largest flood equal to 1.
N is the total number of PDS peaks (samples) in the data set.
r is average number of floods per year

Frequency analysis based on PDS uses all measured discharges above a certain threshold or base discharge. Therefore, selecting an appropriate threshold value is a challenging task. Unfortunately, in practice there is no universally accepted rule for threshold value in PDS frequency analysis. Some of the suggested approaches on which the selection of appropriate threshold discharge for PDS should be based are:

- ✓ The threshold can be either the bankfull discharge, the lowest value of record, or some other recognizable criterion (McCuen, 1998).
- ✓ The threshold discharge generally is selected such that, on average, three to four independent flood-peak discharges, including the annual maximum peak discharge, will exceed the threshold discharge each water year (Soong et al., 2004; McCuen, 1998).

- ✓ The threşhold is selected to assure that all events of interest are evaluated including at least one event per time period (Interagency Advisory Committee on Water Data, 1982).
- ✓ The threshold is generally selected as equal to the lowest annual flood so that at least one flood in each year is included, however in a long record, the threshold is generally raised so that on the average only 3 or 4 floods in a year are included (Dalrymple, 1960)

Another major problem is to assure that each flood magnitude to be incorporated in PDS is hydrologically independent. To avoid the hydrological interdependency among the selected events, the peak floods should be selected so that the time interval between any two events is greater than or equal to one week. Other independency criteria have been utilized, including: each peak be separated by substantial recession in stage and discharge (Dalrymple, 1960), or the recession between two peaks must fall to at least 25% of the first discharge (McCuen, 1998).

Appendix B

B Summary of Morphological Information of Study Streams

1) 02HM004 Wilton Creek near Napanee

Measurement date: March 27, 2007

Geographic location of study reach: $44^0 14' 21''$N, $76^0 50' 58''$ W

Location of the surveyed reach with respect to gauge station: Downstream

Instruments used for measurement

Propeller Current Meter and Electronic Total Station

Bankfull indicators

Top of bank and/or break in channel bank slope. Reliable bankfull indicator found on the left bank. Incision was observed at downstream where the effect of deposited materials from the nearby road seems to vanish and top of bank on the right bank was much higher than the one on the left side.

Bed and bank material

Both bed and bank materials were cohesive and the dominant particles of bed material were silt-clay except the bed substrate at a location very close to bridge (gauge site), which was deposited gravel (expected to be from the nearby road) and organic muck.

Additional observations

Right bank was almost vertical; erosion — undercut and bank-slides (on outer bank) were observed; no debris but there were sand and gravel deposits near the bridge; vegetations: grasses; pool-riffle morphology was not obvious. Land use (only visible areas close to the gauge station): pasture

Figure B.1 Satellite image of Wilton creek survey location (source: Google Earth)

Figure B.2 Wilton Creek looking downstream (taken in August, 2006)

Figure B.3 Wilton Creek focusing on bed and right bank (taken in August 2006).

2) 02HM009 West Branch Little Cataraqui Creek at Kingston

Measurement date: March 27, 2007

Geographic location of study reach: $44^0 14' 24''$N, $76^0 34' 44''$ W

Location of surveyed reach with respect to gauge station: upstream

Instruments used for measurement

Propeller current meter, Electronic Total Station and measuring tape

Bankfull indicators

Top of bank and vegetation; left and right top of bank levels were about the same

Bed and bank material

Both bed and banks were cohesive bank. Clay was the dominant constituent of the bed (confirmed by sieve analysis) and incision to hard clay (shale) bed was observed.

Additional observations

Steep bank banks; incision to clay shale bed and beaver dams were common; vegetations: grasses, shrubs and trees (mostly outer side); pool-riffle morphology was obvious. Land use: high urbanization (in the city of Kingiston)

Figure B.4 Satellite image of West Branch Little Cataraqui creek survey location (source: Google Earth)

Figure B.5 West Branch Little Cataraqui Creek looking upstream (taken on March 27, 2007)

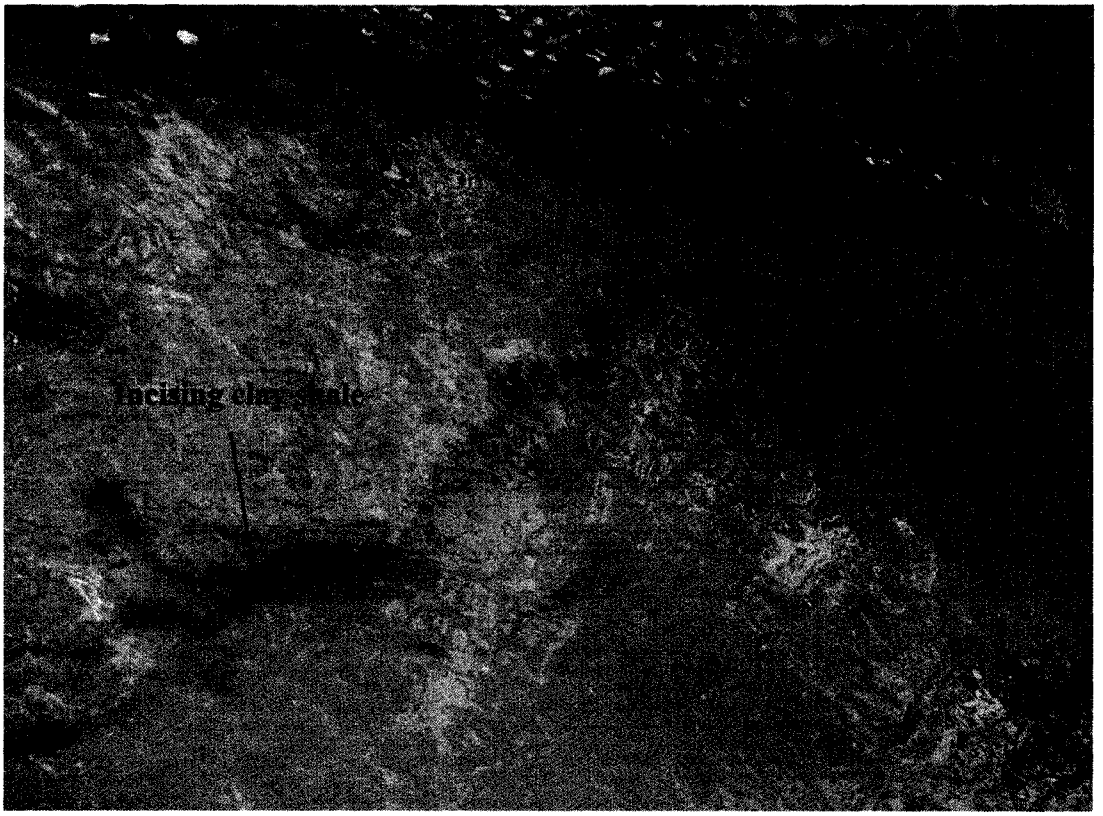

Figure B.6 West Branch Little Cataraqui Creek bed (taken in August, 2006)

4) 02MC001 RAISIN RIVER NEAR WILLIAMSTOWN

Measurement date: April 18, 2007

Geographic location of study reach: $45^{0}09'20''$N, $73^{0}38'16''$ W

Location of the surveyed reach with respect to gauge station: Upstream

Instruments used for measurement

Acoustic Doppler Current Profiler (ADCP), Real Time Kinemetic Differential Global Positioning System (RTK-DGPS) and Electronic Total Station

Bankfull indicator

Top of bank and bank slope change were clearly identifiable indicators. Right and left top of bank levels had substantial difference. The level difference indicates that higher flow frequently overtops the left top of bank while it is still in the channel section on the right side. The right bank indicator was taken as bankfull level of the channel since it was more definite and the flow at that level was well within the reasonable range of the theoretical bankfull discharge based frequency analysis.

Bed and bank material

Both bed and bank materials were cohesive. The river was too deep to wade across; therefore appropriate bed material sampling was not possible. Bed-load sediment has been taken by throwing the Environment Canada bed-load sampler (cylindrical bucket with sharp top edge) into the river and dragging on the bed. This method of sampling does not fully reflect the exact constituent of the bed. But it can be used as reliable indicator for identifying the dominant particle of the bed material. The dominant particle of the bed material was silt-clay (confirmed by sieve analysis of surficial bed material samples).

Additional observations

Benches were encountered; moderate erosion and effect of wood debris; vegetations: Trees, shrubs and grasses. Small to big trees lined up on both side of the bank seemed to play locally bank stabilization roles; pool-riffle morphology was not obvious. Land use: Farming (crops), moderate urbanization.

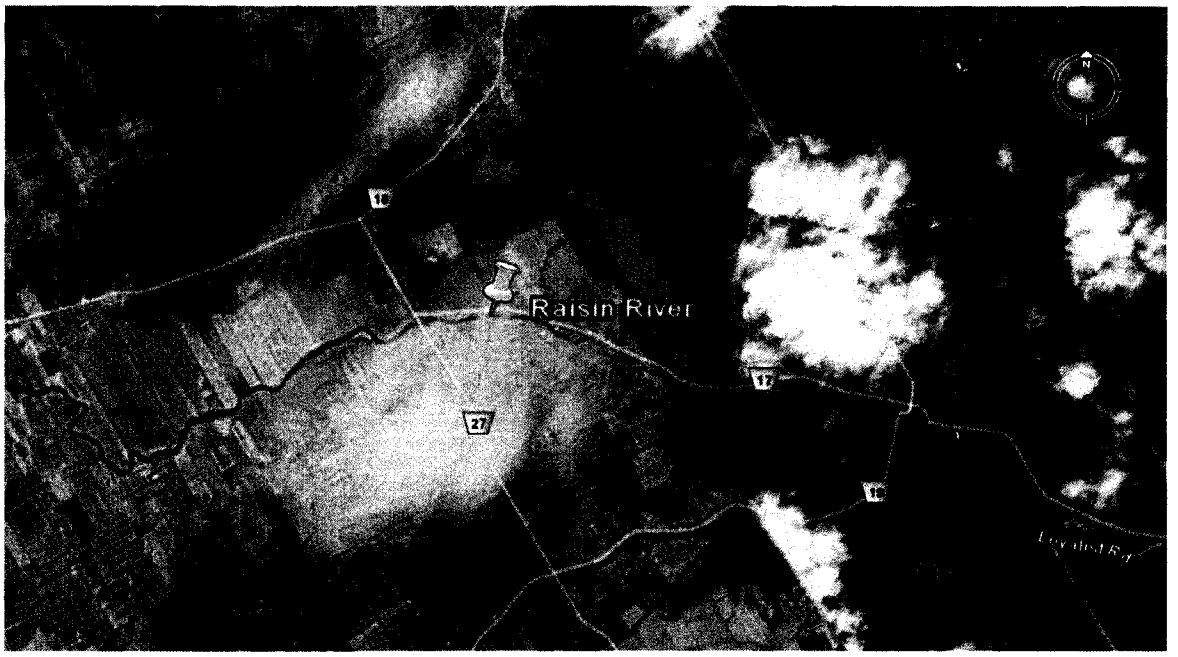

Figure B.7 Satellite image of Raisin River survey location (source: Google Earth)

Figure B.8 Raisin River looking downstream (taken in August, 2006)

6) **02LB007 SOUTH NATION RIVER AT SPENCERVILLE**

Measurement date: April 5, 2007

Geographic location of study reach: $44^0 48' 51''$N, $75^0 34' 20''$ W

Location of the surveyed reach with respect to gauge station:

Far upstream of the gauge site; at Weir road bridge

Instruments used for measurement

Acoustic Doppler Current Profiler (ADCP), Real Time Kinemetic Differential Global Positioning System (RTK-DGPS) and Electronic Total Station

Bankfull indicators

Vegetation and to some extent bank slope were useful indicators to locate the bankfull level on both right and left banks. The magnitude of bankfull levels on both left and right banks were almost the same.

Bed and bank material

Based on surface geology map of the area, the bed material of South Nation River was undoubtedly expected to be cohesive with high silt-clay content. Banks were partially cohesive and boulders and medium size stones were also common on the right bank of the river. Those stones even seemed to play the role of stabilizing right bank. The river was too deep to wade across; hence, the bed material of the river was not appropriately sampled. Surficial bed material was collected by dragging Environment Canada bed-load sampler along the bed. This method doesn't seem to be good enough to properly identify the constituents of the bed material, as it may be biased by the material transported from upstream reaches as bed-load and deposited on the bed. The sieve analysis of surficial bed material sample collected from South Nation river did not confirm cohesive bed.

Additional observations

There were benches; no sign of erosion and pronounced debris, but there were deposition of organic substrates; vegetations: grasses and shrubs (inner bank); and trees, shrubs and grasses (outer bank); pool-riffle morphology was not obvious. The bank stabilizing role of shrubs (left), and trees, shrubs and stones (right) are clearly visible; Land use: crops

Figure B.9 Satellite image of South Nation River survey location (source: Google Earth)

Figure B.10 South Nation river looking downstream (taken on April 5, 2007)

7) 02LA007 JOCK RIVER NEAR RICHMOND

Measurement date: April 18, 2007

Geographic location of study reach: $45^0 17' 07''$N, $75^0 45' 56''$ W

Location of the surveyed reach with respect to gauge station

Far downstream of the gauge site

Instruments used for measurement

Acoustic Doppler Current Profiler (ADCP), Real Time Kinemetic Differential Global Positioning System (RTK-DGPS) and Electronic Total Station

Bankfull indicators

Top of bank, change in bank slope and vegetation

Bed and bank material

Banks were cohesive and organic, and bed is clay at the surveyed reach, although at the reach close to the gauges station (at Modie Drive Road) was rock, cobble and

boulder. The river was too deep to wade across and proper sampling of the bed material was not possible with the instrument used. Only sampling of surficial bed-material was carried out. It was sampled by dragging the Environment Canada bed-load sampler (cylindrical bucket with to sharp edge) on the bed of the river. As it were explained above this sampling method can only help to know the dominant bed material and it is not good enough to exactly classify the bed material since it can be biased by the material transported from up stream reaches and deposited on the bed.

Additional observations

There were benches; moderate sign of erosion and debris barrier; there were considerable organic substrates; vegetations: grasses, shrubs and trees; trees and shrubs seemed to play a local stabilizing role of both right and left bank; pool-riffle morphology was not obvious. Land use: crops and moderate urbanization.

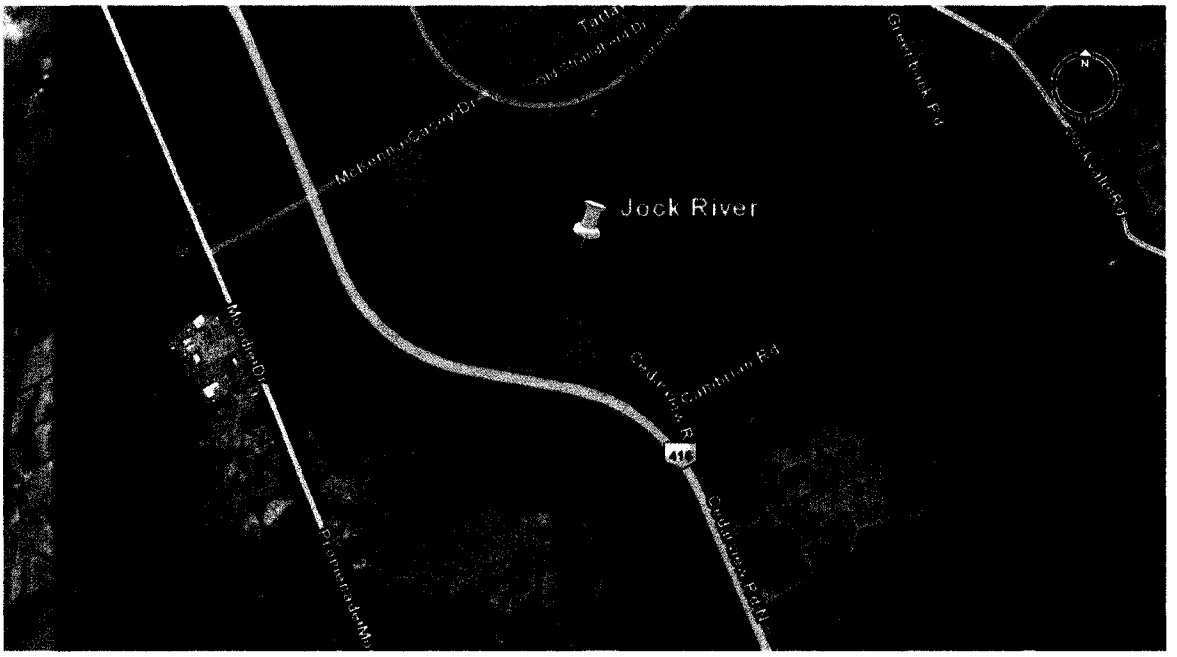

Figure B.11 Satellite image of Jock River survey location (source: Google Earth)

Figure B.12 Jock River looking upstream (taken in August, 2006)

Appendix C

C Cross-sectional Profile Data

Table C.1 South Nation River Cross-sectional Data

CUM_DIS. LB TO RB	BED_AL	AV_BFD	CUM_AREA LB TO RB	SURVEYING METHOD	NOTE
(m)	(m)	(m)	(m^2)		
0.000	80.695			ETS	LB BM
1.543	80.462			ETS	
2.390	80.444	0.000	0.000	ETS	BFL; interpolated
5.232	80.384	0.060	0.086	ETS	
6.768	80.159	0.285	0.351	ETS	
7.900	80.106	0.338	0.703	ETS	
9.400	80.013	0.431	1.280	ADCP_GPS	
9.970	79.887	0.557	1.562	ADCP_GPS	
10.540	79.818	0.626	1.899	ADCP_GPS	
11.110	79.751	0.693	2.275	ADCP_GPS	
11.680	79.692	0.752	2.687	ADCP_GPS	
12.250	79.725	0.719	3.106	ADCP_GPS	
13.056	79.662	0.782	3.711	ADCP_GPS	
13.626	79.595	0.849	4.176	ADCP_GPS	
14.196	79.482	0.962	4.692	ADCP_GPS	
14.766	79.436	1.008	5.253	ADCP_GPS	
15.336	79.375	1.069	5.845	ADCP_GPS	
16.142	79.265	1.179	6.751	ADCP_GPS	
16.712	79.184	1.260	7.446	ADCP_GPS	
17.282	79.106	1.338	8.186	ADCP_GPS	
17.852	79.025	1.419	8.972	ADCP_GPS	
18.658	78.910	1.534	10.162	ADCP_GPS	
19.228	78.820	1.624	11.062	ADCP_GPS	
19.798	78.725	1.719	12.015	ADCP_GPS	
20.368	78.627	1.817	13.023	ADCP_GPS	
20.938	78.513	1.931	14.091	ADCP_GPS	
21.744	78.410	2.034	15.689	ADCP_GPS	
22.314	78.396	2.048	16.852	ADCP_GPS	
22.884	78.377	2.067	18.025	ADCP_GPS	
23.454	78.353	2.091	19.210	ADCP_GPS	
24.024	78.270	2.174	20.426	ADCP_GPS	
24.830	78.377	2.067	22.135	ADCP_GPS	
25.400	78.342	2.102	23.323	ADCP_GPS	
25.970	78.351	2.093	24.519	ADCP_GPS	
26.540	78.365	2.079	25.708	ADCP_GPS	
27.110	78.437	2.007	26.873	ADCP_GPS	
27.916	78.462	1.982	28.481	ADCP_GPS	

28.486	78.471	1.973	29.608	ADCP_GPS	
29.056	78.501	1.943	30.724	ADCP_GPS	
29.626	78.497	1.947	31.833	ADCP_GPS	
30.432	78.495	1.949	33.403	ADCP_GPS	
31.002	78.503	1.941	34.512	ADCP_GPS	
31.572	78.546	1.898	35.606	ADCP_GPS	
32.142	78.623	1.821	36.666	ADCP_GPS	
32.712	78.648	1.796	37.697	ADCP_GPS	
33.518	78.675	1.769	39.134	ADCP_GPS	
34.088	78.711	1.733	40.132	ADCP_GPS	
34.658	78.708	1.736	41.121	ADCP_GPS	
35.228	78.743	1.701	42.101	ADCP_GPS	
35.798	78.824	1.620	43.047	ADCP_GPS	
36.604	79.241	1.203	44.185	ADCP_GPS	
37.174	79.251	1.193	44.868	ADCP_GPS	
37.826	79.610	0.834	45.529	ETS	
38.789	79.966	0.478	46.161	ETS	
39.302	80.377	0.067	46.301	ETS	
39.542	80.444	0.000	46.309	ETS	RB BFL
40.179	80.605			ETS	
40.725	80.738			ETS	
41.163	80.876			ETS	
41.626	81.028			ETS	
42.284	81.148			ETS	
43.443	81.152			ETS/GPS	RB BM

Average water surface level during measurement = 80.377m
Approximated bankfull level = 80.444m

Table C.2 Jock River Cross-sectional Data

CUM_DIS. LB TO RB (m)	BED_AL (m)	AV_BFD (m)	CUM_AREA LB TO RB (m^2)	SURVEYING METHOD	NOTE
0.000	89.180			ETS/GPS	LB BM
1.226	88.986			ETS	
1.382	88.968			ETS	
2.890	88.794			ETS	
4.316	88.629			ETS	
5.012	88.587	0.000	0.000	ETS	LB BFL, interpolated
6.060	88.524	0.063	0.033	ETS	
7.530	88.436	0.151	0.190	ETS	
9.570	88.331	0.256	0.605	ETS	
9.661	88.306	0.281	0.629	ETS	
9.820	88.212	0.375	0.681	ETS	
10.042	88.080	0.507	0.779	ETS	
10.770	88.060	0.527	1.155	ADCP_GPS	
11.230	87.884	0.703	1.438	ADCP_GPS	
11.690	87.794	0.793	1.782	ADCP_GPS	
12.150	87.615	0.972	2.188	ADCP_GPS	
12.610	87.519	1.068	2.657	ADCP_GPS	
13.070	87.501	1.086	3.152	ADCP_GPS	
13.530	87.490	1.097	3.654	ADCP_GPS	
13.990	87.472	1.115	4.163	ADCP_GPS	
14.450	87.471	1.116	4.676	ADCP_GPS	
14.910	87.547	1.040	5.172	ADCP_GPS	
15.370	87.577	1.010	5.644	ADCP_GPS	
15.830	87.511	1.076	6.124	ADCP_GPS	
16.290	87.471	1.116	6.628	ADCP_GPS	
16.750	87.458	1.129	7.144	ADCP_GPS	
17.210	87.447	1.140	7.666	ADCP_GPS	
17.670	87.439	1.148	8.192	ADCP_GPS	
18.130	87.417	1.170	8.725	ADCP_GPS	
18.590	87.393	1.194	9.269	ADCP_GPS	
19.050	87.361	1.226	9.826	ADCP_GPS	
19.510	87.313	1.274	10.401	ADCP_GPS	
19.970	87.239	1.348	11.004	ADCP_GPS	
20.430	87.133	1.454	11.648	ADCP_GPS	
20.890	86.999	1.588	12.348	ADCP_GPS	
21.350	86.848	1.739	13.113	ADCP_GPS	
21.810	86.674	1.913	13.953	ADCP_GPS	
22.270	86.487	2.100	14.876	ADCP_GPS	
22.730	86.301	2.286	15.885	ADCP_GPS	
23.190	86.108	2.479	16.981	ADCP_GPS	
23.650	85.913	2.674	18.166	ADCP_GPS	
24.110	85.717	2.870	19.441	ADCP_GPS	
24.570	85.538	3.049	20.802	ADCP_GPS	

25.030	85.366	3.221	22.244	ADCP_GPS	
25.490	85.219	3.368	23.759	ADCP_GPS	
25.950	85.071	3.516	25.342	ADCP_GPS	
26.410	84.921	3.666	26.994	ADCP_GPS	
26.870	84.781	3.806	28.713	ADCP_GPS	
27.330	84.643	3.944	30.495	ADCP_GPS	
27.790	84.512	4.075	32.339	ADCP_GPS	
28.250	84.393	4.194	34.241	ADCP_GPS	
28.710	84.270	4.317	36.199	ADCP_GPS	
29.170	84.136	4.451	38.216	ADCP_GPS	
29.630	84.044	4.543	40.285	ADCP_GPS	
30.090	83.968	4.619	42.392	ADCP_GPS	
30.550	83.912	4.675	44.530	ADCP_GPS	
31.010	83.778	4.809	46.711	ADCP_GPS	
31.470	83.687	4.900	48.944	ADCP_GPS	
31.930	83.639	4.948	51.209	ADCP_GPS	
32.390	83.588	4.999	53.497	ADCP_GPS	
32.850	83.562	5.025	55.803	ADCP_GPS	
33.310	83.531	5.056	58.122	ADCP_GPS	
33.770	83.503	5.084	60.454	ADCP_GPS	
34.230	83.470	5.117	62.800	ADCP_GPS	
34.690	83.446	5.141	65.159	ADCP_GPS	
35.150	83.422	5.165	67.529	ADCP_GPS	
35.610	83.455	5.132	69.897	ADCP_GPS	
36.070	83.410	5.177	72.268	ADCP_GPS	
36.530	83.392	5.195	74.654	ADCP_GPS	
36.990	83.455	5.132	77.029	ADCP_GPS	
37.450	83.504	5.083	79.378	ADCP_GPS	
37.910	83.549	5.038	81.706	ADCP_GPS	
38.370	83.600	4.987	84.012	ADCP_GPS	
38.830	83.672	4.915	86.289	ADCP_GPS	
39.290	83.789	4.798	88.523	ADCP_GPS	
39.750	83.838	4.749	90.719	ADCP_GPS	
40.210	83.913	4.674	92.886	ADCP_GPS	
40.670	84.041	4.546	95.007	ADCP_GPS	
41.130	84.138	4.449	97.076	ADCP_GPS	
41.590	84.206	4.381	99.107	ADCP_GPS	
42.050	84.280	4.307	101.105	ADCP_GPS	
42.510	84.381	4.206	103.063	ADCP_GPS	
42.970	84.490	4.097	104.973	ADCP_GPS	
43.430	84.590	3.997	106.835	ADCP_GPS	
43.890	84.703	3.884	108.648	ADCP_GPS	
44.350	84.833	3.754	110.405	ADCP_GPS	
44.810	84.992	3.595	112.095	ADCP_GPS	
45.270	85.149	3.438	113.713	ADCP_GPS	
45.730	85.279	3.308	115.265	ADCP_GPS	
46.190	85.403	3.184	116.758	ADCP_GPS	
46.650	85.506	3.081	118.199	ADCP_GPS	
47.110	85.662	2.925	119.580	ADCP_GPS	

47.570	85.839	2.748	120.885	ADCP_GPS	
48.030	86.037	2.550	122.104	ADCP_GPS	
48.490	86.259	2.328	123.226	ADCP_GPS	
48.950	86.478	2.109	124.247	ADCP_GPS	
49.410	86.660	1.927	125.175	ADCP_GPS	
49.870	86.897	1.690	126.007	ADCP_GPS	
50.330	87.076	1.511	126.743	ADCP_GPS	
50.790	87.228	1.359	127.403	ADCP_GPS	
51.250	87.293	1.294	128.013	ADCP_GPS	
52.290	87.307	1.280	129.351	ETS	
53.110	87.318	1.269	130.396	ETS	
55.202	87.347	1.240	133.020	ETS	
55.773	87.392	1.195	133.715	ETS	
56.140	87.540	1.047	134.126	ETS	
56.440	87.660	0.927	134.422	ETS	
56.755	87.787	0.800	134.694	ETS	
56.983	87.850	0.737	134.869	ETS	
57.300	88.016	0.571	135.076	ETS	
57.520	88.131	0.456	135.189	ETS	
57.730	88.244	0.343	135.273	ETS	
58.084	88.436	0.151	135.360	ETS	
58.114	88.452	0.135	135.364	ETS	
58.515	88.587	0.000	135.391	ETS	RB BFL
59.086	88.659			ETS	
60.103	88.771			ETS	
61.165	88.797			ETS	
61.375	88.897			ETS	
62.049	88.968			ETS	
62.816	89.049			ETS	
0.000	89.180			ETS/GPS	RB BM

Water surface level during measurement = 88.968
Approximated bankfull level = 88.587m

Table C.3 Raisin River Cross-sectional Data

CUM_DIS. LB TO RB (m)	BED_AL (m)	AV_BFD (m)	CUM_AREA LB TO RB (m^2)	SURVEYING METHOD	NOTE
0.000	53.036			ETS/GPS	LB BM
0.815	52.943			ETS	
1.359	52.880			ETS	
1.943	52.816			ETS	
2.369	52.677			ETS	
2.543	52.617	0.000	0.000	ETS	BFL; Interpolated
2.780	52.535	0.082	0.010	ETS	
3.345	52.339	0.278	0.112	ETS	
3.740	52.220	0.397	0.245	ETS	
4.373	51.929	0.688	0.588	ETS	
4.742	51.781	0.836	0.869	ETS	
5.059	51.514	1.103	1.176	ETS	
5.370	51.310	1.307	1.551	ETS	
5.823	51.013	1.604	2.210	ETS	
7.220	50.824	1.793	4.583	ETS	
9.070	50.574	2.043	8.131	ETS	
10.848	50.334	2.283	11.977	ADCP_GPS	
11.116	50.215	2.402	12.605	ADCP_GPS	
11.384	50.218	2.399	13.248	ADCP_GPS	
11.652	50.157	2.460	13.899	ADCP_GPS	
11.920	50.058	2.559	14.572	ADCP_GPS	
12.188	50.019	2.598	15.263	ADCP_GPS	
12.456	49.980	2.637	15.964	ADCP_GPS	
12.724	49.973	2.644	16.672	ADCP_GPS	
12.992	49.890	2.727	17.392	ADCP_GPS	
13.260	49.719	2.898	18.146	ADCP_GPS	
13.528	49.653	2.964	18.932	ADCP_GPS	
13.796	49.605	3.012	19.733	ADCP_GPS	
14.064	49.573	3.044	20.545	ADCP_GPS	
14.332	49.427	3.190	21.380	ADCP_GPS	
14.600	49.328	3.289	22.248	ADCP_GPS	
14.868	49.237	3.380	23.142	ADCP_GPS	
15.136	49.144	3.473	24.060	ADCP_GPS	
15.404	49.099	3.518	24.997	ADCP_GPS	
15.672	49.032	3.585	25.949	ADCP_GPS	
15.940	48.924	3.693	26.924	ADCP_GPS	
16.208	48.857	3.760	27.923	ADCP_GPS	
16.476	48.825	3.792	28.935	ADCP_GPS	
16.744	48.774	3.843	29.958	ADCP_GPS	
17.012	48.724	3.893	30.995	ADCP_GPS	
17.280	48.672	3.945	32.045	ADCP_GPS	
17.548	48.642	3.975	33.106	ADCP_GPS	
17.816	48.636	3.981	34.172	ADCP_GPS	

18.084	48.622	3.995	35.241	ADCP_GPS	
18.352	48.604	4.013	36.314	ADCP_GPS	
18.620	48.608	4.009	37.389	ADCP_GPS	
18.888	48.600	4.017	38.464	ADCP_GPS	
19.156	48.581	4.036	39.543	ADCP_GPS	
19.535	48.605	4.012	41.068	ADCP_GPS	
19.803	48.607	4.010	42.143	ADCP_GPS	
20.071	48.608	4.009	43.218	ADCP_GPS	
20.339	48.612	4.005	44.292	ADCP_GPS	
20.607	48.618	3.999	45.365	ADCP_GPS	
20.875	48.629	3.988	46.435	ADCP_GPS	
21.143	48.636	3.981	47.503	ADCP_GPS	
21.411	48.661	3.956	48.567	ADCP_GPS	
21.679	48.703	3.914	49.622	ADCP_GPS	
21.947	48.735	3.882	50.667	ADCP_GPS	
22.215	48.755	3.862	51.705	ADCP_GPS	
22.483	48.783	3.834	52.736	ADCP_GPS	
22.751	48.798	3.819	53.762	ADCP_GPS	
23.019	48.758	3.859	54.791	ADCP_GPS	
23.287	48.765	3.852	55.824	ADCP_GPS	
23.555	48.760	3.857	56.857	ADCP_GPS	
23.823	48.791	3.826	57.887	ADCP_GPS	
24.091	48.817	3.800	58.909	ADCP_GPS	
24.359	48.824	3.793	59.926	ADCP_GPS	
24.627	48.852	3.765	60.939	ADCP_GPS	
24.895	48.838	3.779	61.950	ADCP_GPS	
25.163	48.814	3.803	62.966	ADCP_GPS	
25.431	48.815	3.802	63.985	ADCP_GPS	
25.699	48.863	3.754	64.998	ADCP_GPS	
25.967	48.897	3.720	66.000	ADCP_GPS	
26.235	48.905	3.712	66.996	ADCP_GPS	
26.503	48.940	3.677	67.986	ADCP_GPS	
26.771	48.986	3.631	68.965	ADCP_GPS	
27.039	49.049	3.568	69.930	ADCP_GPS	
27.307	49.104	3.513	70.879	ADCP_GPS	
27.686	49.138	3.479	72.204	ADCP_GPS	
27.954	49.120	3.497	73.139	ADCP_GPS	
28.222	49.117	3.500	74.077	ADCP_GPS	
28.490	49.165	3.452	75.009	ADCP_GPS	
28.758	49.219	3.398	75.927	ADCP_GPS	
29.026	49.307	3.310	76.826	ADCP_GPS	
29.294	49.396	3.221	77.701	ADCP_GPS	
29.562	49.481	3.136	78.553	ADCP_GPS	
29.830	49.562	3.055	79.383	ADCP_GPS	
30.098	49.646	2.971	80.190	ADCP_GPS	
30.366	49.729	2.888	80.975	ADCP_GPS	
30.634	49.795	2.822	81.740	ADCP_GPS	
30.902	49.855	2.762	82.488	ADCP_GPS	
31.170	49.907	2.710	83.221	ADCP_GPS	

31.438	49.959	2.658	83.940	ADCP_GPS	
31.706	50.016	2.601	84.645	ADCP_GPS	
31.974	50.082	2.535	85.333	ADCP_GPS	
32.242	50.178	2.439	86.000	ADCP_GPS	
32.510	50.313	2.304	86.636	ADCP_GPS	
32.778	50.403	2.214	87.241	ADCP_GPS	
33.046	50.414	2.203	87.833	ADCP_GPS	
33.314	50.451	2.166	88.418	ADCP_GPS	
33.582	50.491	2.126	88.993	ADCP_GPS	
33.850	50.544	2.073	89.556	ADCP_GPS	
34.118	50.593	2.024	90.105	ADCP_GPS	
34.386	50.620	1.997	90.644	ADCP_GPS	
34.654	50.633	1.984	91.177	ADCP_GPS	
34.922	50.649	1.968	91.707	ADCP_GPS	
35.190	50.676	1.941	92.231	ADCP_GPS	
35.458	50.714	1.903	92.746	ADCP_GPS	
35.837	50.741	1.876	93.462	ADCP_GPS	
36.105	50.787	1.830	93.959	ADCP_GPS	
36.373	50.852	1.765	94.441	ADCP_GPS	
36.641	50.922	1.695	94.905	ADCP_GPS	
36.909	50.967	1.650	95.353	ADCP_GPS	
37.177	51.010	1.607	95.789	ADCP_GPS	
37.445	51.016	1.601	96.219	ADCP_GPS	
37.713	51.062	1.555	96.642	ADCP_GPS	
37.981	51.141	1.476	97.048	ADCP_GPS	
38.249	51.250	1.367	97.429	ADCP_GPS	
39.280	51.373	1.244	98.775	ETS	
40.363	51.502	1.115	100.052	ETS	
40.741	51.719	0.898	100.432	ETS	
41.130	51.928	0.689	100.741	ETS	
41.433	52.091	0.526	100.925	ETS	
41.505	52.220	0.397	100.958	ETS	
41.610	52.408	0.209	100.990	ETS	
41.727	52.617	0.000	101.002	ETS	RB BFL
41.831	52.677			ETS	
42.292	52.943			ETS	
42.314	52.956			ETS/GPS	RB BM

Water surface level during measurement = 52.943m
Approximated bankfull level = 52.617m

Table C.4 Wilton Creek Cross-sectional Data

CUM_DIS. LB TO RB (m)	BED_AL (m)	AV_BFD (m)	CUM_AREA LB TO RB (m^2)	SURVEYING METHOD	NOTE
0	100.033			ETS	
1.54	99.882	0	0	ETS	LB-BFL
1.87	99.787	0.095	0.016	ETS	
2.2	99.693	0.189	0.063	ETS	
2.58	99.584	0.298	0.156	ETS	
2.975	99.471	0.411	0.296	ETS	
3.103	99.389	0.493	0.354	ETS	
3.362	99.223	0.659	0.503	ETS	
3.951	98.87	1.012	0.995	ETS	
5.051	98.704	1.178	2.2	ETS	
7.004	98.394	1.488	4.803	ETS	
8.519	98.155	1.727	7.238	ETS	
10.14	98.122	1.76	10.064	ETS	
13.434	98.111	1.771	15.88	ETS	
13.77	98.257	1.625	16.451	ETS	
14.06	98.383	1.499	16.904	ETS	
14.24	98.679	1.203	17.147	ETS	
14.38	98.909	0.973	17.299	ETS	
14.53	99.155	0.727	17.426	ETS	
14.845	99.389	0.493	17.618	ETS	
15.13	99.601	0.281	17.728	ETS	
15.32	99.742	0.14	17.768	ETS	
15.499	99.875	0.007	17.781	ETS	
15.52	99.882	0	17.781	ETS	RB-BFL
16.847	100.38			ETS	
19.021	100.429			ETS	

Water surface level during measurement = 99.389m
Approximated bankfull level = 99.882m

Table C.5 West Branch Little Cataraqui Creek Cross-sectional Data

CUM_DIS. LB TO RB (m)	BED_AL (m)	AV_BFD (m)	CUM_AREA LB TO RB (m2)	SURVEYING METHOD	NOTE
0	82.843			ETS	
0.761	82.86			ETS	LB BM
1.435	82.822			ETS	
1.985	82.772	0	0	ETS	LB BFL
2.07	82.707	0.065	0.003	ETS	
2.171	82.63	0.142	0.013	ETS	
2.202	82.478	0.294	0.02	ETS	
2.21	82.436	0.336	0.023	ETS	
2.252	82.228	0.544	0.041	ETS	
3.03	82.149	0.623	0.495	ETS	
3.345	82.132	0.64	0.694	ETS	
3.671	82.193	0.579	0.893	ETS	
3.938	82.033	0.739	1.069	ETS	
4.25	82.015	0.757	1.302	ETS	
4.581	82.056	0.716	1.546	ETS	
4.783	82.029	0.743	1.693	ETS	
5.156	82.07	0.702	1.962	ETS	
5.465	82.109	0.663	2.173	ETS	
5.746	82.168	0.604	2.351	ETS	
6.074	82.213	0.559	2.542	ETS	
6.43	82.358	0.414	2.715	ETS	
6.725	82.478	0.294	2.819	ETS	
7.01	82.644	0.128	2.879	ETS	
7.208	82.759	0.013	2.893	ETS	
7.255	82.772	0	2.893	ETS	RB BFL
7.756	82.915			ETS	
8.65	83.031			ETS	

✓ Abbreviations used in Tables C1 – C5

- CUM_DIS Cumulative distance
- LB TO RB Left bank to right bank
- BED_AL Bed altitude
- AV_BFD Average distance at bankfull level
- CUM_AREA Cumulative area
- RB BFL Right bank bankfull level
- LB BFL Left bank bankfull level
- RB BM Right bank bench bank
- ETS Electronic Total Station
- GPS Global Positioning System

Appendix D

D Field Configuration for ADCP Measurements

I Jock River Field Configuration

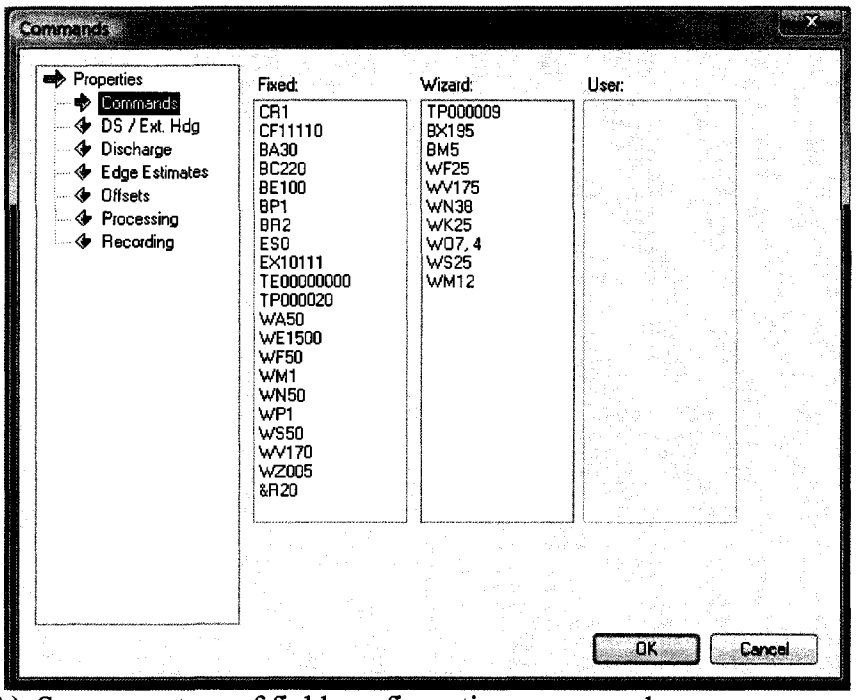

A) Screen capture of field configuration, commands

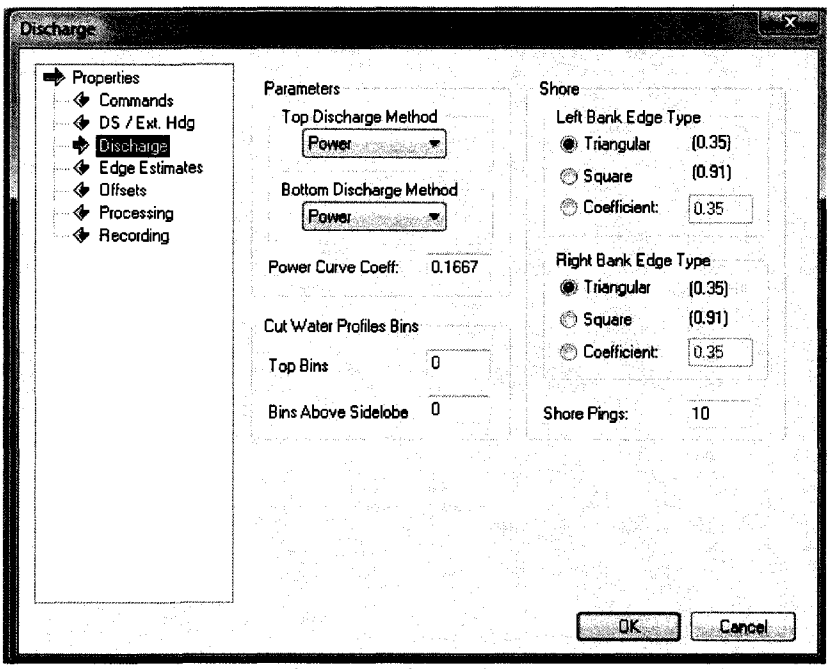

B) Screen capture of field configuration, unmeasured discharge

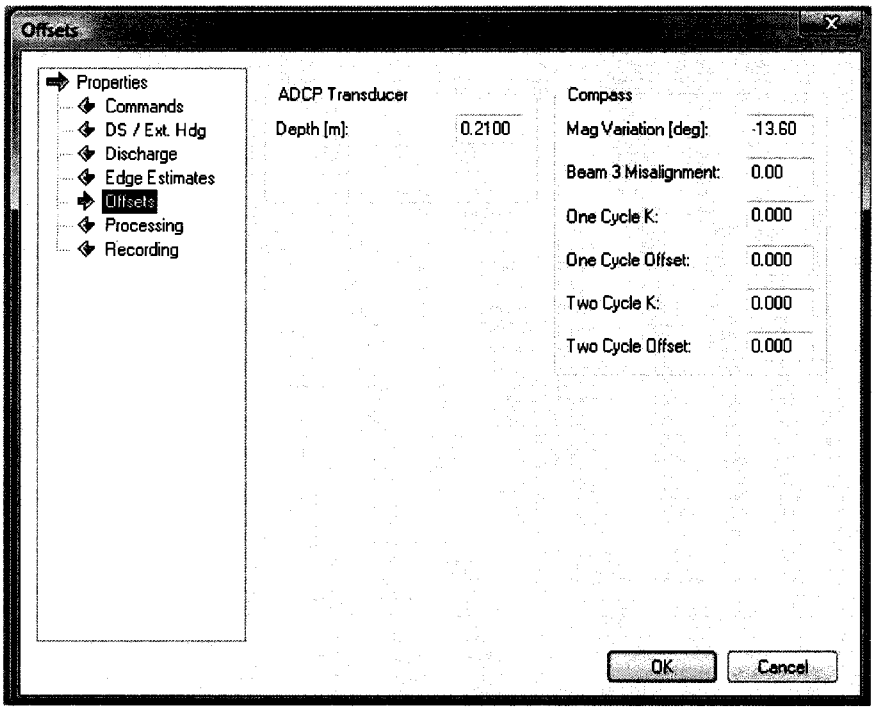

C) Screen capture of field configuration, offsets input

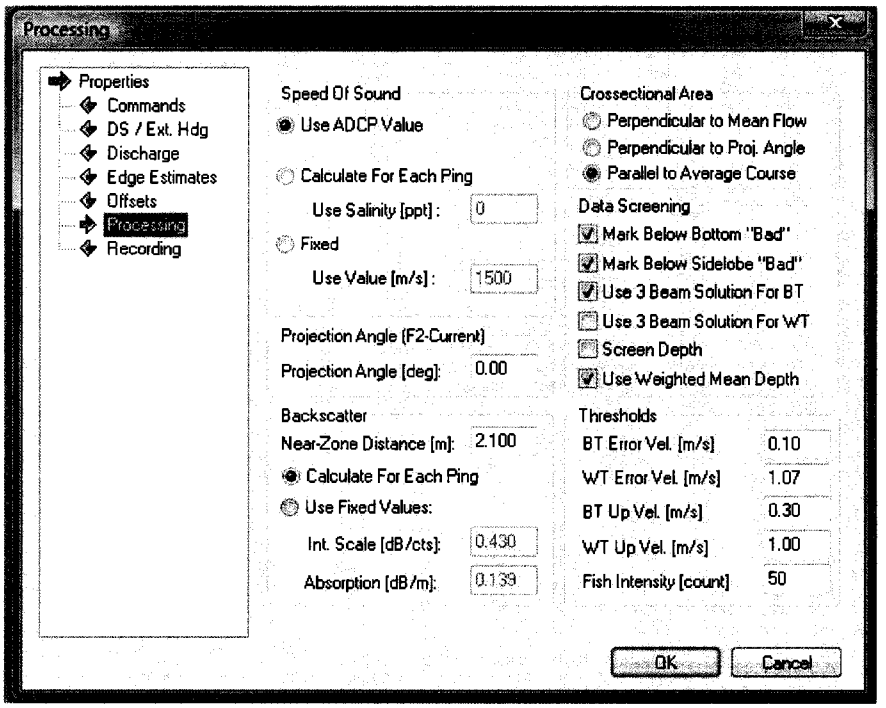

D) Screen capture of field configuration, processing information

II Raisin River Field Configuration

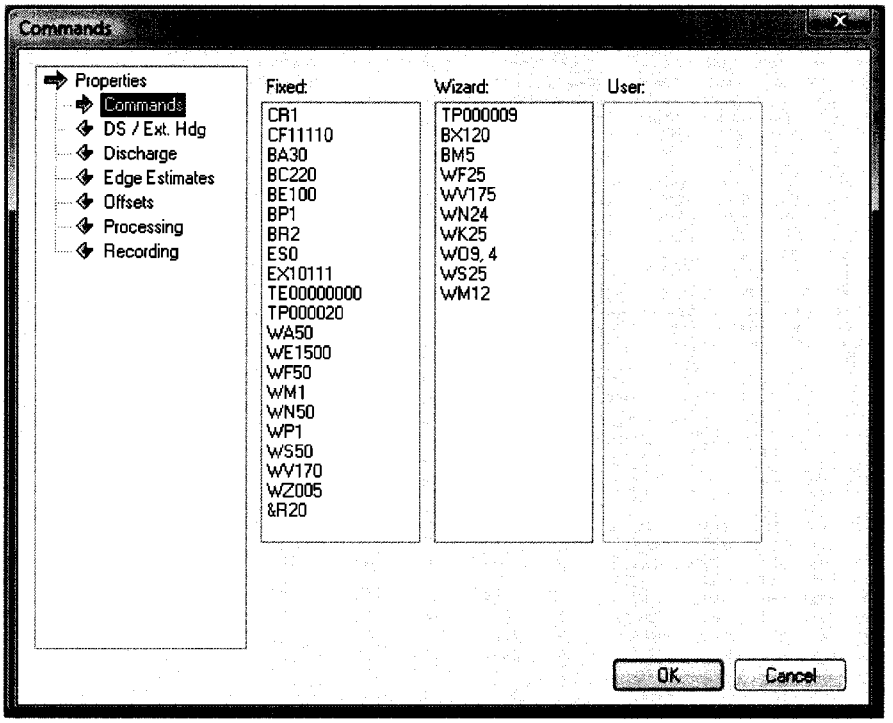

A) Screen capture of field configuration, commands

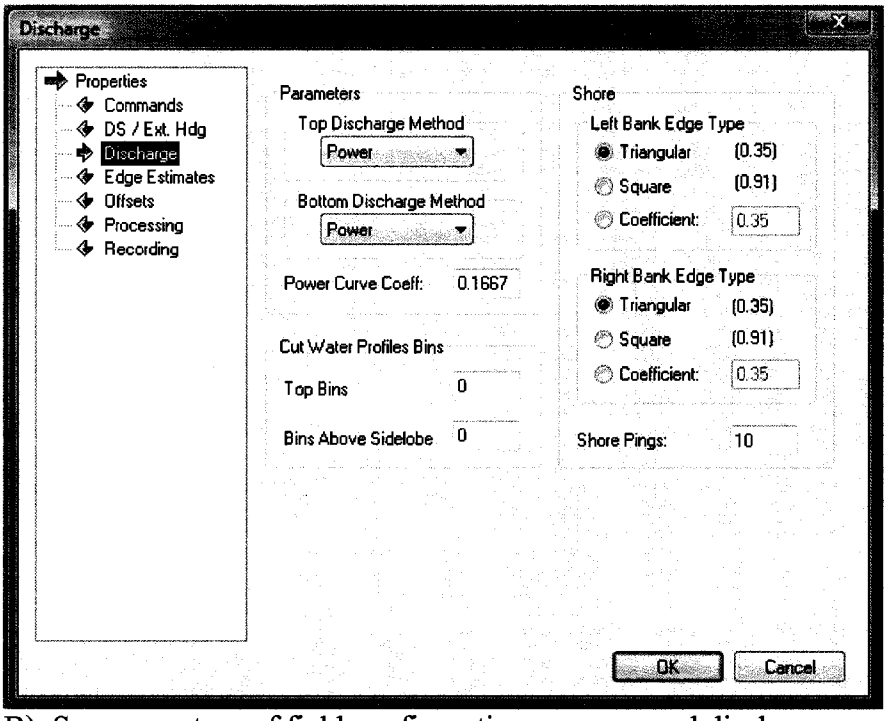

B) Screen capture of field configuration, unmeasured discharge

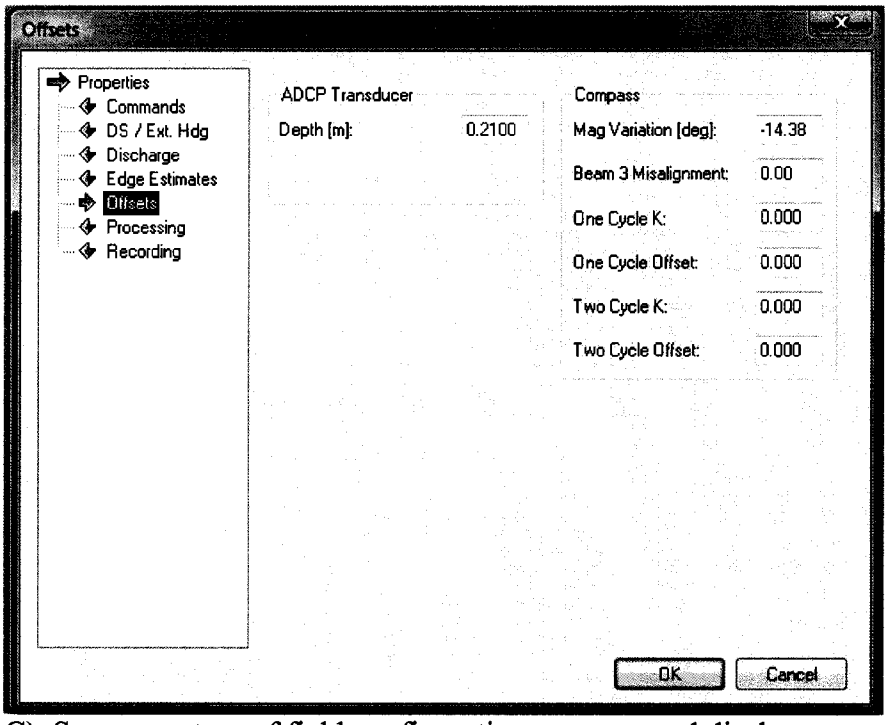

C) Screen capture of field configuration, unmeasured discharge

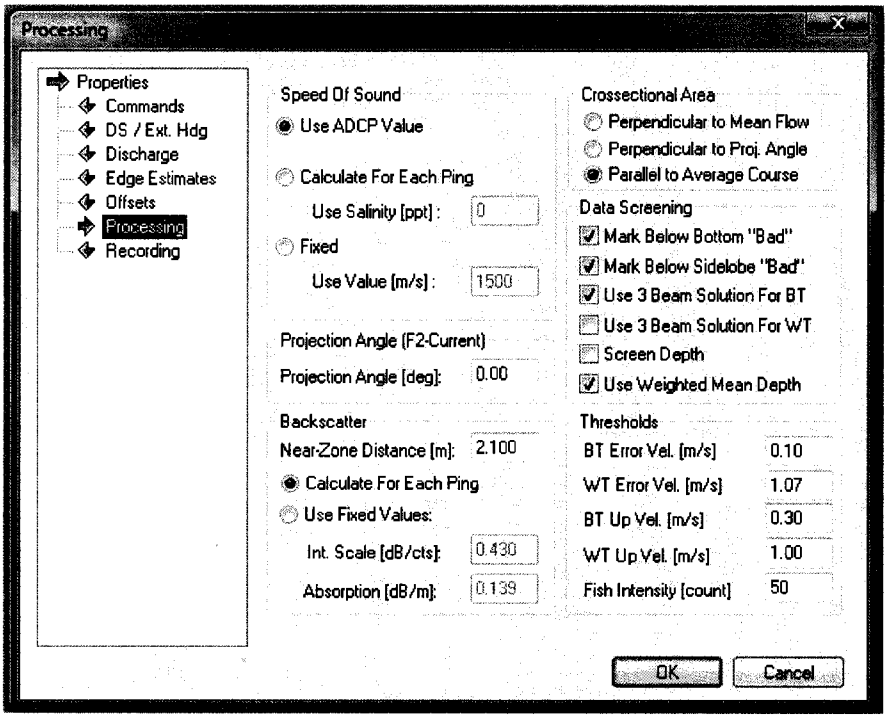

D) Screen capture of field configuration, processing information

III South Nation River Field Configuration

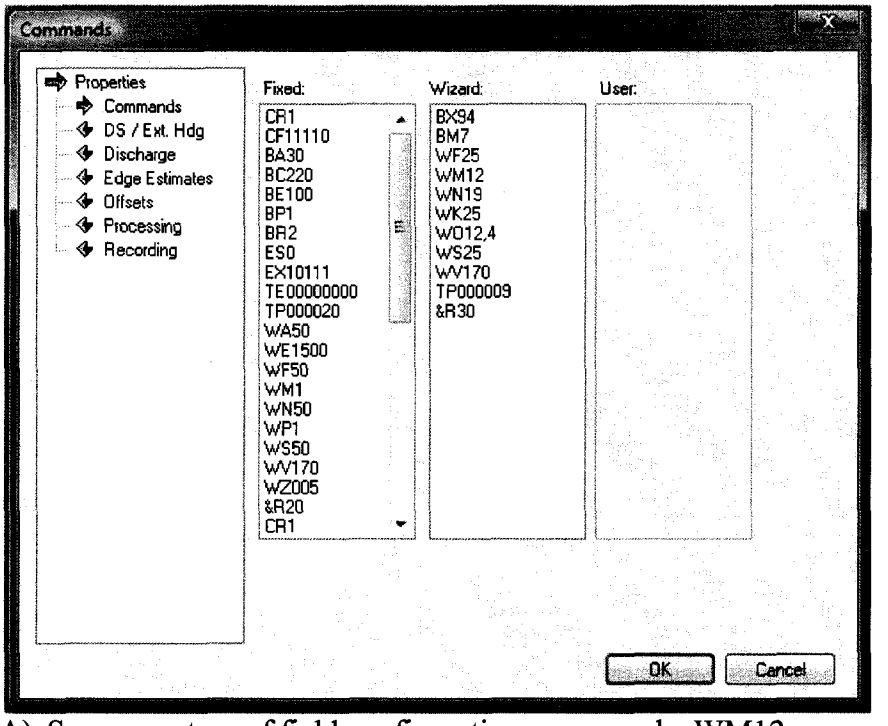

A) Screen capture of field configuration, commands; WM12

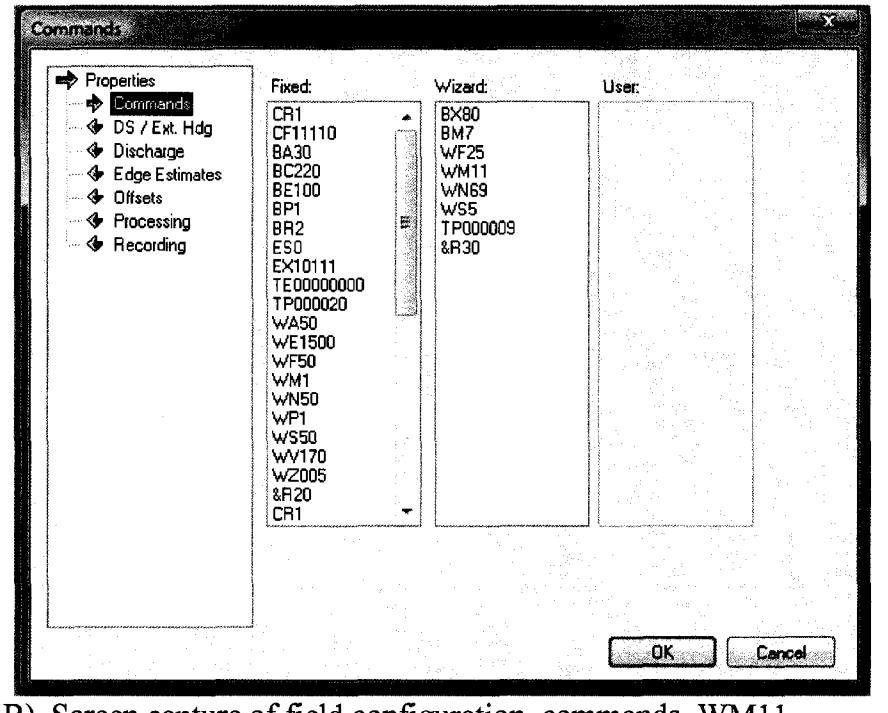

B) Screen capture of field configuration, commands, WM11

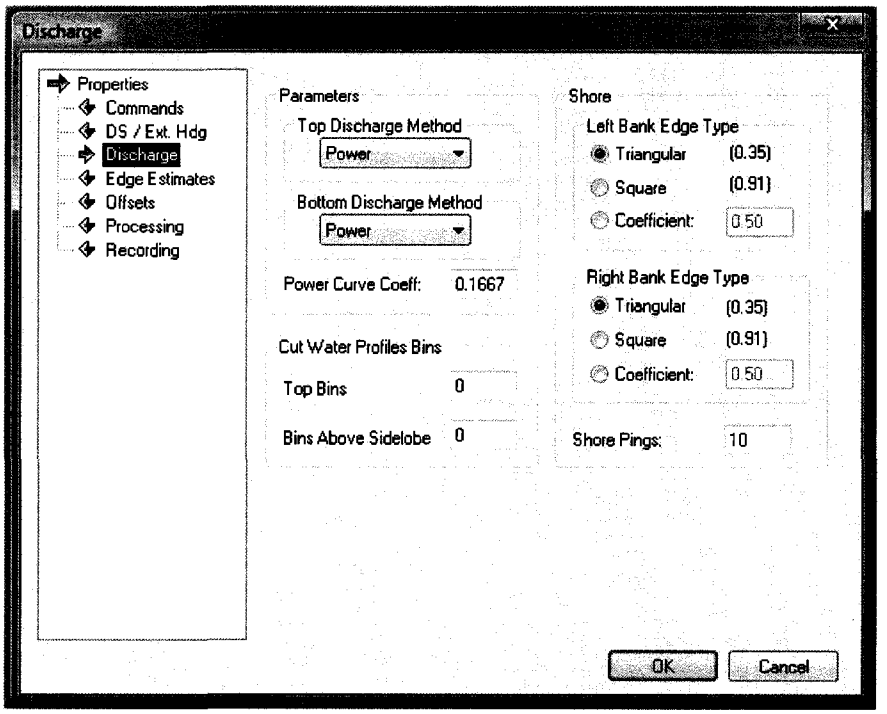

C) Screen capture of field configuration, unmeasured discharge

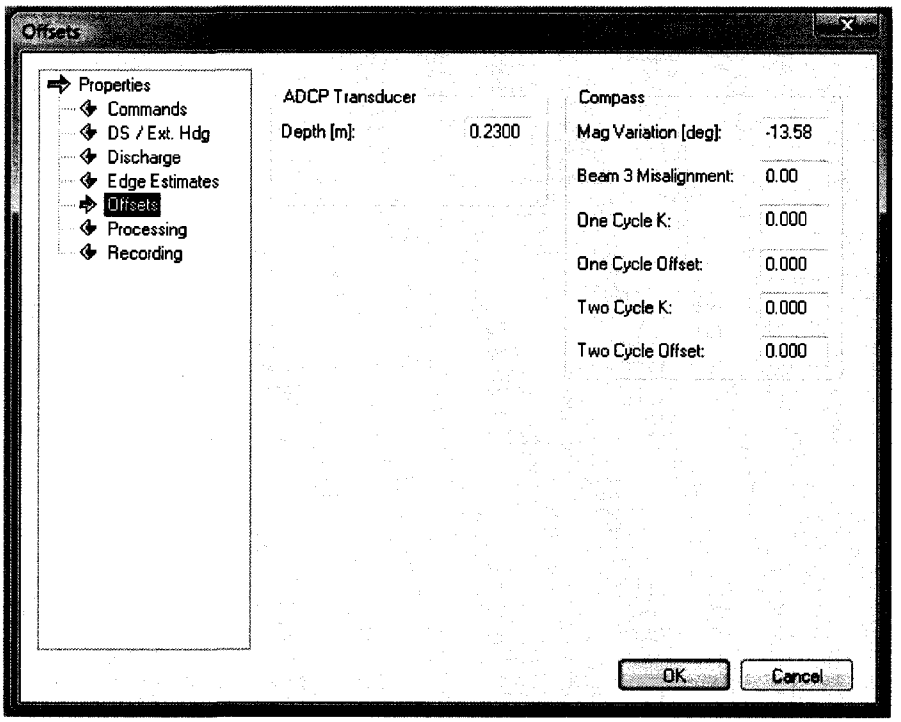

D) Screen capture of field configuration, offsets input

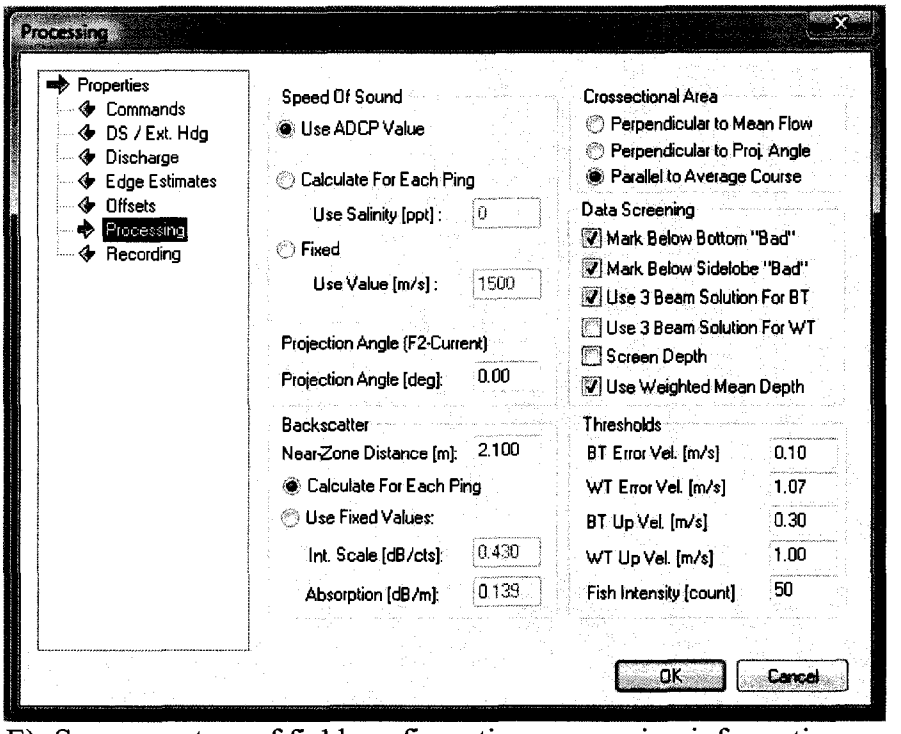

E) Screen capture of field configuration, processing information

Appendix E

E Matlab Code Used to Read PDO Files Created by WinRiver

```
function [Hdr, Inst, Cfg, Sensor, Gps, Wt, Bt, Nmea, Gps2]=pd0wr2(fullName);
%% Read RDI PD0 File Format (WinRiver)
% The function reads the RDI PD0 format raw data as recorded by WinRiver.
% It accounts for the special locations used by WinRiver to store GPS data.
% It should read standard PD0 formatted files but was written specifically
% for PD0 files created by WinRiver.
%
% Data are stored in Matlab data structures to provide easy and efficient
% transfer of data between functions. For numeric data the arrays are
% preallocated with "nan" (not a number) so that no value is assumed for bad
% or missing data. Data coded with -32768 are not stored and default to "nan".
% No filtering of the data is provided, although some units conversion is
% provided for consistency and convience. All data structures begin with an
% upper case letter. All variable names begin with a lower case letter. If
% a specific dimension is associated with a variable the variable name will
% include an underscore "_" followed by the dimension. The dimension
% abrevations used are as follows:
%  cm     - centimeters
%  deg    - degrees
%  degc   - degrees Celsius
%  dm     - decimeters
%  m      - meters
%  mm     - millimeters
%  mmps   - millimeters per second
%  mps    - meters per second
%  msc    - minutes seconds hundreths of a second
%  pascal - pascals
%  ppt    - parts per thousand
%  sec    - seconds
%
% Data that vary with depth are stored so that the bin (depth) varies by
% row and the ensemble varies by column. Most other data are stored so that
% the ensemble varies by row. Data associated with various beams are stored
% with a 3rd dimension reflecting the beam number.
%
% David S. Mueller (dmueller@usgs.gov)
% U.S. Geological Survey
% Office of Surface Water
% July 11, 2005
%
% MODIFIED 6/23/2006 dsm
% 1) Fixed Gps. structure to be consisent with (iensembles,n).
% 2) Added check for checksum
%
% MODIFIED 6/28/2006 dsm
% 3) Added data type '5000' to allow reading of Streampro raw data
%
% MODIFIED 7/25/2006 dsm
% 4) Modified code to correct for bad checksum and to refind a valid
%    ensemble and read remainder of file.
%
```

```
% MODIFIED 4/18/2007 dsm
% 5) Added code to search for a '7F7F' leader_id before proceeding into the
% remainder of the code. Some files have the instrument defined or other
% information prior to the first '7F7F'.
%
% 6) Changed the way the end of file is determined.
%
% 7) Fixed the "other" case to handle undefined data types
%
% 8) Commented out data type '5000' since the code now handles unknown data
% types properly and we don't have the coding information for '5000'.


%% Open File

%%%%%%%%%%%%%%%%%%%%%%%%%%%%%%%%%%%%%%%%%%%%%%%%%%%%%%%%%%%%%%%%%%%%%%%%%%%%%%%%%%
%Miressa Ebisa Fola, University of Ottawa, April, 2007
%Added to facilitate an input of the 'xxx.pd0' file on screen
%To run the code write on screen: >>pd0wr2
%The code and file should be in the same directory (folder)
%fullname: 'xxx.Pd0'; xxx is file name Winriver II pd0 format
%Example: >>Input pd0 File Name:'Jock_TR_001.PD0'
fullName = input('Input pd0 File Name: ');
%%%%%%%%%%%%%%%%%%%%%%%%%%%%%%%%%%%%%%%%%%%%%%%%%%%%%%%%%%%%%%%%%%%%%%%%%%%%%%%%%%

% Get and display file information
FileInfo=dir(fullName)
% Open File
fid=fopen(fullName,'r','l');

%% Read Selected Parameters
% Selected portions of the raw data file are read to determine the number
% of ensembles, the number of bins, and the number of beams. These
% variables are used to preallocate the arrays in the data structures used
% to store the data in Matlab. Although preallocation is not required it
% does improve the performance of Matlab.
  leader_id=dec2hex(fread(fid,1,'uint16'),4);
  if leader_id~='7F7F'
    while ~strcmp(leader_id,'7F7F')
      fseek(fid,-1,'cof');
      leader_id=dec2hex(fread(fid,1,'uint16'),4);
    end
  end
  initialPos=ftell(fid)-2;
% Set the position in the file and read the number of bytes per ensemble.
%fseek(fid,2,'bof');
bytesPerEns=fread(fid,1,'uint16');

% Set the position in the file and read the number of data types in the
% file.
fseek(fid,1,'cof');
nTypes=fread(fid,1,'uint8');
offset=fread(fid,1,'uint16');

% Set the position in the file and read the number of beams and the number
% of bins.
```

```
fseek(fid,initialPos+offset+8,'bof');
ftell(fid)
nBeams=fread(fid,1,'uint8');
nBins=fread(fid,1,'uint8');

% Compute the number of ensembles
nEnsembles=ceil(FileInfo.bytes/(bytesPerEns+2));

%% Define Data Storage Structure.
% A data storage structure is used to provide an easy and efficient method
% for passing large amounts of data between functions. The arrays within
% the structure are preallocated for efficiency.

% Clear variables to be used.
clear Hdr Inst Cfg Sensor Gps Wt Bt  Nmea;

% Data structure for the Binary Header Data
Hdr=struct( 'bytesPerEns', zeros(nEnsembles,1),...
        'dataOffsets', zeros(nEnsembles,nTypes),...
        'nDataTypes', zeros(nEnsembles,1),...
        'dataOK',zeros(nEnsembles,1));

% Data structure for variables related to the instrument
Inst=struct('beamAng', zeros(nEnsembles,1),...
        'beams', zeros(nEnsembles,1),...
        'dataType', repmat(blanks(4),nEnsembles,1),...
        'firmVer', zeros(nEnsembles,1),...
        'freq', zeros(nEnsembles,1),...
        'pat', repmat(blanks(7),nEnsembles,1),...
        'resRDI', zeros(1),...
        'sensorCfg', nan(nEnsembles,1),...
        'xducer', repmat(blanks(12),nEnsembles,1));

% Data structure for direct commands and other configuration information
Cfg=struct( 'ba', nan(nEnsembles,1),...
        'bc', nan(nEnsembles,1),...
        'be_mmps', nan(nEnsembles,1),...
        'bg', nan(nEnsembles,1),...
        'bm', nan(nEnsembles,1),...
        'bp', nan(nEnsembles,1),...
        'bx_dm', nan(nEnsembles,1),...
        'codeReps', nan(nEnsembles,1),...
        'coordSys', repmat(blanks(5),nEnsembles,1),...
        'cpuSerNo', nan(nEnsembles,8),...
        'cq', nan(nEnsembles,1),...
        'cx', nan(nEnsembles,1),...
        'distBin1_cm', nan(nEnsembles,1),...
        'ea_deg', nan(nEnsembles,1),...
        'eb_deg', nan(nEnsembles,1),...
        'ec', repmat(blanks(8),nEnsembles,1),...
        'ex', repmat(blanks(8),nEnsembles,1),...
        'ez', repmat(blanks(8),nEnsembles,1),...
        'headSrc', repmat(blanks(11),nEnsembles,1),...
        'lag_cm', nan(nEnsembles,1),...
        'mapBins', repmat(blanks(3),nEnsembles,1),...
        'nBeams', nan(nEnsembles,1),...
```

```
        'pitchSrc', repmat(blanks(11),nEnsembles,1),...
        'refLayEndCell', nan(nEnsembles,1),...
        'refLayStrCell', nan(nEnsembles,1),...
        'rollSrc', repmat(blanks(11),nEnsembles,1),...
        'salSrc', repmat(blanks(9),nEnsembles,1),...
        'wm', nan(nEnsembles,1),...
        'sosSrc', repmat(blanks(11),nEnsembles,1),...
        'tempSrc', repmat(blanks(11),nEnsembles,1),...
        'tp_sec', nan(nEnsembles,1),...
        'use3beam', repmat(blanks(3),nEnsembles,1),...
        'usePR', repmat(blanks(3),nEnsembles,1),...
        'wa', nan(nEnsembles,1),...
        'wb', nan(nEnsembles,1),...
        'wc', nan(nEnsembles,1),...
        'we_mmps', nan(nEnsembles,1),...
        'wf_cm', nan(nEnsembles,1),...
        'wg_per', nan(nEnsembles,1),...
        'wj', nan(nEnsembles,1),...
        'wn', nan(nEnsembles,1),...
        'wp', nan(nEnsembles,1),...
        'ws_cm', nan(nEnsembles,1),...
        'xdcrDepSrs', repmat(blanks(9),nEnsembles,1),...
        'xmitPulse_cm', nan(nEnsembles,1));

% Data structure for data obtained from the various internal and external sensors.
Sensor=struct( 'ambientTemp', nan(nEnsembles,1),...
        'attitudeTemp', nan(nEnsembles,1),...
        'attitude', nan(nEnsembles,1),...
        'bitTest', nan(nEnsembles,1),...
        'contamSensor', nan(nEnsembles,1),...
        'date', nan(nEnsembles,4),...
        'dateNotY2k', nan(nEnsembles,3),...
        'dateY2k', nan(nEnsembles,4),...
        'errorStatusWord', repmat(blanks(8),[nEnsembles,1,4]),...
        'headingStdDev', nan(nEnsembles,1),...
        'heading_deg', nan(nEnsembles,1),...
        'mpt_msc', nan(nEnsembles,3),...
        'num', nan(nEnsembles,1),...
        'numFact', nan(nEnsembles,1),...
        'orient', repmat(blanks(4),nEnsembles,1),...
        'pitchStdDev', nan(nEnsembles,1),...
        'pitch_deg', nan(nEnsembles,1),...
        'pressureNeg', nan(nEnsembles,1),...
        'pressurePos', nan(nEnsembles,1),...
        'pressureVar_pascal', nan(nEnsembles,1),...
        'pressure_pascal', nan(nEnsembles,1),...
        'rollStdDev_deg', nan(nEnsembles,1),...
        'roll_deg', nan(nEnsembles,1),...
        'salinity_ppt', nan(nEnsembles,1),...
        'sos_mps', nan(nEnsembles,1),...
        'temperature_degc', nan(nEnsembles,1),...
        'time', nan(nEnsembles,4),...
        'timeY2k', nan(nEnsembles,4),...
        'xdcrDepth_dm', nan(nEnsembles,1),...
        'xmitCurrent', nan(nEnsembles,1),...
        'xmitVoltage', nan(nEnsembles,1));
```

```
% Data structure for the water track data. Data are stored in 3-dimensional
% arrays with the 1st dimension (rows) being the bin number, the second
% dimension (column) being the ensemble index, and the 3rd dimension being
% the beam number.
Wt=struct(  'corr', nan(nBins,nEnsembles,nBeams),...
        'pergd', nan(nBins,nEnsembles,nBeams),...
        'rssi', nan(nBins,nEnsembles,nBeams),...
        'vel_mps', nan(nBins,nEnsembles,nBeams));

% Data structure for the bottom track data. Data are stored in 2-dimensional
% arrays with the 1st dimension (rows) being the beam number and the 2nd
% dimension being the ensemble index.
Bt=struct(  'corr', nan(nBeams,nEnsembles),...
        'depth_m', nan(nBeams,nEnsembles),...
        'evalAmp', nan(nBeams,nEnsembles),...
        'extDepth_cm', nan(nEnsembles,1),...
        'pergd', nan(nBeams,nEnsembles),...
        'rssi', nan(nBeams,nEnsembles),...
        'vel_mps', nan(nBeams,nEnsembles));

% Data structure for GPS data
Gps=struct( 'alt_m', nan(nEnsembles,1),...
        'ggaDiff', nan(nEnsembles,1),...
        'ggaHdop', nan(nEnsembles,1),...
        'ggaNStats', nan(nEnsembles,1),...
        'ggaVelE_mps', nan(nEnsembles,1),...
        'ggaVelN_mps', nan(nEnsembles,1),...
        'gsaPdop', nan(nEnsembles,1),...
        'gsaSat', nan(nEnsembles,6),...
        'gsaVdop', nan(nEnsembles,1),...
        'lat_deg', nan(nEnsembles,1),...
        'long_deg', nan(nEnsembles,1),...
        'vtgVelE_mps', nan(nEnsembles,1),...
        'vtgVelN_mps', nan(nEnsembles,1));
Gps2=struct( 'ggaDeltaTime', repmat(blanks(8),nEnsembles,1),...
        'ggaHeader', repmat(blanks(10),nEnsembles,1),...
        'utc', nan(nEnsembles,1),...
        'lat_dm', nan(nEnsembles,1),...
        'latRef', repmat(blanks(1),nEnsembles,1),...
        'lon_dm', nan(nEnsembles,1),...
        'lonRef', repmat(blanks(1),nEnsembles,1),...
        'corrQual', nan(nEnsembles,1),...
        'numSats', nan(nEnsembles,1),...
        'hdop', nan(nEnsembles,1),...
        'alt', nan(nEnsembles,1),...
        'altUnit', repmat(blanks(1),nEnsembles,1),...
        'geoid', nan(nEnsembles,1),...
        'geoidUnit', repmat(blanks(1),nEnsembles,1),...
        'dgpsAge', nan(nEnsembles,1),...
        'refStatID', nan(nEnsembles,1),...
        'vtgDeltaTime', repmat(blanks(8),nEnsembles,1),...
        'vtgHeader', repmat(blanks(10),nEnsembles,1),...
        'courseTrue', nan(nEnsembles,1),...
        'trueIndicator', repmat(blanks(1),nEnsembles,1),...
        'courseMag', nan(nEnsembles,1),...
```

```
        'magIndicator', repmat(blanks(1),nEnsembles,1),...
        'speedKnots', nan(nEnsembles,1),...
        'knotsIndicator', repmat(blanks(1),nEnsembles,1),...
        'speedKmph', nan(nEnsembles,1),...
        'kmphIndicator', repmat(blanks(1),nEnsembles,1),...
        'modeIndicator', repmat(blanks(1),nEnsembles,1),...
        'dbtDeltaTime', repmat(blanks(8),nEnsembles,1),...
        'dbtHeader', repmat(blanks(10),nEnsembles,1),...
        'depth_ft', nan(nEnsembles,1),...
        'ftIndicator', repmat(blanks(1),nEnsembles,1),...
        'depth_m', nan(nEnsembles,1),...
        'mIndicator', repmat(blanks(1),nEnsembles,1),...
        'depth_fath', nan(nEnsembles,1),...
        'fathIndicator', repmat(blanks(1),nEnsembles,1),...
        'hdtDeltaTime', repmat(blanks(8),nEnsembles,1),...
        'hdtHeader', repmat(blanks(10),nEnsembles,1),...
        'heading_deg', nan(nEnsembles,1),...
        'hTrueIndicactor', repmat(blanks(1),nEnsembles,1));

% Data structure for raw NMEA data strings. The strings are stored
% in a character array with rows being the ensemble index and columns
% the characters in the respective string.
Nmea=struct('gga', repmat(blanks(97),nEnsembles,1),...
        'gsa', repmat(blanks(60),nEnsembles,1),...
        'vtg', repmat(blanks(50),nEnsembles,1),...
        'raw', repmat(blanks(100),nEnsembles,1));
%% Read Raw Data
% Data in the PD0 format are organized by leader_id. The leader_id is read
% and the appropriate statements executed to read the data defined by the
% leader_id. All data are read and stored, even data that should not change
% between ensembles. The data are read until the end of file character is
% encountered.
fseek(fid,initialPos,'bof');
iEns=0;
disp('Reading file')
endFileCheck=0;
endFile=FileInfo.bytes;
while endFileCheck<endFile

%  Read leader_id
  leader_id=dec2hex(fread(fid,1,'uint16'),4);

%  Select appropriate code to read data based on leader_id
  switch leader_id

%%     Read Binary Header Data
    case '7F7F'
      i2022=0;
      fileloc=ftell(fid)-2;
      idataTypes=0;
      iEns=iEns+1;
      Hdr.bytesPerEns(iEns)=fread(fid,1,'uint16');
      bytesPerEns=Hdr.bytesPerEns(iEns);

%       Check checksum for valid ensemble
      fseek(fid,fileloc,'bof');
```

```
        Testb = fread(fid,Hdr.bytesPerEns(iEns),'uchar');
        check=sum(Testb);
        checkh=dec2hex(check);
        checkh=checkh(end-3:end);
        fseek(fid,fileloc+Hdr.bytesPerEns(iEns),'bof');
        checksum=fread(fid,1,'uint16');
        if hex2dec(checkh)==checksum
          Hdr.dataOK(iEns)=1;
          fseek(fid,fileloc+5,'bof');
          Hdr.nDataTypes(iEns)=fread(fid,1,'uint8');
          Hdr.dataOffsets(iEns,1:Hdr.nDataTypes(iEns))=fread(fid,Hdr.nDataTypes(iEns),'uint16');
          if (idataTypes+1)<=Hdr.nDataTypes(iEns)
            fseek(fid,(Hdr.dataOffsets(iEns,idataTypes+1)+fileloc),'bof');
          else
            fseek(fid,fileloc+bytesPerEns-2);
          end
        else
          disp('Bad Checksum');
          search_id='  ';
          searchloc=fileloc+2;
          while search_id~=hex2dec('7F7F');
            searchloc=searchloc+1;
            fseek(fid,searchloc,'bof');
            search_id=fread(fid,1,'uint16');
          end
          fseek(fid,searchloc,'bof');
          idataTypes=-1;
        end

%%    Read Binary Fixed Leader Data
      case '0000'
        idataTypes=idataTypes+1;
        Inst.firmVer(iEns)=fread(fid,1,'uint8');
        Inst.firmVer(iEns)=Inst.firmVer(iEns)+fread(fid,1,'uint8')/100;
        bitls=fread(fid,1,'uint8');
        bitls=dec2base(bitls,2,8);

        switch base2dec(bitls(6:8),2)
          case 0;   Inst.freq(iEns)=75;
          case 1;   Inst.freq(iEns)=150;
          case 2;   Inst.freq(iEns)=300;
          case 3;   Inst.freq(iEns)=600;
          case 4;   Inst.freq(iEns)=1200;
          case 5;   Inst.freq(iEns)=2400;
          otherwise; Inst.freq(iEns)=nan;
        end;

        switch base2dec(bitls(5),2)
          case 0;   Inst.pat(iEns,:)='Concave';
          case 1;   Inst.pat(iEns,:)='Convex ';
          otherwise;  Inst.pat(iEns,:)='n/a   ';
        end;

        Inst.sensorCfg(iEns)=base2dec(bitls(3:4),2)+1;

        switch base2dec(bitls(2),2)
```

```
   case 0;    Inst.xducer(iEns,:)='Not Attached';
   case 1;    Inst.xducer(iEns,:)='Attached    ';
   otherwise; Inst.xducer(iEns,:)='n/a         ';
end;

switch base2dec(bitls(1),2)
   case 0;    Sensor.orient(iEns,:)='Down';
   case 1;    Sensor.orient(iEns,:)='Up  ';
   otherwise; Sensor.orient(iEns,:)='n/a ';
end;

bitms=fread(fid,1,'uint8');
bitms=dec2base(bitms,2,8);

switch base2dec(bitms(7:8),2)
   case 0;    Inst.beamAng(iEns)=15;
   case 1;    Inst.beamAng(iEns)=20;
   case 2;    Inst.beamAng(iEns)=30;
   case 3;    Inst.beamAng(iEns)=nan;
   otherwise; Inst.beamAng(iEns)=nan;
end;

switch base2dec(bitms(1:4),2)
   case 4
      Inst.beams(iEns)=4;
   case 5
      Inst.beams(iEns)=5;
      Inst.demod(iEns)=1;
   case 15
      Inst.beams(iEns)=5;
      Inst.demod(iEns)=2;
   otherwise
      Inst.beams(iEns)=nan;
      Inst.demod(iEns)=nan;
end;

switch fread(fid,1,'uint8')
   case 0;    Inst.dataType(iEns,:)='Real';
   otherwise; Inst.dataType(iEns,:)='Simu';
end;

fseek(fid,1,'cof');
Cfg.nBeams(iEns)=fread(fid,1,'uint8');
Cfg.wn(iEns)=fread(fid,1,'uint8');
Cfg.wp(iEns)=fread(fid,1,'uint16');
Cfg.ws_cm(iEns)=fread(fid,1,'uint16');
Cfg.wf_cm(iEns)=fread(fid,1,'uint16');
Cfg.wm(iEns)=fread(fid,1,'uint8');
Cfg.wc(iEns)=fread(fid,1,'uint8');
Cfg.codeReps(iEns)=fread(fid,1,'uint8');
Cfg.wg_per(iEns)=fread(fid,1,'uint8');
Cfg.we_mmps(iEns)=fread(fid,1,'uint16');
Cfg.tp_sec(iEns,:)=sum(fread(fid,3,'uint8').*[60 1 0.01]');
Cfg.ex(iEns,:)=dec2base(fread(fid,1,'uint8'),2,8);

switch base2dec(Cfg.ex(iEns,4:5),2)
```

```
   case 0;    Cfg.coordSys(iEns,:)='Beam ';
   case 1;    Cfg.coordSys(iEns,:)='Inst ';
   case 2;    Cfg.coordSys(iEns,:)='Ship ';
   case 3;    Cfg.coordSys(iEns,:)='Earth';
   otherwise; Cfg.coordSys(iEns,:)='n/a  ';
end;

switch base2dec(Cfg.ex(iEns,6),2)
   case 0;    Cfg.usePR(iEns,:)='No ';
   case 1;    Cfg.usePR(iEns,:)='Yes';
   otherwise; Cfg.usePR(iEns,:)='n/a';
end;

switch base2dec(Cfg.ex(iEns,7),2)
   case 0;    Cfg.use3beam(iEns,:)='No ';
   case 1;    Cfg.use3beam(iEns,:)='Yes';
   otherwise; Cfg.use3beam(iEns,:)='n/a';
end;

switch base2dec(Cfg.ex(iEns,8),2)
   case 0;    Cfg.mapBins(iEns,:)='No ';
   case 1;    Cfg.mapBins(iEns,:)='Yes';
   otherwise; Cfg.mapBins(iEns,:)='n/a';
end;

Cfg.ea_deg(iEns)=fread(fid,1,'int16')*0.01;
Cfg.eb_deg(iEns)=fread(fid,1,'uint16')*0.01;
Cfg.ez(iEns,:)=dec2base(fread(fid,1,'uint8'),2,8);

switch base2dec(Cfg.ez(iEns,1:2),2)
   case 0;    Cfg.sosSrc(iEns,:)='Manual EC  ';
   case 1;    Cfg.sosSrc(iEns,:)='Calculated ';
   case 3;    Cfg.sosSrc(iEns,:)='SVSS Sensor';
   otherwise; Cfg.sosSrc(iEns,:)='n/a        ';
end

switch base2dec(Cfg.ez(iEns,3),2)
   case 0;    Cfg.xdcrDepSrc(iEns,:)='Manual ED';
   case 1;    Cfg.xdcrDepSrc(iEns,:)='Sensor   ';
   otherwise; Cfg.xdcrDepSrc(iEns,:)='n/a      ';
end

switch base2dec(Cfg.ez(iEns,4),2)
   case 0;    Cfg.headSrc(iEns,:)='Manual EH  ';
   case 1;    Cfg.headSrc(iEns,:)='Int. Sensor';
   otherwise; Cfg.headSrc(iEns,:)='n/a        ';
end

switch base2dec(Cfg.ez(iEns,5),2)
   case 0;    Cfg.pitchSrc(iEns,:)='Manual EP  ';
   case 1;    Cfg.pitchSrc(iEns,:)='Int. Sensor';
   otherwise; Cfg.pitchSrc(iEns,:)='n/a        ';
end

switch base2dec(Cfg.ez(iEns,6),2)
   case 0;    Cfg.rollSrc(iEns,:)='Manual ER  ';
```

```
      case 1;    Cfg.rollSrc(iEns,:)='Int. Sensor';
      otherwise; Cfg.rollSrc(iEns,:)='n/a       ';
    end

    switch base2dec(Cfg.ez(iEns,7),2)
      case 0;    Cfg.salSrc(iEns,:)='Manual ES';
      case 1;    Cfg.salSrc(iEns,:)='n/a     ';
      otherwise; Cfg.salSrc(iEns,:)='n/a     ';
    end

    switch base2dec(Cfg.ez(iEns,8),2)
      case 0;    Cfg.tempSrc(iEns,:)='Manual ET ';
      case 1;    Cfg.tempSrc(iEns,:)='Int. Sensor';
      otherwise; Cfg.tempSrc(iEns,:)='n/a       ';
    end

    Cfg.ec(iEns,:)=dec2base(fread(fid,1,'uint8'),2,8);
    Cfg.distBin1_cm(iEns)=fread(fid,1,'uint16');
    Cfg.xmitPulse_cm(iEns)=fread(fid,1,'uint16');
    Cfg.refLayStrCell(iEns)=fread(fid,1,'uint8');
    Cfg.refLayEndCell(iEns)=fread(fid,1,'uint8');
    Cfg.wa(iEns)=fread(fid,1,'uint8');
    Cfg.cx(iEns)=fread(fid,1,'uint8');
    Cfg.lag_cm(iEns)=fread(fid,1,'uint16');
    Cfg.cpuSerNo(iEns,:)=fread(fid,8,'uint8');
    Cfg.wb(iEns)=fread(fid,1,'uint8');
    Cfg.cq(iEns)=fread(fid,1,'uint8');
    if (idataTypes+1)<=Hdr.nDataTypes(iEns)
      fseek(fid,(Hdr.dataOffsets(iEns,idataTypes+1)+fileloc),'bof');
    else
      fseek(fid,fileloc+bytesPerEns-2,'bof');
    end

%%  Read Variable Leader Data
  case '0080'
    idataTypes=idataTypes+1;
    Sensor.num(iEns)=fread(fid,1,'uint16');
    Sensor.dateNotY2k(iEns,:)=fread(fid,3,'uint8');
    Sensor.time(iEns,:)=fread(fid,4,'uint8');
    Sensor.numFact(iEns)=fread(fid,1,'uint8');
    Sensor.numTot(iEns)=Sensor.num(iEns)+Sensor.numFact(iEns)*65535;
    Sensor.bitTest(iEns)=fread(fid,1,'uint16');
    Sensor.sos_mps(iEns)=fread(fid,1,'uint16');
    Sensor.xdcrDepth_dm(iEns)=fread(fid,1,'uint16');
    Sensor.heading_deg(iEns)=fread(fid,1,'uint16')/100;
    Sensor.pitch_deg(iEns)=fread(fid,1,'int16')/100;
    Sensor.roll_deg(iEns)=fread(fid,1,'int16')/100;
    Sensor.salinity_ppt(iEns)=fread(fid,1,'uint16');
    Sensor.temperature_degc(iEns)=fread(fid,1,'uint16');
    Sensor.mpt_msc(iEns,:)=fread(fid,3,'uint8');
    Sensor.headingStdDev_deg(iEns)=fread(fid,1,'uint8');
    Sensor.pitchStdDev_deg(iEns)=fread(fid,1,'uint8')/10;
    Sensor.rollStdDev_deg(iEns)=fread(fid,1,'uint8')/10;
    Sensor.xmitCurrent(iEns)=fread(fid,1,'uint8');
    Sensor.xmitVoltage(iEns)=fread(fid,1,'uint8');
    Sensor.ambientTemp(iEns)=fread(fid,1,'uint8');
```

```
        Sensor.pressurePos(iEns)=fread(fid,1,'uint8');
        Sensor.pressureNeg(iEns)=fread(fid,1,'uint8');
        Sensor.attitudeTemp(iEns)=fread(fid,1,'uint8');
        Sensor.atttitude(iEns)=fread(fid,1,'uint8');
        Sensor.contamSensor(iEns)=fread(fid,1,'uint8');
        Sensor.errorStatusWord(iEns,:,1)=dec2base(fread(fid,1,'uint8'),2,8);
        Sensor.errorStatusWord(iEns,:,2)=dec2base(fread(fid,1,'uint8'),2,8);
        Sensor.errorStatusWord(iEns,:,3)=dec2base(fread(fid,1,'uint8'),2,8);
        Sensor.errorStatusWord(iEns,:,4)=dec2base(fread(fid,1,'uint8'),2,8);
        fseek(fid,2,'cof');
        Sensor.pressure_pascal(iEns)=fread(fid,1,'uint32');
        Sensor.pressureVar_pascal(iEns)=fread(fid,1,'uint32');
        fseek(fid,1,'cof');
        Sensor.dateY2k(iEns,:)=fread(fid,4,'uint8');
        Sensor.timeY2k(iEns,:)=fread(fid,4,'uint8');
        Sensor.date(iEns,:)=Sensor.dateNotY2k(iEns);
        Sensor.date(iEns,1)=Sensor.dateY2k(iEns,1)*100+Sensor.dateY2k(iEns,2);
        if (idataTypes+1)<=Hdr.nDataTypes(iEns)
          fseek(fid,(Hdr.dataOffsets(iEns,idataTypes+1)+fileloc),'bof');
        else
          fseek(fid,fileloc+bytesPerEns-2,'bof');
        end

%%    Read Velocity Data
      case '0100'
        idataTypes=idataTypes+1;
        for iBin=1:Cfg.wn
          for iBeam=1:Inst.beams(iEns)
            dummy=fread(fid,1,'int16');
            if dummy~=-32768
              Wt.vel_mps(iBin,iEns,iBeam)=dummy/1000;
            end;
          end;
        end;
        if (idataTypes+1)<=Hdr.nDataTypes(iEns)
          fseek(fid,(Hdr.dataOffsets(iEns,idataTypes+1)+fileloc),'bof');
        else
          fseek(fid,fileloc+bytesPerEns-2,'bof');
        end
%%    Read Correlation Magnitude
      case '0200'
        idataTypes=idataTypes+1;
        for iBin=1:Cfg.wn
          for iBeam=1:Inst.beams(iEns)
            dummy=fread(fid,1,'uint8');
            if dummy~=-32768
              Wt.corr(iBin,iEns,iBeam)=dummy;
            end;
          end;
        end;
        if (idataTypes+1)<=Hdr.nDataTypes(iEns)
          fseek(fid,(Hdr.dataOffsets(iEns,idataTypes+1)+fileloc),'bof');
        else
          fseek(fid,fileloc+bytesPerEns-2,'bof');
        end
```

```
%%    Read Echo Intensity
    case '0300'
      idataTypes=idataTypes+1;
      for iBin=1:Cfg.wn
        for iBeam=1:Inst.beams(iEns)
          dummy=fread(fid,1,'uint8');
          if dummy~=-32768
            Wt.rssi(iBin,iEns,iBeam)=dummy;
          end;
        end;
      end;
      if (idataTypes+1)<=Hdr.nDataTypes(iEns)
        fseek(fid,(Hdr.dataOffsets(iEns,idataTypes+1)+fileloc),'bof');
      else
        fseek(fid,fileloc+bytesPerEns-2,'bof');
      end

%%    Read Percent-Good Data
    case '0400'
      idataTypes=idataTypes+1;
      for iBin=1:Cfg.wn
        for iBeam=1:Inst.beams(iEns)
          dummy=fread(fid,1,'uint8');
          if dummy~=-32768
            Wt.pergd(iBin,iEns,iBeam)=dummy;
          end;
        end;
      end;
      if (idataTypes+1)<=Hdr.nDataTypes(iEns)
        fseek(fid,(Hdr.dataOffsets(iEns,idataTypes+1)+fileloc),'bof');
      else
        fseek(fid,fileloc+bytesPerEns-2,'bof');
      end
%%    Read Status
%     case '5000'
%       idataTypes=idataTypes+1;
%       if (idataTypes+1)<=Hdr.nDataTypes(iEns)
%         fseek(fid,(Hdr.dataOffsets(iEns,idataTypes+1)+fileloc),'bof');
%       else
%         fseek(fid,fileloc+bytesPerEns-2,'bof');
%       end

%%    Read Bottom Track Data
    case '0600'
      idataTypes=idataTypes+1;
      Cfg.bp(iEns)=fread(fid,1,'uint16');
      long1=fread(fid,1,'uint16');
      Cfg.bc(iEns)=fread(fid,1,'uint8');
      Cfg.ba(iEns)=fread(fid,1,'uint8');
      Cfg.bg(iEns)=fread(fid,1,'uint8');
      Cfg.bm(iEns)=fread(fid,1,'uint8');
      Cfg.be_mmps(iEns)=fread(fid,1,'uint16');
      Gps.lat_deg(iEns,1)=(fread(fid,1,'int32')/2^31)*180;
      for iBeam=1:Inst.beams(iEns)
          dummy=fread(fid,1,'uint16');
          if dummy~=-32768
```

```
        Bt.depth_m(iBeam,iEns)=dummy/100;
      end;
end;
for iBeam=1:Inst.beams(iEns)
  dummy=fread(fid,1,'int16');
  if dummy~=-32768
    Bt.vel_mps(iBeam,iEns)=dummy/1000;
  end;
end;
for iBeam=1:Inst.beams(iEns)
  dummy=fread(fid,1,'uint8');
  if dummy~=-32768
    Bt.corr(iBeam,iEns)=dummy;
  end;
end;
for iBeam=1:Inst.beams(iEns)
  dummy=fread(fid,1,'uint8');
  if dummy~=-32768
    Bt.evalAmp(iBeam,iEns)=dummy;
  end;
end;
for iBeam=1:Inst.beams(iEns)
  dummy=fread(fid,1,'uint8');
  if dummy~=-32768
    Bt.pergd(iBeam,iEns)=dummy;
  end
end;
dummy=fread(fid,1,'uint16');
if dummy~=-32768
  Gps.alt_m(iEns,1)=(dummy-32768)/10;
end
long2=fread(fid,1,'uint16');
Gps.long_deg(iEns,1)=((long1+long2*2^16)/2^31)*180;
if Gps.long_deg(iEns,1) > 180
  Gps.long_deg(iEns,1)=Gps.long_deg(iEns,1)-360;
end;
Bt.extDepth_cm(iEns)=fread(fid,1,'int16');
dummy=fread(fid,1,'int16');
if dummy~=-32768
    Gps.ggaVelE_mps(iEns,1)=dummy*-1/1000;
end
dummy=fread(fid,1,'int16');
if dummy~=-32768
    Gps.ggaVelN_mps(iEns,1)=dummy*-1/1000;
end
dummy=fread(fid,1,'int16');
if dummy~=-32768
    Gps.vtgVelE_mps(iEns,1)=dummy*-1/1000;
end
dummy=fread(fid,1,'int16');
if dummy~=-32768
    Gps.vtgVelN_mps(iEns,1)=dummy*-1/1000;
end
dummy=fread(fid,1,'uint8');
if dummy~=0
  Gps.gsaVdop(iEns,1)=dummy;
```

```
        end
        dummy=fread(fid,1,'uint8');
        if dummy~=0
          Gps.gsaPdop(iEns,1)=dummy;
        end
        dummy=fread(fid,1,'uint8');
        if dummy~=0
          Gps.ggaNStats(iEns,1)=dummy;
        end
        fseek(fid,1,'cof');
        Gps.gsaSat(iEns,5)=fread(fid,1,'uint8');
        Gps.gsaSat(iEns,6)=fread(fid,1,'uint8');
        Gps.ggaDiff(iEns,1)=fread(fid,1,'uint8');
        dummy=fread(fid,1,'uint8');
        if dummy~=0
          Gps.ggaHdop(iEns,1)=dummy/10;
        end
        Gps.gsaSat(iEns,1)=fread(fid,1,'uint8');
        Gps.gsaSat(iEns,2)=fread(fid,1,'uint8');
        Gps.gsaSat(iEns,3)=fread(fid,1,'uint8');
        Gps.gsaSat(iEns,4)=fread(fid,1,'uint8');
        Cfg.bx_dm(iEns)=fread(fid,1,'uint16');
        Bt.rssi(1,iEns)=fread(fid,1,'uint8');
        Bt.rssi(2,iEns)=fread(fid,1,'uint8');
        Bt.rssi(3,iEns)=fread(fid,1,'uint8');
        Bt.rssi(4,iEns)=fread(fid,1,'uint8');
        Cfg.wj(iEns)=fread(fid,1,'uint8');
        for iBeam=1:Inst.beams(iEns)
          dummy=fread(fid,1,'uint8');
          if dummy~=-32768
            Bt.depth_m(iBeam,iEns)=Bt.depth_m(iBeam,iEns)+...
            (dummy*2^16)/100;
          end

        end;
        if (idataTypes+1)<=Hdr.nDataTypes(iEns)
          fseek(fid,(Hdr.dataOffsets(iEns,idataTypes+1)+fileloc),'bof');
        else
          fseek(fid,fileloc+bytesPerEns-2,'bof');
        end
%%    Read  General NMEA Structure
      case '2022'
        i2022=i2022+1;
        idataTypes=idataTypes+1;
        specificID=fread(fid,1,'int16');
        msgSize=fread(fid,1,'int16');
        deltaTime=fread(fid,8,'uchar');
        marker=ftell(fid);
        switch specificID
%
%         Read GGA data
          case 100
            Gps2.ggaDeltaTime(iEns,:)=deltaTime;
            Gps2.ggaHeader(iEns,:)=char(fread(fid,10,'uint16'))';
            Gps2.utc(iEns,:)=str2double(char(fread(fid,10,'uint16'))');
            Gps2.lat_dm(iEns)=fread(fid,1,'float64');
```

```
            Gps2.latRef(iEns)=char(fread(fid,1,'uint16'));
            Gps2.lon_dm(iEns)=fread(fid,1,'float64');
            Gps2.lonRef(iEns)=char(fread(fid,1,'uint16'));
            Gps2.corrQual(iEns)=fread(fid,1,'uint8');
            Gps2.numSats(iEns)=fread(fid,1,'uint8');
            Gps2.hdop(iEns)=fread(fid,1,'float32');
            Gps2.alt(iEns)=fread(fid,1,'float32');
            Gps2.altUnit(iEns)=char(fread(fid,1,'uint16'));
            Gps2.geoid(iEns)=fread(fid,1,'float32');
            Gps2.geoidUnit(iEns)=char(fread(fid,1,'uint16'));
            Gps2.dgpsAge(iEns)=fread(fid,1,'float32');
            Gps2.refStatID(iEns)=fread(fid,1,'int16');
%
%         Read VTG data
          case 101
            Gps2.vtgDeltaTime(iEns,:)=deltaTime;
            Gps2.vtgHeader(iEns,:)=char(fread(fid,10,'uint16'))';
            Gps2.courseTrue(iEns)=fread(fid,1,'float32');
            Gps2.trueIndicator(iEns)=char(fread(fid,1,'uint16'));
            Gps2.courseMag(iEns)=fread(fid,1,'float32');
            Gps2.magIndicator(iEns)=char(fread(fid,1,'uint16'));
            Gps2.speedKnots(iEns)=fread(fid,1,'float32');
            Gps2.knotsIndicator(iEns)=char(fread(fid,1,'uchar'));
            Gps2.speedKmph(iEns)=fread(fid,1,'float32');
            Gps2.kmphIndicator(iEns)=char(fread(fid,1,'uint16'));
            Gps2.modeIndicator(iEns)=char(fread(fid,1,'uint16'));
%
%         Read DBT data
          case 102
            Gps2.dbtDeltaTime(iEns,:)=deltaTime;
            Gps2.dbtHeader(iEns,:)=char(fread(fid,10,'int16'))';
            Gps2.depth_ft(iEns)=fread(fid,1,'float32');
            Gps2.ftIndicator(iEns)=char(fread(fid,1,'uint16'));
            Gps2.depth_m(iEns)=fread(fid,1,'float32');
            Gps2.mIndicator(iEns)=char(fread(fid,1,'uint16'));
            Gps2.depth_fath(iEns)=fread(fid,1,'float32');
            Gps2.fathIndicator(iEns)=char(fread(fid,1,'uint16'));
%
%         Read HDT data
          case 103
            Gps2.hdtDeltaTime(iEns,:)=deltaTime;
            Gps2.hdtHeader(iEns,:)=char(fread(fid,10,'uint16'))';
            Gps2.heading_deg(iEns)=fread(fid,1,'float32');
            Gps2.hTrueIndicactor(iEns)=char(fread(fid,1,'uint16'));
        end
        if (idataTypes+1)<=Hdr.nDataTypes(iEns)
          fseek(fid,(Hdr.dataOffsets(iEns,idataTypes+1)+fileloc),'bof');
        else
          fseek(fid,fileloc+bytesPerEns-2,'bof');
        end

%%    Read DBT NMEA String
      case '2100'
        idataTypes=idataTypes+1;
        marker=ftell(fid);
        fseek(fid,(Hdr.dataOffsets(iEns,idataTypes)+fileloc+2),'bof');
```

```
        Nmea.dbt(iEns,:)=char(fread(fid,38,'char'));
        dummy=zeros(1,38);
        endstr=find(Nmea.dbt(iEns,:)==char(13));
        dummy(1,1:endstr)=Nmea.dbt(iEns,1:endstr);
        Nmea.dbt(iEns,:)=dummy(1,:);
        if (idataTypes+1)<=Hdr.nDataTypes(iEns)
          fseek(fid,(Hdr.dataOffsets(iEns,idataTypes+1)+fileloc),'bof');
        else
          fseek(fid,fileloc+bytesPerEns-2,'bof');
        end

%%    Read GGA NMEA String
      case '2101'
        idataTypes=idataTypes+1;
        marker=ftell(fid);
        fseek(fid,(Hdr.dataOffsets(iEns,idataTypes)+fileloc+4),'bof');
        if idataTypes < Hdr.nDataTypes(iEns)
          num2Read=Hdr.dataOffsets(iEns,idataTypes+1)-Hdr.dataOffsets(iEns,idataTypes)-4;
        else
          num2Read=bytesPerEns-Hdr.dataOffsets(iEns,idataTypes)-6;
        end
        dummy=char(fread(fid,num2Read,'char'));
        dummy1=blanks(97);
        endstr=size(dummy,1);
        dummy1(1,1:endstr)=dummy(1:endstr);
        Nmea.gga(iEns,:)=dummy1(1,:);
        if (idataTypes+1)<=Hdr.nDataTypes(iEns)
          fseek(fid,(Hdr.dataOffsets(iEns,idataTypes+1)+fileloc),'bof');
        else
          fseek(fid,fileloc+bytesPerEns-2,'bof');
        end

%%    Read VTG NMEA String
      case '2102'
        idataTypes=idataTypes+1;
        marker=ftell(fid);
        fseek(fid,(Hdr.dataOffsets(iEns,idataTypes)+fileloc+4),'bof');
        if idataTypes < Hdr.nDataTypes(iEns)
          num2Read=Hdr.dataOffsets(iEns,idataTypes+1)-Hdr.dataOffsets(iEns,idataTypes)-4;
        else
          num2Read=bytesPerEns-Hdr.dataOffsets(iEns,idataTypes)-6;
        end
        dummy=char(fread(fid,num2Read,'char'));
        dummy1=blanks(50);
        endstr=size(dummy,1);
        dummy1(1,1:endstr)=dummy(1:endstr);
        Nmea.vtg(iEns,:)=dummy1(1,:);
         if (idataTypes+1)<=Hdr.nDataTypes(iEns)
          fseek(fid,(Hdr.dataOffsets(iEns,idataTypes+1)+fileloc),'bof');
        else
          fseek(fid,fileloc+bytesPerEns-2,'bof');
        end

%%    Read GSA NMEA String
      case '2103'
        idataTypes=idataTypes+1;
```

```
        marker=ftell(fid);
        fseek(fid,(Hdr.dataOffsets(iEns,idataTypes)+fileloc+4),'bof');
        if idataTypes < Hdr.nDataTypes(iEns)
          num2Read=Hdr.dataOffsets(iEns,idataTypes+1)-Hdr.dataOffsets(iEns,idataTypes)-4;
        else
          num2Read=bytesPerEns-Hdr.dataOffsets(iEns,idataTypes)-6;
        end
        dummy=char(fread(fid,num2Read,'char'));
        dummy1=blanks(60);
        endstr=size(dummy,1);
        dummy1(1,1:endstr)=dummy(1:endstr);
        Nmea.gsa(iEns,:)=dummy1(1,:);
        if (idataTypes+1)<=Hdr.nDataTypes(iEns)
          fseek(fid,(Hdr.dataOffsets(iEns,idataTypes+1)+fileloc),'bof');
        else
          fseek(fid,fileloc+bytesPerEns-2,'bof');
        end

      otherwise
        Hdr.invalid(iEns,:)=leader_id;
        idataTypes=idataTypes+1;
        if (idataTypes+1)<=Hdr.nDataTypes(iEns)
          fseek(fid,(Hdr.dataOffsets(iEns,idataTypes+1)+fileloc),'bof');
        else
          fseek(fid,fileloc+bytesPerEns-2,'bof');
        end
    end;
    if idataTypes>=Hdr.nDataTypes(iEns)
      Inst.resRDI=fread(fid,1,'uint16');
      checksum=fread(fid,1,'uint16');
    end;
    endFileCheck=ftell(fid);
end;
disp('File complete')

%%%%%%%%%%%%%%%%%%%%%%%%%%%%%%%%%%%%%%%%%%%%%%%%%%%%%%%%%%%%%%%%%%%%%%%%%%%%
%Miressa Ebisa Fola, University of Ottawa, April, 2007
%Added to write Gps2 and Nmea outputs to excel file
%Ensemble number
EnsNum=Sensor.num;
%UTC for each ensemble
utcGps2=Gps2.utc;
%Latitude in degree minute corresponding to each ensemble
latGps2=Gps2.lat_dm;
%Longitude in degree minute corresponding to each ensemble
lonGps2=Gps2.lon_dm;
%Rover GPS antenna altitude corresponding to each ensemble
altGps2=Gps2.alt;
%Number of Satellites used by GPS corresponding to each ensemble
numSatsGps2=Gps2.numSats;
%RTK-DGPS data quality indicator
corrQualGps2=Gps2.corrQual;
%Horizontal Dilution of Precision (HDOP) for GPS data
hdopGps2=Gps2.hdop;
%Depths measured by transducers corresponding to each ensemble
Btd=transpose(Bt.depth_m(1:4,:));
```

```
%Nmea output (UTC, Altitude, Number of satellites and GPS quality, ...)
Nmeaout=Nmea.gga;
%Configuration data output
wmCfg=Cfg.wm;
bmCfg=Cfg.bm;
wpCfg=Cfg.wp;
ws_cmCfg=Cfg.ws_cm;
lag_cmCfg=Cfg.lag_cm;
distBin1_cmCfg=Cfg.distBin1_cm;
%Input excel file name on screen.
fname = input('Input Output File Name: ', 's');
xlswrite(fname,[EnsNum utcGps2 latGps2 lonGps2 altGps2 corrQualGps2 numSatsGps2 hdopGps2
Btd],'Gps2','B1');
xlswrite(fname,[Nmeaout],'Nmeagga','B1');
xlswrite(fname,[EnsNum wmCfg bmCfg wpCfg ws_cmCfg lag_cmCfg distBin1_cmCfg],'cfg','B1');
fclose('all');
```

Appendix F

F Leave One out Regression Analysis

A leave one out analysis was performed to assess the reliability of the regression equations. This was necessary due to the small data set. First, downstream hydraulic geometry equations of all hydraulic variables were derived by leaving one variable out (i.e., only 8 data points were used for the derivation instead of 9 for each case). This was performed for all available data, i.e., nine different regression equations were generated, each time leaving a different datum out of the regression. Second, for each regression equation the estimated hydraulic variables were computed from the regression equation for the datum that was left out of the analysis (Table F.1). This produced an error estimate for each datum (Fig. F.1), from which error statistics were determined (Table F.2).

Table F.1 Summary of measured data and estimated values using the hydraulic geometry equation derived from leaving one variable out.

Q_{bf}	W_{bf}		D_{bf}		V_{bf}		A_{bf}	
(m^3/s)	(m)		(m)		(m/s)		(m^2)	
M	M	E	M	E	M	E	M	E
38.58	53.50	36.55	2.53	2.80	0.28	0.38	135.39	101.68
26.55	39.18	31.20	2.58	2.10	0.26	0.40	101.00	65.16
1.14	5.08	5.61	0.57	0.41	0.39	0.50	2.90	2.30
12.63	13.98	23.52	1.27	1.56	0.71	0.34	17.78	36.52
27.94	25.67	37.94	2.38	2.25	0.46	0.33	61.09	84.94
1.13	6.69	5.21	0.22	0.49	0.77	0.44	1.46	2.58
0.40	1.86	3.76	0.24	0.26	0.88	0.42	0.46	0.95
0.71	5.79	3.82	0.43	0.32	0.28	0.59	2.51	1.19
1.84	9.75	6.84	0.70	0.53	0.28	0.50	6.69	3.63

M: Measured data; E: Estimated data

Table F.2 Root mean square error and mean absolute deviation of estimated data

Hydraulic Variables	MAD	RMS
W_{bf} (m)	6.17	8.24
D_{bf} (m)	0.21	0.25
V_{bf} (m/s)	0.24	0.27
A_{bf} (m^2)	13.19	19.30

MAD: Mean absolute deviation
RMS: Root mean square error

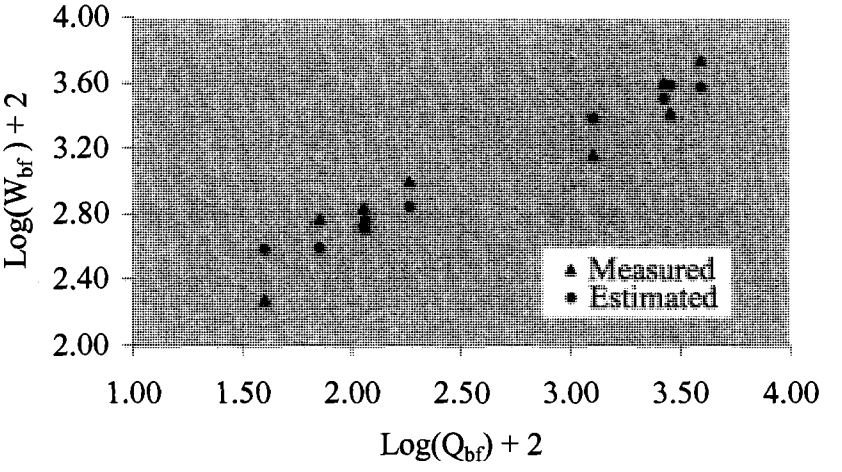

A) Bankfull width versus bankfull discharge

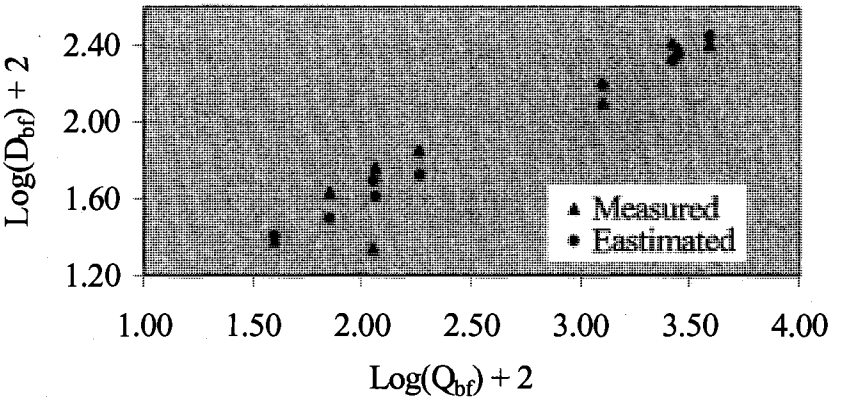

B) Bankfull mean depth versus bankfull discharge

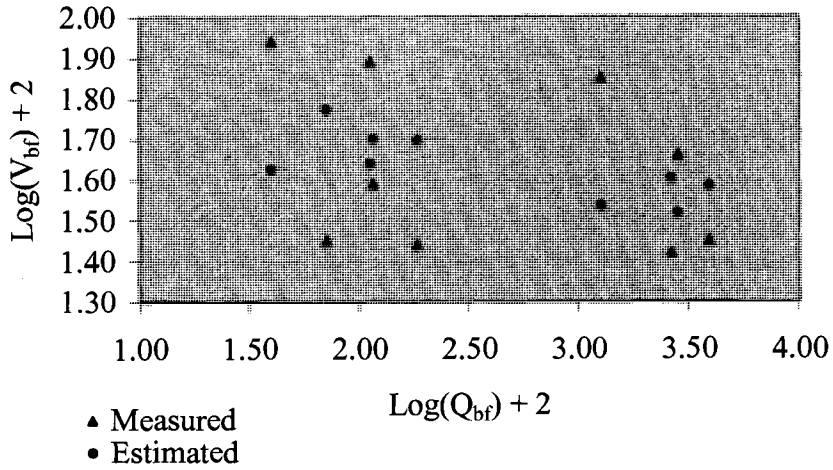

C) Bankfull mean velocity versus bankfull discharge

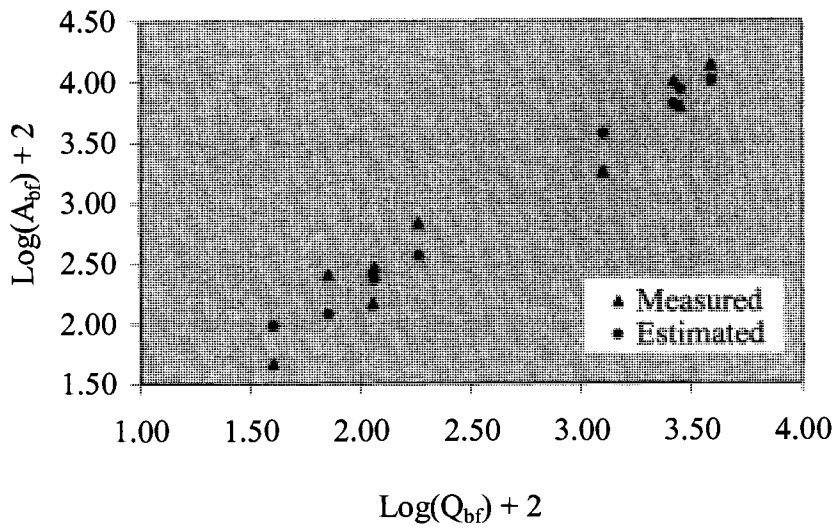

D) Bankfull area versus bankfull discharge

Figure F.1 (A - D) Graphs indicating the relationship between measured and estimated hydraulic variables versus discharge.